

# Novae II. Model, multi-band outburst, bipolar ejecta, accretion disk, relativistic electrons ....

Nimisha G. Kantharia  
National Centre for Radio Astrophysics,  
Tata Institute of Fundamental Research,  
Post Bag 3, Ganeshkhind, Pune-411007, India  
*Email: nkprasadnetra@gmail.com*  
*URL: <https://sites.google.com/view/ngkresearch/home>*

September 2017

arXiv:1709.09400v1 [astro-ph.HE] 27 Sep 2017

## Contents

<b>1</b>	<b>Introduction</b>	
<b>2</b>	<b>Background on novae</b>	
2.1	Novae at minimum . . . . .	3
2.2	Novae in outburst . . . . .	4
2.2.1	Optical light curve . . . . .	4
2.2.2	Optical spectra . . . . .	4
2.2.3	Fe II and He/N novae . . . . .	6
2.3	Existing astrophysical model for novae . . . . .	7
2.4	White dwarf primary . . . . .	8
<b>3</b>	<b>The updated model for novae</b>	
3.1	Accretion disk, accreted envelope, bipolar/ellipsoidal ejecta . . . . .	9
3.2	Novae in quiescence . . . . .	11
3.2.1	Eclipsing novae . . . . .	14
3.3	Novae in outburst . . . . .	15
3.4	Origin of multifrequency emissions . . . . .	31
<b>4</b>	<b>Case studies</b>	
4.1	Classical novae . . . . .	33
4.1.1	DQ Herculis 1934 . . . . .	34
4.1.2	V339 Delphini 2013 . . . . .	37
4.2	Recurrent novae . . . . .	39
4.2.1	RS Ophiuchi . . . . .	40
4.2.2	T Pyxidis . . . . .	42
4.3	Evolution of novae to SN 1a . . . . .	43
<b>5</b>	<b>Conclusions</b>	

## Abstract

**2** The study of novae is continued and a self-consistent updated physical model for classical/recurrent novae derived from multi-wavelength observations is presented. **3**  
**3** In particular, observations of novae support the origin of the optical continuous emission in the outburst ejecta, mass-based segregation and clump formation in the ejecta, origin of the Orion, diffuse enhanced lines and dust in the clumps, prompt Fe II line formation in swept-up material, energising of electrons to relativistic velocities by the explosion and the existence of a large cool envelope around the accreting white dwarf in quiescence. The rapid transfer of thermonuclear energy should be adiabatic which energises and ejects all the particles in the overlying layers. Our study results in the following conclusions which are relevant for novae and other astrophysical systems: **9**  
(1) Electrons are instantaneously energised in the explosion alongside the heavier atoms and ions. In sufficiently energetic explosions, electrons should acquire highly relativistic velocities due to their small mass and emit synchrotron emission in a magnetic field. No post-ejection shock acceleration needs to be invoked. **33**  
(2) Rotation of an incompressible spherical accreting object modifies the effective potential felt by infalling particles. The combined effect of gravitational and centrifugal forces will lead to a latitude-dependent potential such that the accretion rate will be maximum at the poles and minimum at the equator. The mass accumulation at the poles will exceed that at the equator leading to the formation of a prolate-shaped or bipolar envelope around the object. Energetic expulsion of this envelope will result in a bipolar/prolate shaped ejecta/outflows. Such outflows cannot be ejected from non-rotating spherical objects. **44**  
(3) The latitude-dependent accretion rates in a rotating accreting object will also lead to accumulation of the infalling matter outside the object in the non-polar regions thus forming an accretion disk. The angular momentum of the incoming matter plays no role in the

formation of an accretion disk. Accretion disks cannot form around a non-rotating object.

## 1 Introduction

Novae are highly energetic explosions on the accreting white dwarf in a semi-detached binary system hosting a gaseous companion star. Such an explosion in a classical nova ejects matter and brightens the binary by 8-20 magnitudes within a day or so whereas it leads to brightening upto 6 magnitudes in a dwarf nova. While the return to brightness of the pre-outburst phase takes much longer, the explosion, energising and ejection of matter in classical novae are rapidly accomplished supporting a dominantly adiabatic transfer of energy.

Most nova outbursts follow the maximum magnitude relation with decline time (MMRD) which is an inverse relation between the peak V band luminosity of a nova and its decline time with the latter following an inverse relation with the ejecta velocity derived from the spectral lines. This relation should have dispelled all doubts of a separate origin of the optical spectrum and continuum emission. However, literature continues to attribute the origin of the optical continuum to the pseudo-photosphere of the white dwarf inflated by the explosion and the spectrum to the ejecta. We also recall that the MMRD derived using simple physical arguments by Kantharia (2017) was able to improve the MMRD fit to existing data on novae, thus giving strong support to its validity. The observed relation between the ejecta velocity  $v_{ej}$  and time taken by the light curve to decline by two magnitudes  $t_2$ , which is used to calibrate the MMRD is straightforward to understand if their origin is in the ejecta - a rapidly expanding ejecta (large  $v_{ej}$ ) will quickly become optically thin and find its emission measure dropping rapidly, so that its light output will also decline faster (smaller  $t_2$ ). However this relation is difficult to understand if the continuum emission arises in the pseudo-photosphere as explained here. A rapidly expanding ejecta surmised from the spectral lines would also indicate a fast expanding pseudo-photosphere and the optical continuum will quickly brighten. However the decline in the light curve will now be attributed to the contraction of the photosphere after it has expanded to some maximum size. In this case, it is difficult to understand why a fast ejecta should lead to a faster contraction of the photosphere and hence a faster drop in the optical continuum i.e. shorter  $t_2$ . One can also resort to a temperature change in the photosphere but again the problem is why the temperature of the photosphere should change rapidly in a nova in which the ejecta is rapidly expanding. To explain the optical continuum from the photosphere requires contrived explanations. The most obvious solution is that both the optical continuum emission and spectrum arise in the ejecta.

We point to the empirical result that while classical and recurrent novae are found to obey the MMRD, data on dwarf novae suggests a weak opposite correlation between

peak luminosity and decline time, if any (Figure 3a in Kantharia, 2017). This supports a different origin location of the optical continuum in dwarf novae and a strong contender is the expanded photosphere (outer surface of the accreted envelope) due to energy injection. If the optical continuum was due to the isothermal expansion of a photosphere then a brighter dwarf nova outburst would indicate a larger photosphere whereas a faint dwarf nova outburst would indicate a smaller photosphere. For example, consider a dwarf nova outburst results in an envelope which is ten times the radius of the white dwarf core ( $R_{WD}$ ) as compared to another dwarf nova which is inflated to five times  $R_{WD}$ . The black body luminosities of the two novae assuming both photospheres are at the same temperature will differ by a factor of four. Even if both the photospheres are contracting at the same rate of say  $0.1R_{WD}$  per day then after 10 days, the photospheres would have contracted by a  $R_{WD}$ . This means that the radius of the envelope which was  $5R_{WD}$  would be  $4R_{WD}$  i.e. 80% of the maximum radius whereas for the photosphere of  $10R_{WD}$ , the radius will be  $9R_{WD}$  ie 90% of the maximum radius and the luminosities would have decreased to 64% and 81% of the peak respectively. The contraction of the larger photosphere (i.e. brighter dwarf nova outburst) takes longer so that  $t_2$  is longer compared to the fainter dwarf nova with the smaller photosphere. This, then, would explain why dwarf novae do not follow MMRD but show a weak opposite trend. Moreover the photospheric origin also explains the observed flat maximum in dwarf novae - the photosphere having expanded to a maximum size, will stop expanding but remain at that radial extent for some time before it starts shrinking and the light curve declines. Thus, the behaviour of the MMRD in classical and dwarf novae encompass the physical processes in these systems.

The existing multi-wavelength observational results offer us an opportunity to coherently understand the evolution of a nova outburst and we attempt the same in this paper. There exist a range of ill-understood phenomena such as ejecta morphology so that some are spherical and others are aspherical, increasing blue-shifted velocity displacement of absorption lines when the light curve is in the early decline phase, only some novae emit radio synchrotron, origin of energetic  $\gamma$ -rays, sites of dust formation, an old nova being brighter than its components etc. which we discuss in this paper and then update the existing model used to explain novae.

Since a nova outburst is representative of an explosive phenomenon in which a huge quantity of energy is pumped into a system in a short time, we extend our results to other similar transient explosive systems such as supernovae and jets in active nuclei and find parallels so that several phenomena happening there can be explained by extending our nova model. All of this is also used to further our understanding of basic physical processes such as accretion rates and formation of accretion disks, bipolar outflows; electron acceleration and distribution of electron energies. The results, some supporting existing astrophysical theories and some leading to a paradigm shift in exist-

ing astrophysical theories within the framework of known physics are discussed in the paper. Throughout, the aim has been to adhere to the simplest picture that obeys the laws of physics, explains observational results, is logically consistent and requires the minimum of assumptions and personal biases to be introduced.

We begin by giving a background on novae and the well-defined behaviour of their light curves and spectra. This is followed by a summary of the existing model used to explain novae and introduction to white dwarfs. Then we describe the updated model which is used to understand the observations of a few novae and end with conclusions.

## 2 Background on novae

Soon after novae were identified, there existed suspicions that the star on which the energetic event occurred and which was a blue star (Humason, 1938; Kraft, 1964b) was a white dwarf (e.g. Humason, 1938; McLaughlin, 1941; Greenstein, 1957; Kraft, 1959, 1962; Paczyński, 1965) but the combination of brighter absolute magnitudes, distinct colours, larger estimated masses and lower densities of the blue star (Humason, 1938; McLaughlin, 1941) compared to isolated white dwarfs seems to have caused the blue star to be misidentified as a hot sub-dwarf. However as the number of novae in which a white dwarf could be unequivocally identified increased, it became clear that the blue star was a white dwarf. From the early studies it was clear that the explosion was very energetic which led to upto million times increase in the luminosity of the star and several different origins for the energy were explored ranging from collisions between two stars to an origin in a thermonuclear explosion (e.g. Mestel, 1952; Marshak, 1940; Kraft, 1964a; Paczyński, 1965) which is now known to be the cause. There existed doubts regarding the explosion being within the degenerate core of a white dwarf or on in the surface layer. The energy output if the explosion occurred within the degenerate core was estimated to resemble the energy release in a supernova explosion (Mestel, 1952) and was ruled out and the surface explosion was favoured (e.g. Paczyński, 1965; Gallagher & Starfield, 1978). Detection of expanding shells around old novae which show enhanced CNO abundance with respect to hydrogen as compared to other nebulae (Williams et al., 1978) have since supported the thermonuclear origin of the energy pulse in classical nova outbursts. It was also found that several of these explosions were in binary systems (Sanford, 1947; Joy, 1954; Walker, 1954; Kraft, 1962) and this seems to have been established as a basic property of novae when Kraft found that seven out of the ten old novae he had examined were unambiguously binary systems (Kraft, 1964b). It was also suggested that hydrogen fuel was being transferred from the red companion to the blue star which was a semi-degenerate object on its way to becoming a white dwarf and this was inducing superficial outbursts on the blue star (Kraft, 1964a) and the emission lines from a nova were arising in the disk of material formed around the blue star (e.g. Kraft, 1959). It is

also worth noting that from early observations of novae it was obvious to astronomers that classical, recurrent and dwarf novae consisted of the same basic components. It was suggested that the nature of the observed spectra of nova outbursts can be explained if they arose in an expanding sphere of hot gases that cooled as it expanded so that the spectral lines appeared in absorption or emission and were broadened (Pickering, 1901). From the observed character of the light curve, it was also suggested that the nova outburst whatever its cause led to a major ejection of matter which was followed by continuous ejection in the form of winds (e.g. McLaughlin, 1943). It is instructive to appreciate how the binary nature and its member stars, the origin of the outburst energy, important physical processes etc have gradually been unravelled from interpretation of observations constrained by physics so that our knowledge on novae is now extensive.

Classical novae are identified when in outburst. The progenitor system can often be identified in sky images taken before the outburst once its position is known. The system observed outside the outburst region is in its minimum state and observations of this state have been useful in understanding several features of the binary. We discuss this next.

### 2.1 Novae at minimum

From a study of 16 old novae, Humason (1938) established that these were blue stars since all the objects showed a strong continuum spectrum which extended upto the violet and half of them also showed emission lines of hydrogen, carbon and neutral or ionized helium. No absorption lines were detected. The temperatures for these blue stars were estimated to be between 20000 K and 50000 K similar to O or early B type main sequence stars (Humason, 1938). McLaughlin (1941) followed up this work on novae in quiescence and derived radii of  $\sim 0.1 - 0.2 R_{\odot}$  and densities of  $\sim 10^3 \rho_{\odot}$  for the blue star using the Stephen-Boltzmann law. For comparison, the nominal radii of white dwarfs are  $\sim 0.01 R_{\odot}$  and densities are  $\geq 10^4 \rho_{\odot}$ . Due to these different physical properties, both these authors concluded that the old novae could not be true white dwarfs but were sub-dwarf stars. Since recurrent novae present quiescent periods between outbursts which represent both the post-nova and pre-nova phases, these have been studied to understand the blue star. The spectrum of the recurrent nova RS Ophiuchi from 1937 (after its outburst in 1933) was similar to its spectrum from 1923 with both showing bright hydrogen and Fe II lines on a continuous spectrum indicating both were the minimum spectrum - the only difference seemed to be in the presence of the He II 4686A line in 1937 which was absent in 1923. However the spectrum taken in 1936 was quite different (McLaughlin, 1941) indicating that the nova was not yet back to its inter-outburst state. A spectrum of T Pyxidis taken 14 years after its outburst in 1920 is similar to other old novae showing a continuous spectrum with a bright He II 4686A line and faint hydrogen lines (McLaughlin, 1941). Such studies that established the similarity between the spectra of recurrent

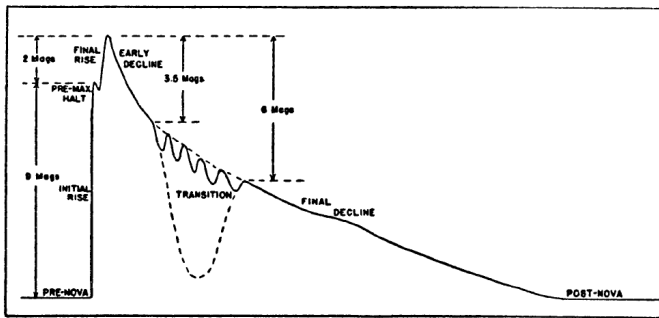


Figure 1: A schematic showing the typical optical light curve of a nova reproduced from McLaughlin (1943). The main phases in the evolution of a typical light curve are labelled in the figure.

novae in the inter-outburst period and classical novae at minimum support similar physical processes in classical and recurrent nova outbursts. McLaughlin (1941) argues that although there are differences in the spectra of classical novae and U Geminorum stars (dwarf novae); there also are strong resemblances which argue for the underlying processes being similar in nature. These studies helped infer that pre-nova and post-nova stars have similar physical properties and ruled out any model which involved destroying the star. It argued for a superficial explosion on a star (McLaughlin, 1943).

## 2.2 Novae in outburst

There is a sudden brightening of 8 – 20 magnitudes in the optical bands when a nova goes in outburst making several of them visible to the naked eye before their brightness starts to decline. While the rise to maximum is extremely rapid in most novae, they show a range in the decline rates using which they are classified into speed classes i.e. slow and fast novae. The light curves and spectra of novae evolve after the outburst and exhibit similar pattern of evolution. We describe the observational details on the nova light curves and spectra.

### 2.2.1 Optical light curve

A typical optical light curve showing the evolution of light in a nova outburst is schematically shown in Figure 1 (McLaughlin, 1943). Light curves of novae were discussed in detail by McLaughlin (1939a,b). Based on his own and other scientists' observational inferences, McLaughlin divided the light curve into different evolutionary phases between the pre-nova and post-nova stages and identified them as the initial rise, pre-maximum halt, final rise, early decline, transition and final decline as labelled in Figure 1. All novae are observed to follow this kind of progression with the differences being limited to the presence of the pre-maximum halt or the transition phase in the form of oscillations or a deep minimum. This, then gives a template to understand the underlying physical processes in the nova responsible for the light evolution. Most no-

vae show similar spectral patterns in a particular phase of light curve evolution and these are summarised in Table 1 which is copied from McLaughlin (1943). That most novae adhere to such a well-defined evolution indicates that it has an astrophysical origin and cannot be attributed to a random, chancy effect.

We describe the different stages labelled in Figure 1. In the *initial rise*, the nova rapidly brightens from minimum to about two magnitudes below maximum which is a rise of 6-18 magnitudes in a day or so. Some novae remain at this stage, which is known as the *pre-maximum halt*, for a considerable time and this stage is typically observable in slow novae detected before maximum. The *final rise* to maximum brightness after the pre-maximum halt is slower than the initial rise. Most fast novae are detected just before or after the maximum brightness often leading to uncertainty in the peak magnitude. Slow novae spend a longer time near maximum brightness whereas fast novae begin to decline soon after reaching maximum. The time a nova takes to decline by two or three magnitudes from peak brightness is known as the decline times  $t_2$  and  $t_3$  and are used to identify the speed class of the nova. Around 3 to 3.5 magnitudes below maximum, the transition phase sets in when the light curve of some novae show oscillations in the visible light whereas some slow novae show a steep drop in the light curve (Figure 1). The transition phase in novae was first identified as the phase in which the spectrum changes from a stellar (absorption lines) to a nebular (emission lines) type (Stratton, 1920). The change from a stellar spectrum to a nebular spectrum was found to be correlated to the phase of the light curve which showed oscillations or a steep fall and hence referred to by the same name i.e. transition phase. When the nova light stops oscillating or when it recovers from the steep drop, it is generally  $\geq 6$  magnitudes below maximum and into the nebular phase characterised by emission lines and absence of absorption lines. The nova begins its final decline which is very slow in most novae and can take upto a decade or longer. At the end of the final decline, the nova reverts to its pre-nova brightness. While all novae pass through the same light curve phases, the time taken by different novae to evolve through the various phases of the light curve differ. Light curves of classical nova outbursts take several years to complete their decline whereas recurrent novae outbursts get over in a year or so. The spectral changes (see Table 1) are generally observed to occur close to the labelled light curve changes with respect to the maximum. Such well-determined evolution of novae light curves and spectra indicate well-defined processes at work.

### 2.2.2 Optical spectra

The evolution of the optical spectra of most novae in outburst is closely related to the light curve evolution as quantified in Table 1 and demonstrated by the efficacy of the MMRD. The spectrum recorded soon after the outburst consists of absorption dips located on the blue side of the wide emission bands which are seen to extend both bluewards and redwards of the rest frequency i.e. P Cygni

Table 1: Table showing the correlated spectral and light curve phases. Copied from McLaughlin (1943).

Absorption system	Emission system	Duration mag from max	Part of light curve
1.Pre-maximum	Pre-maximum	-	Rise(decline)
2.Principal	Principal	0.6 to 4.1	Early decline
3.Diffuse enhanced	Diffuse enhanced	1.2 to 3.0	Early decline
4.Orion	Orion(hazy bands)	2.1 to 3.3	Early decline
5. Nitrogen(Orion)	'4640' (Orion)	3 to 4.5	Transition
6. -	Nebular(principal)	4 to 11	Transition-final decline
7. -	Post-nova narrow stellar emissions	8 to min.	Final decline and post-nova

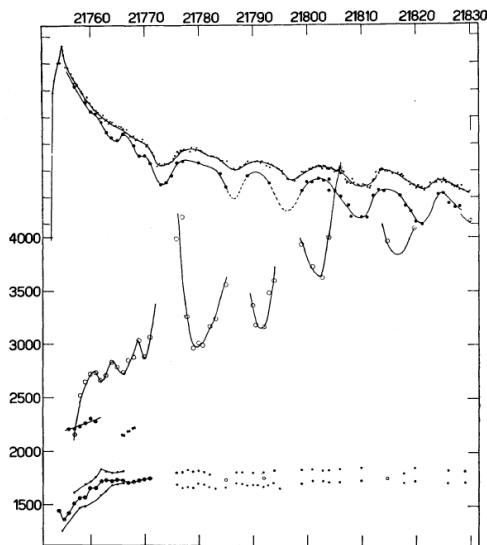


Figure 2: Figure showing light curve of nova V603 Aquilae (upper curves) and the change in the velocity of absorption features (lower curves). The velocity curve right below the light curve shows the variation in the displacement of the Orion line feature. Note its anti-correlation with the light changes. Figure has been reproduced from Gaposchkin (1957).

profiles although sometimes only the absorption component is detected. The excitation level, profile shape and velocity displacement of the absorption lines change as the nova evolves. The changes were identified and classified into a few well-defined stages and the spectral evolutionary sequence of novae was presented (e.g. Stratton, 1920; McLaughlin, 1937a, 1942) as summarised in Table 1. Subsequent observations have given fresh inputs to this basic picture of spectral evolution of novae in addition to validating the basic model put forward to explain the nova spectra.

McLaughlin (1943) has described the joint evolution of the optical light curve and line spectrum in novae (Table 1). The nova exhibits characteristics typical of a supergiant of a spectral type which varies with its light curve evolution. In the pre-maximum phase, the nova spectrum resembles an early spectral type like B or A which evolves to a relatively later type during and after maximum like spectral type F. So, for example, GK Persei exhibited ex-

citation typical of a B9 star in the pre-maximum phase, an A0 type during maximum and A2 after maximum (e.g. McLaughlin, 1960b) whereas DQ Herculis changed from B to A to F0 (McLaughlin, 1954). An important difference between the nova spectrum and that of a supergiant is the presence of absorption lines of oxygen and carbon in the nova spectrum which is not typical of a supergiant star (McLaughlin, 1943).

McLaughlin divided the optical spectral lines observed from novae into four main systems based on the velocity displacement of the absorption component and excitation of the spectrum namely the pre-maximum, principal, diffuse enhanced and Orion spectral systems. The onset and disappearance of these systems were correlated with well-defined phases of light curve evolution as listed in Table 1. The following discussion is mainly based on McLaughlin (1943) and McLaughlin (1960b). The pre-maximum spectrum is observed before the light curve rises to maximum brightness and the lines of hydrogen, Ca II, Na I, O I, C I are detected. The absorption lines are blue-shifted and show the lowest velocity displacement compared to the lines which are detected later. Just after the maximum in the light curve, the principal system of spectral lines appear and the absorption component is displaced to a larger blue-shifted velocity than the pre-maximum lines. The pre-maximum system either disappears as soon as the principal system shows up or at times is detected alongside the principal spectrum for a short while. The principal spectrum resembles that of a star of type A or F. The principal spectrum shows a composition similar to the pre-maximum spectrum with a few additional lines of Mg II, Ti II, Fe II, He I, Si II. The principal absorptions disappear about 4 magnitudes below maximum. Strong absorption lines fade faster so that lines of Mg II, O I, C I and Si II are the first to disappear whereas the hydrogen lines are the last to fade. Some of the principal absorptions are found to split into double or triple components. The principal emission bands are long-lived and are even detected from the nebular shells observed to expand around some old novae many years after the outburst. After the light curve has declined by about a magnitude from maximum, the diffuse enhanced system of lines consisting of hydrogen and metallic lines such as Ca II, Mg II, O I, Na I, Fe II appear. These absorption features show a blue shift which is larger than the principal system by a factor of 1.5 – 2. These lines which are wide and hazy are often

seen to split into multiple sharp components. Around 2 magnitudes below optical maximum, the Orion system of lines generally appear consisting of higher excitation lines like O II, N II, He I, N III at similar or larger velocity displacement than the diffuse enhanced lines. The presence of higher excitation lines as observed in OB associations like in the Orion star forming region prompted McLaughlin to name this system as the Orion system. An important peculiarity of the Orion system is that hydrogen is often missing in this system of lines unlike the spectral systems that preceded it. The velocity displacement of the Orion absorption lines with respect to principal lines is 1.6 to 3.3 times and the emission components are wide and diffuse. These lines are not observed to split into several sharp components although at times multiple wide components are identified. The Orion lines are more evident in slow novae than in fast novae. The Orion lines are most sensitive to light curve oscillations. The simultaneous existence of the principal, diffuse enhanced and Orion systems in the nova spectrum when the light curve is about 1-4 magnitudes below maximum, indicates the range of excitation and physical conditions that exist in a nova. While the principal system of emission lines continue to be present, the diffuse enhanced and Orion system of lines disappear in the transition phase which sets in when the nova has faded by about 3 magnitudes. The principal absorption lines also disappear in the transition phase. The composition and excitation of the emission bands of the principal spectrum changes in the transition phase but the velocity displacement remains the same. The transition phase defines the changeover from a stellar to a nebular spectrum i.e. all absorption features disappear leaving behind wide emission bands which also engulf the absorption velocities. In the transition phase, the light curve of several novae show oscillations and alongwith the light changes, the Orion system lines show correlated changes in excitation levels and velocity displacement as shown in Figure 2. The excitation level and the blue-shifted velocity displacement of the absorption lines increase when the light curve undergoes a minimum in the oscillation and vice versa (Figure 2). The velocity displacement of the principal system of lines are not observed to change with the light oscillations. However in a few novae, the oscillating light is seen to result in the oscillating detection of high excitation principal lines like He II and N III such that lines appear at the secondary light minimum and fade at the secondary maximum. After the transition phase, the spectrum of the nova evolves to a nebular nature. When the nova is on the final decline, the spectrum continues to be nebular with only emission lines typically of [O III], N II, He II, [Ne III] and C II being detected with velocity displacements and widths typically of the principal spectral system. The spectrum also frequently shows the presence of high excitation coronal, forbidden and Neon lines. The nebular spectrum, which is fully developed around 7 magnitudes below optical maximum, closely resembles that of a planetary nebula except for the larger emission linewidths and some differences in the composition. The nebular stage lines are detected as long as the expanding ejecta around

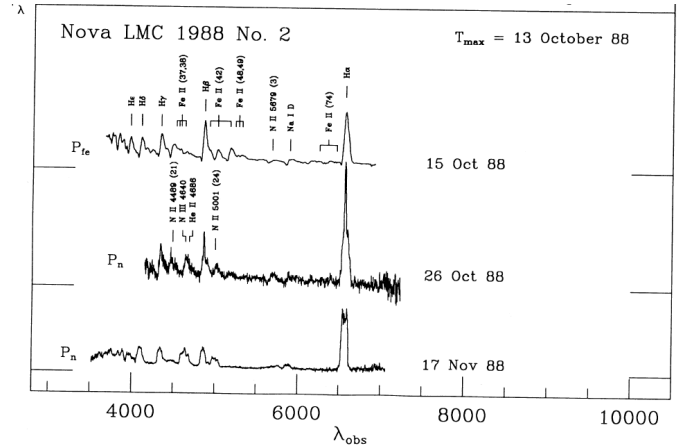


Figure 3: Typical spectra of a hybrid (Fe II and He/N) nova. Figure reproduced from Williams et al. (1991).

the nova retains its identity and is detectable. When it has been possible to separate the emission from the central star and the nebula in the later stages of evolution, it is found that the emission bands arise in the expanding shell whereas the continuum is predominantly from the central star and as the nebula fades, only the spectrum of the star is detected (McLaughlin, 1960b).

### 2.2.3 Fe II and He/N novae

In addition to the classification of spectral stages and light curve phases in the evolution of a nova outburst described in the previous section, it was found that novae could be classified into two types depending on the atomic species other than hydrogen which showed the strongest lines in the optical band soon after maximum (Williams et al., 1991; Williams, 1992). Study of the post-maximum spectra of several novae revealed that the strongest spectral line (other than the Balmer lines) in the nova spectra were either of Fe II or of helium and nitrogen which led to the classification of novae into Fe II and He/N classes (Williams, 1992). Spectra of a nova in the Large Magellanic Cloud (LMC) taken at a few epochs following optical maximum are shown in Figure 3. Several P Cygni profiles are detected in the spectrum taken two days after optical maximum which appears to be very different from the spectrum taken 13 days after maximum indicating changes in the composition of the spectrum, line strengths and widths. The non-Balmer dominant lines are of iron in the spectrum taken two days after maximum which are replaced by lines of helium and nitrogen in the later spectra. The H $\alpha$  profile is seen to change from a gaussian shape to a double component line with a narrow feature perched on a broad feature to a double-peaked profile. While P Cygni profiles are noticeable in the spectrum in the top panel, only emission lines are detected in the spectrum in the lowest panel. In Nova LMC 1998 No 2 (see Figure 3), features due to Fe II and He/N were simultaneously detected and subsequently the Fe II features were replaced by He/N features. Such novae are termed as hybrid novae (Williams, 1992). The vice versa i.e. early post-maximum

detection of He/N and subsequent replacement by Fe II is generally not observed. At this point, it is interesting to note that spectral observations of the slow recurrent nova T Pyx in its pre-maximum phase revealed the presence of high ionization emission lines of helium, nitrogen and other metals which were soon replaced by P Cygni lines of Fe II near maximum (Surina et al., 2014). Since few novae are studied in the pre-maximum phase due to its rapid rise, this result gives us a rare glimpse into the pre-maximum evolution of the nova spectrum. However it does not change the classification into Fe II and He/N types which is based on the post-maximum spectrum.

The Fe II class of novae display narrower lines ( $\text{HWZI} < 2500 \text{ km s}^{-1}$ ), P Cygni profiles, lines of lower excitation and the prompt post-maximum light curve decline is generally slower ( $t_2$  is long). The He/N class of novae are characterised by broad lines ( $\text{HWZI} > 2500 \text{ km s}^{-1}$ ; often broader than  $5000 \text{ km s}^{-1}$ ), jagged flat-topped emission lines often without P Cygni absorption, higher excitation and the post-maximum light curve decline is faster ( $t_2$  small) (Williams, 1992). The above classification has also been extended into the near-infrared bands where the main difference between the two types is found to lie in the presence of neutral carbon lines in Fe II type novae and absence of the same in He/N novae which is inferred to indicate the different excitation conditions in the two types of novae (Banerjee & Ashok, 2012). Dust shows a tendency to form more often in Fe II novae (e.g. Banerjee & Ashok, 2012).

### 2.3 Existing astrophysical model for novae

Observations of novae in outburst have motivated a model which is summarised here. Most of the following is based on McLaughlin (1943). It is interesting to note that the paper makes it a point to mention that the velocity displacements of the absorption lines and widths of the emission lines are due to the Doppler effect in an expanding shell of gas as was suggested by Pickering (1901). Although this is something we take for granted today, it was not obvious then and shows how our knowledge has gradually built up over time from the sincere efforts of many scientists. The model describes the outburst by a ‘main burst’ in which most of the mass and energy are expelled and which is followed by continuous expulsion of matter at a lower rate for a long time i.e. a wind. Since there is no change in the star, the model supports release of energy below the superficial layer which then expands outward. The inner regions of the expanding cloud are dense and radiate as an effective photosphere while the outer layers become progressively tenuous. Since the photosphere is an optical depth extent, it lags behind as the ejecta expands. The observed optical continuous emission in this model arises from the photosphere of the white dwarf. The changing spectral class in this model is explained by the expanding photosphere which cools and changes the energy distribution in the continuum and hence the spectral class. At optical maximum, the photosphere and sur-

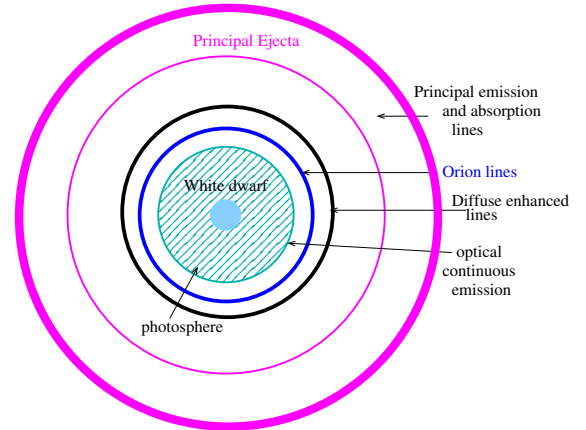


Figure 4: Model summarised by McLaughlin (1943) to explain observations of novae soon after outburst upto about 4 magnitudes below optical maximum. The principal ejecta is enclosed by the magenta lines. The diffuse enhanced (black) and Orion (blue) spectra arise in later faster ejection from the central star. Optical continuum comes from the expanded photosphere of the central star.

rounding atmosphere will resemble a supergiant star with a radius of  $\sim 150R_{\odot}$ . A rapid drop in the rate of ejection is inferred just before light maximum and around maximum, the ejecta is taken to detach from the photosphere. The entire ejecta becomes optically thin after the optical maximum. The continuous spectrum starts to decline after the maximum. The post-maximum model consists of a detached expanding optically thin ejecta and an attached cloud of a relatively smaller radial extent around the star which is expanding at a rate which is lower than the rate at which the photospheric surface is moving inwards. This inward motion of the photospheric surface is due to the expansion of the inner shell which leads to a decrease in the radial extent of the  $\tau = 1$  surface i.e. a contracting photosphere due to decreasing densities. The photosphere keeps shrinking within the smaller expanding cloud around the central star. As the photosphere shrinks, the  $\tau = 1$  surface gets closer to the star and hence hotter. The model uses this argument to explain the observed increase in the colour temperature as the light declines. For example, Nova Herculis 1934 and Nova Lacertae 1936, had colour temperatures of about 6000 K near optical maximum which increased to  $\sim 30000$  K when the light dropped by four magnitudes after maximum (McLaughlin, 1941). McLaughlin suggests that the emergence of the principal spectrum with a larger blue shift and disappearance of the pre-maximum spectrum are due to the radiation pressure exerted by the stellar radiation field on the inner dense layers which are then pushed forward at a higher velocity and leads to the entire outer shell being ejected and going optically thin. He explains the bright wide bands in the principal shell as being emission from

the entire shell and the absorption lines being formed in the outer layers of the shell which absorb the light of gas immediately behind them i.e. the regions of emission and absorption merge into one another in the principal ejecta shell. However an alternate interpretation in literature is that the absorption lines are formed due to absorption of the continuous light of the star. Irrespective of that, as the shell expands, the number of atoms which can absorb keeps decreasing and most absorption lines weaken and eventually fade. As densities fall below the critical densities, forbidden lines appear in the spectra of several novae.

In this model, winds continue to blow from the star well after the main burst which sets forth the ejecta. The model locates the diffuse enhanced and Orion spectral lines in these winds. These winds are postulated to blow out at even higher velocities than the main ejecta and hence explain the higher blue shifted velocities of the diffuse enhanced and Orion systems (see Figure 4). The appearance of the diffuse enhanced P Cygni features happens when sufficient atoms have accumulated in the winds. The multiple sharp components which the diffuse enhanced lines often evolve into are explained as forming in the winds moving outwards in the form of concentric independent shells and the broad diffuse absorption is produced in the outer layers of the envelope. The formation of Orion lines is explained as being in a later but faster ejection from the star. The shrinking photosphere exposes a still hotter surface which is inferred as the reason for the higher excitation of the spectral lines of the Orion system. It is suggested that the hard radiation field weakens the metallic lines of the diffuse enhanced system due to ionization. The model explains that the multiple lines of the diffuse enhanced system disappear when the shells become thin. All through the spectral evolution, the photosphere around the white dwarf is contracting and when the Orion system reaches its maximum strength, McLaughlin estimates the photosphere to be  $\sim 10R_{\odot}$ . As the excitation increases, N III absorption and 4640 emissions emerge as part of the Orion system while the lines He I, O II, N II fade. Since the diffuse enhanced and Orion systems are produced in gas located just outside the photosphere in this model, the larger emission line widths are attributed to enhanced turbulence near the star. The disappearance of the Orion N III lines is attributed to the increased ionization due to the appearance of the hotter inner levels as the photosphere recedes towards the star. It is suggested that subsequently the radiation field is so hard that the diffuse enhanced and Orion lines disappear and no further observable lines are produced although winds continue to be blown by the sub-dwarf star. At this time, the principal shell has expanded to several astronomical units and emission lines are detected from it as the nebular spectrum. This model advocates continuous ejection of matter over a period of years after the main burst. McLaughlin says that ‘The highest velocity of expulsion was reached in the ‘4640’ stage but the greatest violence (in terms of total momentum of the matter ejected in unit time) occurred near light maximum in the eruption of the principal ‘shell’ or ‘main burst.’ In this model, the secondary max-

ima of light observed after maximum and the oscillations in the transition phase are seen as secondary outbursts which lead to temporary increase in ejection rates of the wind. These increase the radius of the effective photosphere with an associated decrease in its temperature. The ejected gases also react to the transient change in the temperature of the photosphere which explains the observed correlations at the secondary maxima. The deep minimum in the transition phase exhibited by some slow novae (see Figure 1) was suggested to be due to dust formation in the ejecta (McLaughlin, 1935, 1937b) or presence of molecules (Stratton, 1945). However the dust explanation was favoured since molecular lines had seldom been detected in the nova spectra. The recovery of the light curve was taken to be indicative of dispersion of the dust so that the obscuring agent had disappeared. McLaughlin (1943) ends his model exposition by stating ‘Greater radiation pressure at the higher temperature may be suggested tentatively as a possible cause of the velocity-magnitude correlation.’ McLaughlin (1941) also inferred that novae were hottest during the final decline at a few magnitudes above quiescence and that the nebulous shell contributed to the light curve from about six to nine magnitudes below maximum.

This model was comprehensive and could explain most of the optical observations. A schematic which summarises some points of this model is shown in Figure 4.

## 2.4 White dwarf primary

The existence of massive objects (white dwarfs) whose gravity is balanced by the pressure of degenerate electrons was first suggested by Fowler (1926) and a detailed theoretical treatment which resulted in an upper mass limit for white dwarfs was derived by Chandrasekhar (1931). A white dwarf consists of two distinct parts - a degenerate core surrounded by a shallow layer of non-degenerate matter which obeys the ideal gas laws and has a thickness of  $\sim 10\%$  of the core radius (Chandrasekhar, 1939). The degenerate electron gas will have a high kinetic temperature ( $10^7 - 10^8$  K) when it is formed. The high conductivity of this degenerate electron gas ensures that the core is isothermal. A white dwarf will radiate, cool and finally settle down as a black dwarf at zero temperature unless there is an additional source of energy. The cooling has no effect on the degenerate electron pressure which will continue to support the gravity of the black dwarf. The cooling timescales for isolated white dwarfs are estimated to be of the order of billions of years due to radiative losses occurring from the cooler non-degenerate layer. The white dwarf would have cooled considerably faster if the hot degenerate core was radiating at 100 million K. The non-degenerate layer can contain hydrogen, helium and other metals leftover from the earlier phase of evolution of the white dwarf. A steep radial gradient in the temperature of this shallow layer has been determined so that the surface temperature is much lower than the core temperature (Marshak, 1940). It was surmised that the core was bereft of hydrogen and helium and the energy source of white



dwarfs was not thermonuclear in nature otherwise their lifetimes would be much shorter than has been estimated (Marshak, 1940). If hydrogen or helium were present in the core, then the high temperatures therein ( $\geq 10^8$  K) would instantly lead to a thermonuclear explosion which in turn would lift the degeneracy (Mestel, 1965). Marshak (1940) estimated a core temperature of  $1.5 \times 10^7$  K, surface temperature of  $9 \times 10^5$  K and a radius of  $5.7 \times 10^8$  cm for the white dwarf Sirius B. The radius he estimated was discrepant by a factor of two with the observational estimate of  $13.6 \times 10^8$  cm by Kuiper. It was difficult to understand the discrepancy which was tentatively attributed to a larger non-degenerate accreted envelope around Sirius B which is in a binary. This issue was resolved when new observations modified the radius of Sirius B to a value smaller by a factor of two (Greenstein et al., 1971) which matched the theoretical value estimated by Marshak (1940). The surface temperature of Sirius B was measured to be 32000 K (Greenstein et al., 1971) which was much lower than the value estimated by Marshak (1940). Surface temperatures of white dwarfs in cataclysmic variables have been determined to span a wide range - 8500 to 50000 K (Sion, 1999).

An accreting white dwarf can accumulate a hydrogen-rich surface layer in which thermonuclear reactions can ignite if its temperature rises and which is not improbable since the internal temperature of the white dwarf is very high (Mestel, 1965). If the temperature in the surface layer increased to  $2 \times 10^8$  K then the hydrogen within would explosively ignite via the Bethe cycle especially if trace amounts of carbon, nitrogen and oxygen are present (Bethe, 1939). In the CNO (Bethe) cycle, the liberated energy is a very sensitive function of temperature since the nitrogen reaction (capture of protons by  $N^{14}$  which is the main process in which energy is liberated) depends very strongly on temperature ( $\propto T^{18}$ ) (Bethe, 1939). Thus the energy production rises steeply with temperature. The thermonuclear reaction when the temperature rises beyond  $10^8$  K can be explosive and all the hydrogen can be transmuted into helium in matter of seconds releasing huge quantities of energy which can eject the overlying layers of matter to infinity (Mestel, 1965). We now know that this summarises the nova explosion. On the other hand, the energy production also drops rapidly as the temperature decreases.

Novae are semi-detached binaries and by definition the companion star fills its Roche lobe and hence the size of the companion star gives an idea of the binary separation. The separation and orbital period are larger when the companion star is a red giant of radius  $\sim$  an astronomical unit as compared to when it is a main sequence star of radius  $\sim R_\odot$ . For a mass ratio of one i.e. both the white dwarf and the companion are of the same mass (say  $\sim M_\odot$ ) and for a typical binary separation of  $1 R_\odot$ , the Roche lobe extent will be  $0.207R_\odot$  and the product of the orbital period  $P$  and density of the outer parts of the companion star  $\rho$  will be  $P\sqrt{\rho} = 0.4168$  (Eggleton, 1983). For a typical orbital period  $P = 0.25$  days, the density will be  $\rho = 2.8 \text{ gm cm}^{-3}$ . For a red giant com-

panion with same mass ratio and a binary separation of  $100 R_\odot$ , the Roche lobe extent will be  $20.7R_\odot$  (Eggleton, 1983) and for an orbital period of 300 days will result in density  $\rho = 1.9 \times 10^{-6} \text{ gm cm}^{-3}$ . The densities in the outer parts of a main sequence star of a solar mass will be a million times larger than in the outer parts of a red giant star of the same mass. The implication for novae would be that the white dwarf is likely to be immersed in a higher density ambient medium with a main sequence companion as compared to a red giant companion which could also have some implications on the accretion rates.

Accretion of matter on the white dwarf will release gravitational energy which can also contribute to the heating of the accreted hydrogen-rich matter. The combination of internal temperature of the white dwarf, gravitational energy and compression of the accreted matter will contribute to the heating of the accreted layer on the white dwarf.

### 3 The updated model for novae

The last section was mainly based on optical observations where sufficient data had been collected and analysed to warrant a model. We now have at our disposal, data on novae at wavebands ranging from  $\gamma$ -rays at the high frequency end to radio waves at the low frequency end of the electromagnetic spectrum which arise due to different physical processes in the nova. These can, hence, be used to modify and update the existing model. Here we put forward a modified physical model based on the multi-band detections. Before we embark on updating the nova model, we begin with a discussion on accretion of matter by a white dwarf and formation of an accretion disk alongwith other associated changes in the system expected from basic physical considerations. This is included here because this explanation deviates significantly from the standard explanation given for the formation of accretion disks in literature. Moreover formation of bipolar outflows have continued to intrigue us with our understanding being limited to some connection with an accretion disk. The following discussion is valid for any accreting massive object.

#### 3.1 Accretion disk, accreted envelope, bipolar/ellipsoidal ejecta

The existing model attributes the formation of a rotating accretion disk around a massive object to the angular momentum carried by the infalling matter. It is believed that the accretion disk facilitates the loss of angular momentum for the particle prior to being accreted on the white dwarf. This means that the formation of the accretion disk does not depend on the rotation of the accretor and will form around both rotating and non-rotating accreting objects. In this case, one would expect the rotation axis of the accretion disk to be oriented along the angular momentum axis of the incoming matter and all the matter should have the same angular momentum axis to be able to form

a massive accretion disk. This means that the accretion disk should have a rotation axis which should bear no relation to the rotation axis of the accretor and hence the two axes should be rarely aligned. However observations give contrary results that the accretion disk is predominantly formed in the equatorial plane of the accretor and shares its rotation axis. While one can invent several explanations for this, it should be borne in mind that such a strong correlation suggests a significant role of the accretor in the formation of the accretion disk but which seems to have been largely ignored in literature. Additionally it appears contrived to suggest that all the infalling particles have the same spin axis. While a fixed angular momentum axis would be expected if a massive object like a star remained intact while being accreted, most of the accretion is of particles which are likely to have a random spin axis and this is especially true of a white dwarf in a nova. These appear to be major irreconcilable problems with the existing theory used to explain the formation of the accretion disk. Unless we can understand it, preferably in the purview of known physics, it will remain a bottleneck in furthering our understanding of any accretion-related phenomenon. It is likely that a physical understanding of this process will also lead to the resolution of several other perplexing observables. We, hence, examine the physics which should dictate the formation of an accretion disk.

Rigid rotation of a gravitating spherical object of radius  $R$  modifies the effective attractive potential felt by the infalling matter. While at the poles the effective potential will be equal to the gravitational potential, the combined effect of gravitational and centrifugal forces in the non-polar regions will lead to a latitude-dependent effective potential such that the attractive potential is lowest at the equator where the effect of the centrifugal force is maximum. This indicates that within a given time, more matter should fall in at the poles than at the equator i.e. a latitude-dependent accretion rate should be set up such that it is maximum at the poles and minimum at the equator. The extent of the accreted envelope will be proportional to the accreted mass and hence the larger accretion rate at the poles will lead to the formation of a prolate-shaped envelope (see Figure 5). For a uniform rate of infall around the object, the matter in the non-polar regions will accumulate outside the object due to the lower accretion rates. This matter should form the accretion disk. An accretion disk, thus formed, should have the largest radial extent at the equator where the accretion rates are lowest and it will taper down towards the poles. The thickness of the accretion disk should depend on the rotation speed of the object so that it will be thick for a fast rotating object and thin for a slowly rotating object. The matter in the accretion disk will be dragged along by the gravitating object and will start rotating. Thus around an accreting rotating body, the formation of an accretion disk and a prolate-shaped envelope are unavoidable although the extent, thickness of the accretion disk and the ellipticity of the envelope will depend on the rotation speed of the object. Significantly, formation of the accretion disk has no dependence on the angular momen-

tum of the infalling matter. In fact considering that the matter being accreted can have different spin axis, if at all, it does appear far fetched to attribute the formation and rotation of the accretion disk to the angular momentum of the infalling matter. *To summarise, a rigidly rotating accreting body will set up a latitude-dependent accretion rate with maximum rates at the poles and minimum rates at the equator. This will result in a prolate-shaped envelope which in the extreme case can be bipolar. The low equatorial accretion rates lead to matter accumulation in the non-polar regions forming an accretion disk which is dragged along by the accretor's rotation. This, then, explains the formation of accretion disks and prolate-shaped envelopes/outflows around compact massive objects. Both require that the accretor is rotating.*

The outwardly directed centrifugal force acting on a particle of mass  $m$  on the surface of the object at a latitude  $i$  will be  $F_{c,i} = mv_i^2/r_i$  and since for a rigidly rotating body  $v_i = r_i\omega$ , it follows that  $F_{c,i} = mr_i\omega^2$ .  $\omega$  is a constant and  $r_i$  is the radial separation between the rotation axis and a point on the accreting body at latitude  $i$  hence the centrifugal force varies as  $r_i$ .  $r_i = R$  at the equator whereas  $r_i = 0$  at the poles which quantifies the varying centrifugal force as a function of latitude and hence the varying effective potential that a particle at different latitudes would experience. The gravitational force is the same over the entire surface of radius  $R$ .

In a spherically accreting non-rotating white dwarf, matter should be accreted at the same rate over the entire surface and a spherical envelope around the white dwarf can be expected (see Figure 5). No accretion disk will form.

We summarise the effect of rotation and accretion on compressible and incompressible objects. If in a compressible object, rotation has led to an originally spherical object evolving to a prolate-shaped ellipsoid then the accretion rate across the entire object will be constant. This will lead to the formation of a prolate-shaped envelope on the object mimicking the shape of the object, but no accretion disk will form. In an incompressible object, rotation cannot modify the shape of the object and it will remain spherical but the effective potential across the surface will vary with latitude. The accretion rates will also be a function of latitude with highest rates at the poles. This will lead to the formation of a prolate-shaped ellipsoidal envelope around the object. The lower accretion rates at the equator will lead to accumulation of the infalling matter in an accretion disk. Thus in an incompressible object which cannot be distorted, rotation and accretion will lead to the formation of a prolate-shaped envelope and an accretion disk.

An instability, at the base of the accreted envelope on a white dwarf, which injects copious amounts of energy into the envelope can lead to its ejection. For a non-rotating white dwarf the spherical envelope will form a spherical ejecta while for a rotating white dwarf the prolate-shaped envelope will be observed as a prolate ellipsoidal ejecta. A bipolar ejecta will be an extreme case of a prolate-shaped ejecta and would indicate a fast-rotating white

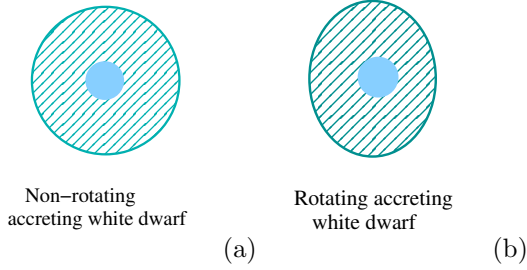


Figure 5: Schematic showing the effect of rotation on the morphology of the accreted envelope. (a) a non-rotating white dwarf will accrete a spherical envelope around it and a nova outburst will result in a spherical ejecta. (b) A rotating white dwarf will accrete a prolate-shaped envelope around it and a nova outburst will result in an elliptical ejecta.

dwarf wherein most of the mass has accumulated at the poles due to extremely low accretion rates at the equator. Ellipsoidal ejecta have been observed in several novae such as DQ Herculis, HR Delphini while there are also novae whose bipolar emission morphologies in early times evolved to spherical morphology at later times (e.g. RS Ophiuchi). The presence of an accretion disk could influence the morphology and speed of mass ejection in the non-polar regions. An accretion disk might quench the outburst in the equatorial regions either through its disruption or by absorbing the ejecta energy, in either case, slowing down the ejecta in the equatorial regions. Faster polar expansion has been noted in nova ejecta e.g. HR Delphini. These are secondary observable effects.

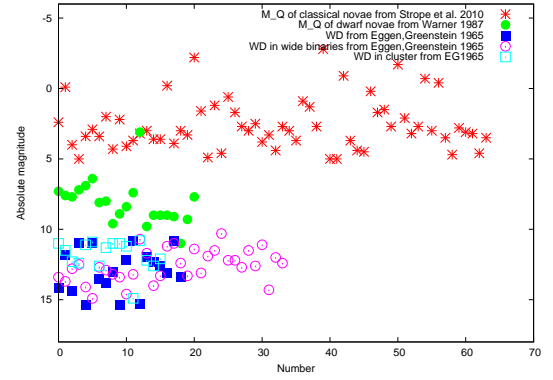
The main inferences derived in this section are: (1) Accretion disks are formed around accreting rotating white dwarfs and their formation is triggered by the latitude-dependent effective potential that the infalling matter experiences which leads to low equatorial accretion rates. The formation of the accretion disk has no dependence on the angular momentum carried by the accreted material (2) detection of a bipolar ejecta/jets indicates the presence of a prolate envelope which indicates a rotating white dwarf.

We now discuss novae in quiescence and in outburst where the above discussion will be useful.

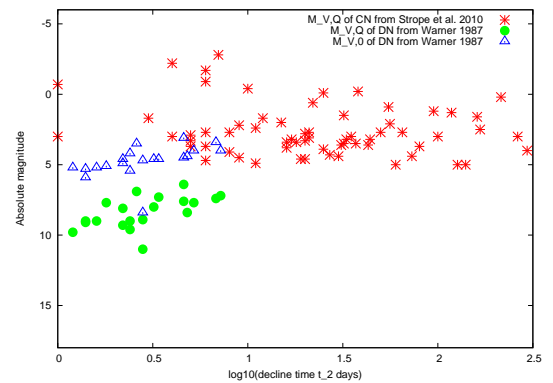
### 3.2 Novae in quiescence

We begin by examining properties of novae in quiescence which will be dictated by the binary components. These can help us better understand the equilibrium configurations of the white dwarf and the companion star which would then result in an initial condition for the outburst.

The quiescence absolute magnitude in the V band  $M_{V,q}$  of classical, recurrent, dwarf novae and of isolated white dwarfs are plotted in Figure 6a with data on novae taken from Strope et al. (2010), Warner (1987) and on white dwarfs from Eggen & Greenstein (1965). In Figure 6b, the data on novae are plotted as a function of the decline time and data on the outburst peak  $M_{V,0}$  of dwarf



(a)



(b)

Figure 6: (a) Figure shows the absolute magnitudes of classical novae, dwarf novae in quiescence and white dwarfs. (b) The quiescence magnitudes of classical novae and dwarf novae and outburst maximum of dwarf novae are plotted as a function of the decline time  $t_2$ . The required data have been taken from Strope et al. (2010) Warner (1987), Eggen & Greenstein (1965), Kantharia (2017).

novae are also included. The  $M_{V,q}$  of classical novae are estimated from the difference between the peak absolute magnitude ( $M_{V,0}$ ) determined using the MMRD calibration in Kantharia (2017) and the outburst amplitude (and  $t_2$ ) taken from Strope et al. (2010). The three different symbols used to denote  $M_V$  of white dwarfs in Figure 6 indicate the different methods used to determine the distance by Eggen & Greenstein (1965) based on the environment of the white dwarf. Trigonometric parallaxes for isolated white dwarfs, wide binary and Galactic cluster membership is indicated by the different symbols. A few inferences can be drawn from Figure 6: (1)  $M_V$  of white dwarfs is significantly lower than  $M_{V,q}$  of novae especially classical and recurrent novae (2) the  $M_{V,q}$  of dwarf novae is systematically lower than that of classical novae. The outburst peak luminosity of dwarf novae merges with the  $M_{V,q}$  of classical novae as seen in Figure 6b and (3)  $M_{V,q}$  of classical novae shows no dependence on the decline time unlike dwarf novae.

The mean quiescent absolute magnitude of classical novae is  $\langle M_{V,q} \rangle = 2.59 \pm 0.23$  magnitudes, for dwarf novae is  $\langle M_{V,q} \rangle = 8.37 \pm 0.25$  magnitudes whereas the mean outburst peak luminosity of dwarf novae is  $\langle M_{V,0} \rangle = 4.75 \pm 0.25$  magnitudes. The absolute magnitudes of white dwarfs were found to divide into two types with one type following the relation  $M_V = 11.65 + 0.85(U - V)$  magnitudes and another fainter population following a relation which is steeper (Eggen & Greenstein, 1965). The quiescent luminosity of the system is a combination of the white dwarf and the companion star and hence is expected to be brighter than an isolated white dwarf. Since both classical and dwarf novae are semi-detached binaries in most cases hosting either a late type main sequence star or sub-giant or giant companions, one would have expected similar distribution of quiescence luminosities. The observed difference in their quiescence brightness is, hence, perplexing and needs to be understood since it indicates differences in their equilibrium physical properties. We note that a few classical novae like GK Persei 1901 now undergo dwarf nova outbursts. The secondary star in GK Persei is a sub-giant of type K2IV type (Sherrington & Jameson, 1983) and the system has a  $M_{V,q} = 4$  magnitudes for a distance of 337 pc (Warner, 1987). A K0 subgiant is expected to have an absolute magnitude of +3.2 magnitudes (Allen, 1973) indicating that in GK Persei, the companion star likely dominates the combined luminosity. In other cases like V446 Her, the system showed dwarf nova-like eruptions a few years before the classical nova outburst (Robinson, 1975). These results also argue for similar binary components in dwarf novae and classical novae and hence the distinct distribution of their quiescence magnitudes is puzzling. We note that literature tends to attribute luminosity changes in novae at times other than outburst to the companion star suggesting that the luminosity of the nova in quiescence is dominated by the companion star. We investigate this further.

The companion stars in novae have been identified to be either late main sequence or subgiant or giant stars. Most systems host a faint main sequence companion as inferred from their short orbital periods of a few hours and the difficulty encountered in detecting their spectroscopic or photometric presence. It is easier to detect a subgiant or red giant companion. The visible band absolute magnitude of main sequence stars of types G0 to M0 range from +4.6 to +9 magnitudes (Allen, 1973). A sub-giant of spectral type K0 is expected to have  $M_V = +3.2$  magnitudes. A main sequence star of spectral type F0 to F5 will have  $M_V$  of +2.6 to +3.4 magnitudes (Allen, 1973). The  $M_{V,q}$  of most classical novae lie between 0 and 5 magnitudes (Figure 6). If the observed  $M_{V,q}$  of the novae is dominated by the companion star then in classical novae, the companion stars have to be main sequence or subgiant stars of types A0 to G4 or giants while in dwarf novae the companions can only be main sequence stars of types K7 and later. While this is possible, such a difference seems not to have been noticed and also seems to be difficult to reconcile with the observed duality of a few novae in showing both dwarf nova and classical nova

outbursts. We could not find a study devoted to this aspect of novae in literature. It would be useful to examine data for any systematic difference between the companion stars in classical and dwarf novae. For the current study, we suggest that the distinct  $M_{V,q}$  of classical and dwarf novae with statistically similar types of companion stars argue for differences in the properties of the white dwarf.

The  $M_{V,q}$  of recurrent novae plotted in Figure 6 show the largest values - for example, RS Ophiuchi has  $M_{V,q} \sim -2.8$  magnitudes, T CrB has  $M_{V,q} \sim -1.7$  magnitudes, U Sco has  $M_{V,q} \sim -0.7$  magnitudes and T Pyx has  $M_{V,q} \sim 0.1$  magnitudes. The companion stars in the four cases have been identified to be a red giant, red giant, sub-giant and a main sequence star respectively. So while it appears that the companion star could dominate the quiescent luminosity in case of RS Oph, T CrB and U Sco it would need to be a hot late B type star in case of T Pyx to explain its large minimum luminosity. Since the companion star in T Pyx is deduced to be a low mass main sequence star like the sun, it suggests that the quiescent brightness of the system might be because of a brighter-than-usual white dwarf. Thus while the quiescence luminosity, in some cases, is indeed dominated by the companion star, it is not universally the case. This supports our earlier conclusion that the accreting white dwarfs in novae can have different properties which contribute to the luminous quiescent states.

We now examine the contribution of the white dwarf to the quiescent luminosity of novae. Classical novae appear brighter by  $\geq 8$  magnitudes than an isolated white dwarf. We recall that a white dwarf consists of a degenerate core surrounded by a thin layer of non-degenerate matter. While the radius of the degenerate core will shrink with increasing mass, the non-degenerate layer will expand with increasing mass. Thus, an accreting white dwarf will increase the thickness of the layer of non-degenerate matter (see Figure 7) as it accretes matter from the companion star. The increase in the radial extent of the outer layer should be accompanied by a drop in surface temperature assuming there is no change in the heating source. However it should be kept in mind that the gravitational energy released due to accretion would contribute to heating the non-degenerate layer as will compression in the lower layers. Thus, two important differences in an accreting white dwarf is a larger envelope and a lower surface temperature. Assuming the white dwarf emits as a black body, the bolometric luminosity can be estimated as  $L_b = 4\pi R^2 \sigma T^4$  where  $T$  is the surface temperature,  $R$  is the radius of the white dwarf and  $\sigma = 5.67 \times 10^{-8} \text{ W m}^{-2} \text{ K}^{-4}$  is the Stefan-Boltzmann constant. To convert the luminosity to the magnitude scale we use  $L_\odot = 3.826 \times 10^{26}$  Watts and 4.75 magnitudes (Allen, 1973) as the bolometric absolute magnitude of the sun in the formula  $M_b - M_\odot = -2.5 \log_{10} L_b / L_\odot$ . The bolometric correction (BC) which is a function of the temperature is then used to convert this to V band magnitude i.e.  $M_V = M_b - BC$ .  $BC = -0.08$  for the sun giving  $M_V = 4.83$  magnitudes (Allen, 1973). For a typical isolated white dwarf of  $R = 6000$  km and temperature of

$10^5$  K,  $L_b = 2.56 \times 10^{27}$  Watts and  $M_b = 2.69$  magnitudes. For  $10^5$  K,  $BC = -7$  (Allen, 1973) which gives  $M_V = 9.69$  magnitudes. A white dwarf with  $R = 6000$  km and  $T = 10^4$  K will have  $M_V = 13.04$  magnitudes since  $BC = -0.36$  (Allen, 1973). While the hotter white dwarfs can explain the minimum luminosity of dwarf novae when not dominated by the companion star, none of the white dwarfs with surface temperature between  $10^4$  to  $10^5$  K and radius of 6000 km will be bright enough to explain the  $M_{V,q}$  of classical novae. We now include the effect of an inflated envelope due to accretion. An expanded envelope of surface temperature  $10^4$  K and  $R = 10 \times 6000$  km  $\sim 0.1R_\odot$  will result in a much brighter  $M_V = 8.04$  magnitudes as compared to  $M_V = 13.04$  magnitudes estimated for a white dwarf of radius 6000 km. A larger increase in the size of the accreted envelope would then result in a still more luminous white dwarf in a classical nova. This result which follows from incorporating the expected effect of accretion of matter on the white dwarf prompts us to suggest that the differences in the  $M_{V,q}$  of classical and dwarf novae are due to the differing extents of the accreted envelopes around the white dwarf. The accreted envelope is smallest in an isolated white dwarf, larger in a dwarf nova and largest in a classical nova (see Figure 7). This could, amongst other factors, reflect the different accretion rates that have been surmised for a dwarf nova (lower) and a classical nova (higher). The argument can be taken further to be suggestive of still larger envelopes in recurrent novae which have higher accretion rates than most classical novae. We recall that to explain the luminosity of old novae, McLaughlin (1941) estimated a radius of  $0.1R_\odot$  and density of  $1000\rho_\odot$  for the nova star using similar arguments. However this preceded the identification of the binary nature of novae and the white dwarf as the primary star. In fact, ironically these physical parameters were the reason that a white dwarf was ruled out as a nova star. We find ourselves arriving at similar dimensions for the white dwarf but with the added knowledge that these are accreting white dwarfs in close binaries which support the existence of such inflated lower density envelopes on white dwarfs.

While most novae show similar pre-nova and post-nova luminosities, there do exist a few cases wherein they differ. We suggest these can be attributed to changes in the size or temperature of the accreted envelope. For example, V533 Her recorded  $m_V = 14.2$  magnitudes well before the outburst which brightened to 12 magnitudes over a 2 year period before it exploded as a classical nova in 1963 (Robinson, 1975). A possible explanation, which needs to be verified, is that the brightening in the pre-nova phase was caused by an increase in the radius of the envelope attributable to enhanced radiation pressure exerted by an increase in the temperature at the base of the envelope. The possibility of an increase in the luminosity of the white dwarf before a classical nova outburst has been considered in literature (e.g. Warner, 1987). In the cases where the post-nova is brighter than the pre-nova, it could indicate that the white dwarf in the post-nova has not yet declined to its pre-nova luminosity. This could then be attributed

Table 2: T denotes the surface temperature of the white dwarf, R denotes the radius of the white dwarf in units of  $R_{WD} = 6000$  km,  $L_b$  denotes the bolometric luminosity in units of  $L_\odot$ .  $M_{V,\odot} = 4.83$  magnitudes is used. Note how the white dwarf brightens as the accreted envelope increases in size.

<b>T</b> K	<b>R</b> $R_{WD}$	<b><math>L_b</math></b> $L_\odot$	<b><math>M_b</math></b> mag	<b><math>M_V</math></b> mag
$10^4$ (BC= -0.36)	1	0.00067	12.68	13.04
	10	0.067	7.68	8.04
	20	0.27	6.17	6.53
	100	6.75	2.68	3.03
	$10^4$	$6.75 \times 10^4$	-7.32	-6.96
$10^5$ (BC=7)	1	6.67	2.69	9.69
	2	26.7	1.18	8.18
	4	106.8	-0.32	6.68
	10	667.5	-2.3	4.69

to the higher temperature of the post-nova white dwarf following the outburst. Thus, we find that changes in the accreted envelope around the white dwarf can explain observations.

To quantify the above, we list the expected V band absolute magnitudes of white dwarfs for combinations of its surface temperature  $T$  and radius  $R$  estimated using the Stefan-Boltzmann law assuming black body emission from the white dwarf in Table 2. Two surface temperatures of  $10^4$  K and  $10^5$  K are used and most white dwarfs in cataclysmic variables have been noted to have temperatures between 8500 K and 50000 K (Sion, 1999) so the two values for which we estimate the emission from white dwarfs define the lower and upper limits. We estimate the bolometric luminosity for white dwarf radius ranging from  $R_{WD}$  to  $10^4 R_{WD}$  where  $R_{WD} = 6000$  km for  $T = 10^4$  K and for radius ranging from  $R_{WD}$  to  $10R_{WD}$  for  $T = 10^5$  K. This is done keeping in mind that the temperature of the white dwarf stripped of its accreted envelope in an outburst will be higher. The post-outburst white dwarf will be hotter as also been observationally found and the remaining envelope will be much smaller since the quiescent state envelope would have been ejected (see Figure 7). If the envelope is made very large then the temperature is likely to reduce or it will become optically thin and not emit as a black body. Thus for the higher temperature we only consider radius upto  $10R_{WD}$ . Some of the inferences we can draw from the table are: (1) For a white dwarf with radius of  $R_{WD} = 6000$  km,  $M_V$  will lie between 13.04 to 9.69 magnitudes for surface temperature between  $10^4$  K and  $10^5$  K. We note that this encompasses the range of observed absolute magnitudes of isolated white dwarfs. (2) The quiescent mean  $M_V$  of dwarf novae can be explained by a white dwarf of  $T \sim 10^4$  K with an envelope of radius  $< 10R_{WD}$  or  $T \sim 10^5$  K with envelope of radius  $< 2R_{WD}$ . It appears that the white dwarf in a quiescent dwarf nova has temperature ranging from about  $10^4$  K to  $10^5$  K and a radius of the accreted envelope ranging from a few  $R_{WD}$  to  $R_{WD}$ . (3) Classical novae in quiescence have an envelope with radius

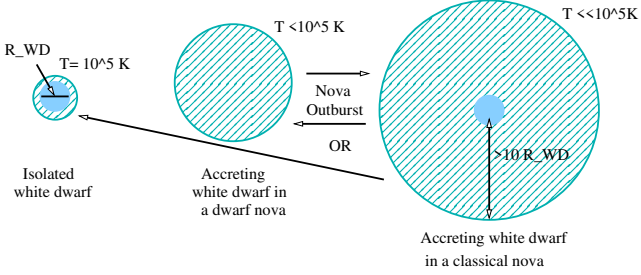


Figure 7: Schematic comparing the varying sizes of the accreted envelopes around an isolated white dwarf (left) and accreting non-rotating white dwarfs in a dwarf nova (middle) and classical nova (right) in quiescence. It also pictorially demonstrates our suggestion that the white dwarf in dwarf nova (middle) has a smaller envelope than a classical nova (right). The envelope size following an outburst in either might resemble the other since dwarf nova inflates its envelope whereas a classical nova ejects it. Alternatively classical nova can eject the entire envelope and resemble an isolated white dwarf for a short time before accretion restarts.

$\geq 10R_{WD}$ . If the surface temperature is low ( $\leq 10^4$ ) then the envelope can even be  $\geq 100R_{WD} \sim R_{\odot}$ . Since the accretion rates in dwarf novae are lower ( $\sim 10^{-10}M_{\odot}\text{yr}^{-1}$ ) compared to classical novae ( $\sim 10^{-8}M_{\odot}\text{yr}^{-1}$ ), this might be one of the causes for the different envelope dimensions. However there could also be other factors. If the accreted mass distributed in an envelope of radius  $100R_{WD}$  on the white dwarf is  $10^{-5}M_{\odot}$  then the hydrogen number densities will be  $\geq 10^{16}\text{cm}^{-3}$ . The discussion here assumes spherical accretion on a white dwarf which leads to the formation of a spherical/ellipsoidal envelope and ignores the contribution of the accretion disk to the luminosity of the white dwarf.

Old novae which contain an accreting white dwarf were expected to be strong emitters of soft X-rays. Observations have shown otherwise so that most old novae rarely emit X-rays and if X-rays are occasionally detected they are generally with energies  $> 5$  keV, (e.g. Cordova et al., 1981; Ferland et al., 1982). We find that this result is as expected from the discussion above wherein the cool accreted envelope will hide the hot X-ray emitting surface of the white dwarf and no soft X-rays should be detectable from the nova in quiescence. In an outburst the cool envelope is ejected exposing a hot surface with a temperature  $\geq 10^5$  K which will emit soft X-rays explaining their detection during an outburst.

There are other observational results which support the establishment and existence of inflated envelopes around the accreting white dwarf in quiescent novae. For example, a decrease in excitation was noted towards the end of the final decline in the light curve in a few novae like Nova Aquilae 1918, Nova Cygni 1920 and it was suggested that the last 1-1.5 magnitudes decline in the light curve is due to the lowering of the temperature of the superficial layers of the star (McLaughlin, 1953). In Nova Gemino-

rum 1912, observations indicated a decrease in excitation about 21 years after outburst and observations showed that the excitation definitely declined between 1917 to 1933 (McLaughlin, 1953). The luminosity of Nova Gemino- rum 1912 was found to decrease alongwith the decreasing excitation so that the apparent magnitude was 11.3 in 1914, 12 in 1916 and 14.5 magnitudes in 1933 (McLaughlin, 1953). It is also deduced that the excitation in RS Ophiuchi is lower in the inter-outburst period than near the end of the decline from maximum (McLaughlin, 1953). The B - V colour of DQ Herculis indicated a temperature of  $\sim 10^4$  K for the star (Walker, 1956) and a radius of  $0.1R_{\odot}$  has been estimated (McLaughlin, 1960b). All these results support the formation of a lower density cooler envelope of several times the radius of the core on the white dwarf and changes in its physical properties especially radius and temperature.

### 3.2.1 Eclipsing novae

We estimate the luminosities of the binary members from the quiescence light curve of a white dwarf in a few eclipsing systems. The main assumptions in doing so are that the primary eclipse is total and that the white dwarf is eclipsed by the secondary star. The former assumption will introduce some errors in the luminosities if the eclipse is partial. Higher order emission lines of the Balmer series in hydrogen which are detected in the non-eclipsing spectrum of DQ Herculis disappear during the eclipse (Walker, 1956). Since high excitation lines are associated with the white dwarf, such results indicate that the primary eclipse is due to the occultation of the white dwarf by the companion star. Moreover the 71 second light modulation observed in DQ Herculis and deduced to be indicative of the rotation period of the white dwarf vanishes during part of the primary eclipse (Walker, 1961). Thus both assumptions are reasonable. The method we use is as follows. We estimate the peak absolute magnitude  $M_{V,0}$  of the classical/recurrent nova outburst using the MMRD calibration of Kantharia (2017) and then use the amplitude of the outburst  $A_n$  and estimate the quiescent absolute magnitude of the nova  $M_{V,q}$ .  $t_2$ ,  $A_n$  and the observed eclipse depth  $\Delta m$  of the novae are taken from literature. The luminosity of the nova at deepest point of the primary eclipse will correspond to the luminosity of the secondary star. This is estimated from the difference between  $M_{V,q}$  and  $\Delta m$  (see Table 3). Magnitudes are converted to the luminosity scale from  $M_V - M_{V,\odot} = -2.5\log_{10}L_V/L_{V,\odot}$ . The V band magnitude of the sun  $M_{V,\odot}$  is 4.83 magnitudes and  $L_V$  is estimated in units of  $L_{V,\odot}$ . The luminosities of the nova and secondary star are determined and their difference corresponds to the luminosity of the white dwarf which can be converted to the magnitude scale as above. The resultant absolute magnitudes of the binary components are listed in Table 3. The white dwarf and the companion star are of comparable V band luminosities. Both the components of the recurrent nova U Scorpii are bright whereas both components of the dwarf nova U Geminorum are faint. In most cases, the white dwarf is the brighter member of the

Table 3: Estimating the absolute magnitude of the white dwarf and companion star using the eclipse depth  $\Delta m$  under the assumption of complete occultation of the white dwarf during the eclipse. Bolometric absolute magnitudes required for estimating radius of the white dwarf  $r_{WD}$  are estimated from  $M_{V,WD}$  using the bolometric correction at the two temperatures and it is assumed that the white dwarf emits like a black body.

Nova	$m_{V,q}$	$m_{V,0}$	$A_V$	$\Delta m$	$t_2$	$M_{V,0}$	$M_{V,q}$	$M_{V,sec}$	$M_{V,WD}$	$r_{WD}$ ( $R_\odot$ )	
	mag	mag	mag	mag	days	mag	mag	mag	mag	$10^4$ K	$10^5$ K
DQ Herculis 1934	15	1.4	13.6	$1.3^1$	67	-6.9	6.7	8.0	7.1	0.13	0.0008
U Scorpii*	17.6	7.5	10.1	$1.3^2$	1	-10.8	-0.7	0.6	-0.31	4	0.74
U Geminorum**	14.6	9.4	5.2	$0.7^3$	-	4.3	9.6	10.3	10.4	0.03	0.000038
V1494 Aql	17.1	4.1	13	$0.35^4$	8	-8.9	4.1	4.4	5.5	0.3	0.004
BT Monocerotis 1939	$15.4^5$	-		$2.7^5$	-	-	$4.0^5$	6.7	4.1	0.5	0.01

<sup>1</sup> From Walker (1956); <sup>2</sup> From Schaefer et al. (2010a); <sup>3</sup> From Krzeminski (1965); <sup>4</sup> From Kato et al. (2004);

<sup>5</sup> From Robinson et al. (1982); \* Recurrent nova; \*\* Dwarf nova

binary. We convert the  $M_V$  to the bolometric magnitude using the bolometric correction and estimate the radius of the white dwarf assuming it emits as black bodies at temperatures  $10^4$  K and  $10^5$  K. These are listed in the last two columns of Table 3 and inform us of the range of radius of the white dwarf required to explain its luminosity. It is clear that for temperatures between these two extremities, most of the white dwarfs in classical/recurrent novae require an inflated envelope to explain their brightness and the data on eclipsing novae have given strong support to the presence of these envelopes. As a next step, the measured surface temperatures of the white dwarf in eclipsing novae can be used to get a better estimate of the size of the envelope for particular novae. This seems to be one of the few methods, applicable only to eclipsing novae, available to us to study the physical properties of the binary components of a nova.

We move to the next section where we discuss novae in outburst and update the existing model. To summarize the initial conditions we start with: (1) The white dwarf in a nova is several times brighter than an isolated white dwarf and the main reason is attributed to the presence of an inflated accreted envelope. (2) One important difference between classical and dwarf novae is in the size of the accreted envelope explaining the difference in their quiescence luminosity. (3) Rotation of the white dwarf leads to the formation of prolate-shaped ellipsoidal envelope and equatorial accretion disks, both due to the latitude-dependent accretion rate.

### 3.3 Novae in outburst

In this section, we update the nova outburst model. It includes known and fresh aspects which coherently explain the outburst and the model is schematically summarised in Figure 8. We refer to Figures 1 and 2 for the observed changes in the light curve and spectra. To preserve continuity the known and fresh aspects of the model are not explicitly distinguished in the explanation but the expert should face no difficulty in identifying these. One can also refer to the details of the existing model in section 2. The updated model incorporates the knowns of a nova system namely that it consists of a binary with an accreting white dwarf and gaseous companion and when the physical con-

ditions in the accreted non-degenerate envelope of matter are appropriate, a thermonuclear runaway ignites and injects copious amounts of energy to the envelope leading to its expulsion. We first summarise some of the common observational features of a nova outburst mainly in the optical (already detailed earlier in the paper) which any model should self-consistently explain and then we address the different ill-understood aspects of the nova outburst which helps build the comprehensive model:

- Sudden optical brightening of a star and evolution of its light with time including peculiarities such as light oscillations and steep drop in the light curve.
- Continuously evolving optical spectrum of the star and simultaneous detection of the pre-maximum, principal, diffuse enhanced and Orion line systems with different velocity displacements and ionization/excitation levels.
- Correlated changes between the evolution of the optical light curve and spectrum shown by most novae.
- The existence of dominant Fe II or He/N spectral lines in the post-maximum spectrum.
- Detection of multi-band emission at particular times and durations with respect to the optical maximum.

The model can be summarised as follows: Accreted matter accumulates in an envelope around the white dwarf. The base of this envelope is compressed and heated. When it heats to  $\geq 10^8$  K, an explosive thermonuclear ignition of the hydrogen-rich normal matter exhausts the fuel in a short time and leads to an energy pulse. There appears no need to invoke degeneracy in this matter which is not likely to be present since the accreted matter will lie above the non-degenerate layer of matter that a white dwarf is born with. This energy can lead to the expansion of the same highly pressured layer and it can adiabatically transmit the energy to the overlying layers increasing the latter's internal energy which can be in the form of mechanical energy imparted to each chemical constituent/particle. Noting that the layer in which the explosion occurred will be at  $10^8$  K ( $T_h$ ) and the overlying layers will be much cooler at  $\leq 50000$  K ( $T_c$ ), the energy transfer efficiency based on



the Carnot cycle  $((T_h + T_c)/T_h)$  can be 99%. Thus most of the energy can be adiabatically injected into the overlying layers as mechanical energy, ejecting them to infinity and also imparting a random motion to all the particles therein. Depending on the total energy injection and mass which is ejected, each particle will acquire some random velocity component and a forward expansion component. While the forward motion component will necessarily have to be larger than the escape velocity of the white dwarf if the ejecta is to leave the system, the random velocity of the particle will be indicative of the remnant energy. The ejected matter consisting of electrons, atoms, ions will start expanding with similar velocities. Electrons can acquire random velocities which are relativistic in sufficiently energetic explosions. Sometimes the relativistic electrons can also precede the main ejecta. The nova and expanding ejecta give rise to multi-band emission. We explain in detail below.

**Optical emission from ejecta:** There exist several points of evidence which suggest that the sudden optical brightening of the nova is due to the increasing emission from the ejecta. In the short duration that the accreted envelope is getting energised by the burst of thermonuclear energy and before it is ejected, one can consider the photosphere as defining the outer boundary of the ejecta. Once the envelope is ejected, evidence suggests that the origin of the optical continuous emission like the line spectrum is in the ejecta and not in the photosphere of the white dwarf. The strongest evidence for the common origin of the optical continuous emission and spectral lines in the ejecta comes from (1) the inference that most novae follow the maximum magnitude relation with decline time (MMRD) wherein the maximum visible luminosity of the nova outburst is strongly correlated with the decline time of light and the ejecta velocity (also see Section 1) and (2) the correlated evolution of the optical light curve and line spectrum in a nova outburst. The simplest explanation for the observed nature of the light curve is that as the ejecta expands, the optical emission reaches a maximum when the optical depth drops to one and then the emission fades as the ejecta expands further and its emission measure declines. Slow novae expand at a slower rate than fast novae so the change in its emission measure (or density) is also gradual and the light curve continues to hover near the maximum for a longer time. A drop of two magnitudes in the peak V band luminosity would require the luminosity to change by a factor of 6.3 which will be due to a drop in the emission measure of the ejecta. A slow nova will take longer to achieve the drop than a fast nova if we assumed that similar masses were ejected. Thus the observed evolution of the light curve is trivially explained if it arises in the ejecta. *Thus we conclude that the optical continuous emission from the nova outburst is dominated by the ejecta near the maximum and weakens as the ejecta expands.*

We now discuss the optical emission from the ejecta and the light curve evolution. The typical temperatures of the white dwarf in cataclysmic variables has been measured

to be between 8500 K and 50000 K (Sion, 1999). The explosion will inject energy into this envelope and eject this hot material. Electron temperatures around 5000 – 10000 K are measured for the ejecta indicating that the outburst energy is sufficient to retain these temperatures and the ejecta starts to radiate in the optical and ultraviolet bands through the free-free and free-bound processes. The optical emission is observed to quickly (within a day or so) strengthen by several magnitudes before it is halted around two magnitudes below maximum. Some novae show a short plateau at this point and we suggest this is because the optically thick ejecta is shining entirely as a result of the energy input from the explosion. Around this time, radiation of the hot white dwarf will also start contributing to the physical state of the ejecta and to the light curve. The radiation field of the white dwarf can exert radiation pressure on the optically thick ejecta and once the ejecta is optically thin, the white dwarf can become optically visible through most of the ejecta and if it is optically brighter compared to quiescence, then it will contribute to the nova brightness in the optical band. We suggest that the white dwarf radiation contributes the final  $\leq 2$  magnitudes rise of brightness to optical peak in many novae. Thus, in some novae it might contribute as much as 2 magnitudes and in some novae, the white dwarf might not contribute anything especially if a large fraction of the ejecta continues to obscure the white dwarf radiation field. An increase by two magnitudes can be contributed by a post-outburst white dwarf which emits 6.3 times its quiescence optical luminosity. The brightness contribution to the light curve by the white dwarf, if any, will remain constant over a longer duration while the contribution by the ejecta will keep declining as it expands. This inference is supported by the observation that the colour temperature estimated from multifrequency optical light curves increases as the light curve declines i.e. the light gets bluer. If the fractional contribution of the cooler ejecta to the optical emission is reducing and that of the hot white dwarf is increasing, the colour should get bluer as is observed. The excitation of the expanding ejecta is constantly changing in the initial phases so that it resembles a hot B/A type star before the optical maximum and then evolves to later A/F types at/after maximum. These will be the combined effect of the explosion energy, expansion of the ejecta and the white dwarf radiation field.

**Generation of relativistic electrons:** The source of energy in a nova has been shown to be in a thermonuclear runaway reaction. When the temperature at the base of the accreted hydrogen/helium envelope rises to  $\sim 10^8$  K due to compression and accretion heating, then even the presence of trace amounts of carbon, nitrogen and oxygen can set up an explosive CNO reaction cycle (Bethe, 1939) which in a matter of seconds can burn the accreted hydrogen with the net reaction products being:  $4\text{H}^1 + 2e^- \rightarrow \text{He}^4 + 2\nu_e + 3\gamma + 26.7 \text{ MeV}$ .  $\nu_e$  are neutrinos and  $\gamma$  are  $\gamma$ -ray photons. The energy liberated in the CNO cycle is  $\propto T^{18}$  (Bethe, 1939). Since the proton-proton chain can ignite at lower temperatures, it could be



the process that happens in some novae, especially dwarf novae where the energy released is lower. The energy liberated in a proton-proton chain is  $\propto T^4$  i.e. is not so sensitive to temperature changes unlike the CNO cycle. This sudden energetic event will release copious quantities of neutrinos,  $\gamma$ -ray photons and heat energy. Since the observational properties of the pre-nova and post-nova are similar, the explosion does not affect the degenerate core of the white dwarf. The released particles are energised to velocities higher than escape velocity and erupt outwards from the white dwarf. The escape velocity from a white dwarf of mass  $0.5M_{\odot}$  and radius  $0.015R_{\odot}$  will be  $3600 \text{ kms}^{-1}$ , from a mass  $1M_{\odot}$  and radius  $0.01R_{\odot}$  will be  $6300 \text{ kms}^{-1}$  and from a mass  $1.3M_{\odot}$  and radius  $0.005R_{\odot}$  will be  $10200 \text{ kms}^{-1}$ . It appears likely that a thermonuclear burst is also the mechanism for a dwarf nova outburst but which only leads to expansion of the accreted envelope and not ejection. This origin can explain the observed light curves of dwarf novae which show a rapid rise, a flat top and then a gradual decrease - all accomplished within a month or so as being due to the expansion and subsequent contraction of the envelope. An outburst amplitude upto five magnitudes which is typical of dwarf novae is possible if the accreted envelope isothermally expands to  $\leq 0.1R_{\odot}$  which as discussed in the previous section will be similar to the extent of the envelope of the white dwarf in a quiescent classical nova.

All the matter in the envelope - atoms, ions, electrons is adiabatically energised by the thermonuclear energy which will result in two velocity components - an outward directed radial velocity and a random velocity. In classical novae, the envelope will detach once it acquires an outward velocity which is of the order of the escape velocity. If we assume equal energy is imparted to all particles and that all particles acquire similar expansion velocity then the electrons can acquire very high random velocities whereas the random velocity component will be smaller for the relatively heavier ions and atoms. It is also likely that the electrons can also acquire higher expansion velocities and we note that imaging observations of radio synchrotron emission seem to support this hypothesis wherein the radio synchrotron emission arises from a region ahead of the thermally emitting region which is the main ejecta. Since the mass ratio of a proton and an electron is 1846, the velocities can differ by a factor  $\leq \sqrt{1846} \sim 42$ . If the bulk ejecta velocity in a classical nova is  $v_{ej} = 3600 \text{ kms}^{-1}$  then each proton will acquire this velocity which translates to an energy of  $1.0368 \times 10^{-14}$  Joules per proton. The electrons will also be imparted this energy and it can be translated to a velocity using the relativistic formula for energy namely  $E_e = (\gamma - 1)m_e c^2$ . This gives  $\gamma = 1.127$ . Since  $\gamma = 1/\sqrt{1 - v_e^2/c^2}$ , this gives  $v_e = 0.4885c$ . If  $v_{ej} = 6300 \text{ kms}^{-1}$  then electrons have energy of  $\gamma = 1.3877$  and  $v_e = 0.8167c$  and if  $v_{ej} = 15000 \text{ kms}^{-1}$  then electrons can have energies of  $\gamma = 3.2$  i.e.  $v_e = 0.9499c$ . These  $\gamma$  factors could indicate the mean energy of the electrons or the highest energy and it is difficult to comment further on this. We can only say that electrons are ejected in a nova outburst with relativistic velocities especially for

large bulk expansion velocities. All nova ejections have been reported to expand with velocities  $< 15000 \text{ kms}^{-1}$  which could indicate that the electrons in a nova outburst have energies around  $\gamma = 3.2$ . The electrons are relativistic and can emit synchrotron emission in a magnetic field. This demonstrates that a population of relativistic electrons should be energised alongwith the main ejecta when expansion velocities are  $\geq 6500 \text{ kms}^{-1}$  and definitely for ejecta velocities  $> 10000 \text{ kms}^{-1}$  and these novae are likely to be synchrotron emitters. Since it has been noted in some novae that high velocities recorded before the pre-maximum halt decline rapidly; it should be kept in mind that there might be several novae in which the initial expansion velocities indicative of the outburst energy are sufficiently high to generate a relativistic electron population. Since few novae are detected in the initial rise phase which is extremely fast, it remains a difficult task to determine the original expansion velocity otherwise that would be able to predict the possible detection of radio synchrotron emission from the system. This explains the detection of radio synchrotron emission from the fast recurrent novae - RS Ophiuchi and V745 Scorpii both of which recorded early ejecta velocities  $> 10000 \text{ kms}^{-1}$ . We believe that radio synchrotron emission from nearby fast classical novae ( $v_{ej} \geq 10000 \text{ kms}^{-1}$ ) should be detectable immediately after the outburst since the foreground obscuration which delays the detection of radio synchrotron emission especially in recurrent novae is likely to be low. We note that since magnetic field is required it can either be frozen in the ejecta if the relativistic electron population is coexistent with the ejecta or an ambient medium in which the field is frozen is required for the electrons to radiate. In GK Persei 1901, the early ejecta velocities were recorded to be only  $1000 - 1500 \text{ kms}^{-1}$  but we detect radio synchrotron emission from its remnant even today indicating that the outburst was highly energetic and injected a relativistic electron population into the circumstellar medium. We do know that GK Persei exploded within its planetary nebula and the high ambient densities could have contributed to the rapid deceleration of the main ejecta which might have erupted at much higher velocities than recorded. This is suggested to explain the observed radio synchrotron emission. The nuclear reaction also emits  $\gamma$ -ray photons. While the photons released before the relativistic electrons have been ejected will leave the system, the photons emitted later can form the seed photon population which can be inverse Compton boosted to energies  $\geq 100 \text{ MeV}$  which have been detected from several classical novae. In a typical nova explosion which generates a relativistic electron population with  $\gamma \sim 3.2$ , detection of  $\gamma$ -ray photons of energy  $\geq 100 \text{ MeV}$  can be explained as being due to inverse Compton boosting of seed photons of energy  $\sim 7.3 \text{ MeV}$ . Since the CNO reaction will emit  $\gamma$ -ray photons of such energies, this explanation appears to be a plausible one for the origin of high energy  $\gamma$ -rays detected soon after the outburst. The duration over which these photons are detected then define the duration of the thermonuclear reactions on the surface of the white dwarf. Once the reaction dies down, low energy  $\gamma$ -ray photons

are extinguished and so are the  $\geq 100$  MeV photons. This is supported by the detection of  $\gamma$ -rays only for a few days near the optical maximum. *To summarise the discussion till now, we have pointed out that a relativistic electron population and hence synchrotron radio emission and energetic  $\gamma$ -rays are all expected from the explosive nuclear reaction on the surface of the white dwarf and there is no need to invoke any post-explosion shock acceleration.*

**Mass-based segregation in ejecta:** We shift our attention to the bulk ejecta and its evolution. The explosion energises and ejects the overlying layers and the expansion velocity has to be  $\geq$  escape velocity of the white dwarf. If all novae explosions release similar energies then a more massive envelope should acquire a lower expansion velocity while a lower mass ejection would be faster. However a detailed correlation is not expected since the energy released in the CNO cycle is a very sensitive function of temperature beyond  $10^8$  K ( $\propto T^{18}$ ) and which should lead to a range of values for the energy released in novae explosions. As mentioned in the previous item, if equal energy is imparted to each particle, it will result in a forward expansion velocity component and a random component. For particles of mass  $\geq$  mass of proton, the random velocity component appears to be a small fraction of the expansion velocity. Since hydrogen is generally the most abundant element in the ejecta, the average expansion velocity should be dictated by the velocity acquired by hydrogen atoms. Observations detect different line widths for emission lines of hydrogen (larger) and iron (smaller) which could indicate slightly different expansion velocities and which can cause the heavier atoms to lag behind in the ejecta. This, then, can lead to mass-based segregation in the main ejecta so that lower mass elements will lead while heavier elements will lag behind in the ejecta (see Figure 8). For simplicity, we assume that this rearrangement within the ejecta does not change the thickness of the ejecta which continues to be of the quiescent envelope size i.e. nominally  $\geq 0.1R_{\odot}$ . Within the main ejecta, the highest velocities are acquired by hydrogen atoms followed by helium atoms, carbon atoms, nitrogen atoms, oxygen atoms and so on.

Segregation, based on mass of the emitting atom, in the ejecta appears to be supported by the following observational results. Distinct line profiles are detected for different elements which suggests that various emitting species have distinct spatial distributions and/or there exist ionization gradients in the ejecta (e.g. Helton et al., 2012). Another point of support emerges from the different types of dust such as amorphous carbon, silicates and hydrocarbons which are detected in the same nova indicating abundance gradients within the ejecta (Evans & Gehrz, 2012). We discuss implications of such mass-based segregation and how it successfully explains several observational results which increases our confidence in such a phenomenon.

**Swept-up matter and Fe II, He/N lines in novae:** The ejecta is expanding with supersonic velocities and will

set up a shock and entrain (heat and accelerate) the matter it encounters on its expansion path. Thus, the spectral signatures from a nova after outburst can be a combination of the accreted envelope which is ejected, matter native to the white dwarf which is ejected and ambient matter which the ejecta sweeps up. While the spectra soon after outburst should be dominated by the lines from the accreted envelope which is ejected, there are likely to be signatures of the other two components. It might be difficult to differentiate these in many cases, but it does appear possible to occasionally separate this from their observational signatures. For example, in DQ Herculis 1934, when the light curve suffered a steep drop and long after most spectral lines had disappeared, emission lines of hydrogen, Fe II and Ca II continued to be detectable. Since the obscuration had to arise either in front of or within the ejecta, this observation indicated that these lines were forming in the outermost part of the ejecta at that time and which was not yet obscured. While hydrogen could be from the ejected material, it seems more likely that the Fe II and Ca II lines were arising in the swept-up material of the companion star as the ejecta expanded, and hence located in the outermost part of the ejecta. Mass-based segregation in the ejecta would have led to the ejected iron and calcium lagging to the rear of the ejecta. This suggestion is strengthened when we realise that the atmospheres of late type stars (later than F) are characterised by iron and calcium lines (e.g. Allen, 1973). Another point of support for some of the detected iron lines forming in the swept up material of the companion star comes from the observations of symbiotic stars wherein the Fe II lines are found to show a distinct radial velocity behaviour with orbital phase as compared to other spectral lines. This observation indicated the origin of the iron lines in the companion star and was instrumental in establishing the binary nature of symbiotic stars. Unless we encounter serious observational contradictions to the hypothesis of mass-based segregation within the ejecta, we assume that this is indeed the case and try to understand observations in its context. At no point we resort to contrived explanations to support our hypothesis since we believe that requiring such an approach means that the hypothesis is incorrect and non-physical. To our satisfaction, the hypothesis works within the ambit of known parameters.

We suggest that the distinction of novae into the Fe II and He/N classes based on the post-maximum spectrum is indicative of the dominance of lines forming in the swept up material and the ejecta respectively. A Fe II type nova shows narrower P Cygni like lines more often than He/N types which show broad jagged flat-topped lines. As discussed in an earlier point, the optical continuum from a nova is predominantly from the ejecta till about the nebular phase. The P Cygni absorption features in Fe II lines support their formation in the outer parts of the ejecta so that the cool ions absorb the emission lines or the continuum emission arising behind them. This, in turn, supports their formation in the swept-up ambient material. With passage of time, this material entrained by the leading part of the ejecta (or shock) will also sink to the rear part

of the ejecta due to lower expansion velocities acquired by these heavier ions. On the other hand, the He/N novae show emission lines with larger widths and seldom P Cygni absorption so that these must arise in the bulk of the hot ejecta with little continuum emission to absorb or cool atoms which can absorb. This is also supported by the observation that in hybrid novae the early detections of Fe II lines are replaced by He/N lines but never vice versa. Since swept-up material should be present in all novae, the reasons for lines from it being detectable in some novae and not in others should be a function of other properties such as the detailed physical conditions in the ejecta, its expansion velocity and the ambient densities. We also note that there is a predominance of main sequence companions in the Fe II type novae and of sub-giants or red giants in the He/N type novae. For example, V1534 Sco, V1535 Sco and Master OT J010603.18 are classified as He/N type novae and the companion stars are identified as giant, giant and sub-giant whereas V2949 Oph, V3661 Oph, TCP J18102829-2729590 and ASASSN-16ma are classified as Fe II novae (Munari et al., 2017) and the companion star is likely to be a main sequence star. Moreover the recurrent novae with main sequence companions - T Pyx and IM Nor are Fe II novae (Darnley et al., 2012). The companion star will be the main source of the ambient medium in the nova. We recall that the matter densities in the outer parts of the Roche lobe of a main sequence star are almost a million times higher than that of a red giant (see Section 2.4). Thus, the shock/ejecta can sweep up more matter in case of a main sequence companion than a giant star and can explain the presence of sufficient swept-up matter for the Fe II lines to be detectable. As the nova ejecta evolves, several of these become hybrid novae with the detection of strong He/N lines from the ejecta. The expanding ejecta soon clears the companion star and hence the swept up matter does not increase indefinitely with time. Moreover, the swept-up matter composed of heavy atoms will sink to the rear part of the ejecta and will soon be indistinguishable from the ejected matter.

Before we proceed, we enumerate the main points of the model discussed till now:

- It is shown that the quiescence luminosity of the nova is high due to the presence of a white dwarf with a large accreted envelope ( $\geq 0.1R_{\odot}$  for a classical nova). Eclipsing novae give quantitative support to this hypothesis.
- The common origin of the sudden optical brightening of a nova outburst and spectral lines is in the ejecta which explains the efficacy of the MMRD and the correlated changes in the optical light curve and spectra. The hotter white dwarf contributes less than two magnitudes to the luminosity after the pre-maximum halt.
- It is suggested that even dwarf nova outbursts are due to a thermonuclear explosion on the white dwarf. However the energy released is much lower than in classical novae and only leads to an expansion of the envelope in dwarf novae.

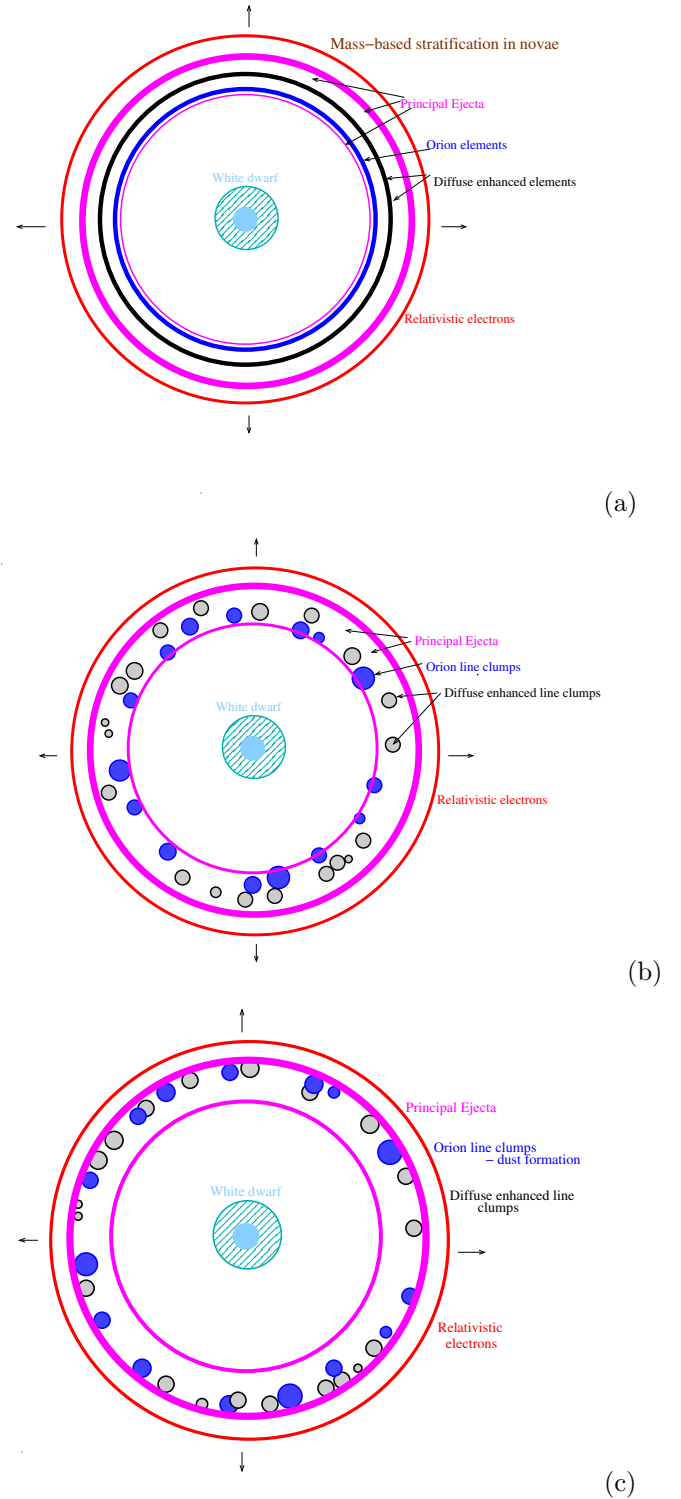


Figure 8: Schematics showing some points of the updated model to explain nova observations. The magenta lines enclose the main ejecta while the outermost red circle shows the location of the relativistic electrons. (a) Mass-based segregation of elements in the ejecta. The heavier atoms/ions accumulate in the inner parts of the ejecta while lighter elements like hydrogen lead the ejecta. (b) Clumps form in the inner part of the ejecta where metals have accumulated. Diffuse enhanced and Orion lines form in these clumps. (c) The clumps are accelerated by radiation pressure from the hot white dwarf and move ahead in the principal shell. Dust forms in the Orion clumps.

- The explosion sets up a blast wave, energises electrons to relativistic velocities and ejects the envelope supersonically, all of which propagate outwards.
- It is suggested that there is mass-based segregation within the ejecta such that the heavier elements having acquired slightly lower velocities occupy the rear parts of the ejecta and the lighter elements lead the ejecta.

### Spectral systems and clump formation in the ejecta:

In this point, we examine observational results on the four main spectral systems namely the pre-maximum, principal, diffuse enhanced and Orion (see Table 1) which can be identified in a nova spectrum as the light curve evolves. In the pre-maximum phase of the light curve, a spectrum consisting of blue-shifted absorption lines of low excitation are detected at a certain velocity displacement. In the new model, the energy input to the ejecta till the pre-maximum is entirely due to the explosion energy. The velocity of the pre-maximum spectrum, if constant since ejection will signify the energy output of the explosion if the ejected mass is known. However some novae like DQ Herculis have shown a rapid decline in this velocity likely due to dense ambient medium. At the optical light curve maximum, a new spectral system is detected in which the absorption lines appear at a higher blue-shifted velocity compared to the pre-maximum spectrum and show associated wide emission bands. This is referred to as the principal spectrum and which replaces the pre-maximum spectrum. Since the major energy and mass release in the nova outburst occurs in a single episode, this subsequent increase in the velocity displacement observed in many novae and indicative of an increase in the expansion velocity of the ejecta has been intriguing. We have suggested that the white dwarf radiation field acts on the ejecta after the pre-maximum halt which is supported by observations. The ejecta is dense and optically thick before the optical maximum. Thus the radiation field of the white dwarf can exert a radiation pressure on the ejecta and accelerate it to higher velocities and the absorption lines appear at a higher blue-shifted velocity and the emission bands become wider. After this final push by the white dwarf radiation field, most of the ejecta becomes optically thin and no further push to the entire ejecta is possible, which is supported by the observation that the emission lines of the principal spectrum are never replaced by another line system. In fact, the principal spectrum lines and velocities survive through the evolution of the outburst and are also detected in nova shells observed several years following the outburst. We do note that in the earlier models, radiation pressure had been invoked to explain some observations e.g. the detachment of the envelope at the optical maximum from the white dwarf. There also exist models in which the entire nova outburst is attributed to the effect of radiation pressure.

About a magnitude below maximum, another independent system of absorption lines at still bluer velocities and associated wider emission bands appears in the nova spec-

trum and are referred to as the diffuse enhanced lines. About a couple magnitudes below maximum another independent system of absorption lines at still bluer velocities and wider emission bands are identifiable in the optical spectra of several novae. These lines are of higher excitation than those of the diffuse enhanced system and are referred to as the Orion system. In the existing model, these two systems have been attributed to faster and newer mass loss from the white dwarf. In the updated model, we argue that these lines are also formed in the same ejecta and no fresh ejection of matter from the white dwarf is warranted. We refer to mass-based segregation of elements in the ejecta so that heavier elements lag behind lighter elements as shown in Figure 8. We suggest that the diffuse enhanced and Orion lines are formed in these regions. In Figure 8, it is schematically suggested that the elements giving rise to the diffuse enhanced lines accumulate near the centre of the ejecta and those giving the Orion lines occupy the rear of the ejecta. The justification for this arrangement is the chronology of their detection, the differences in the spectral line properties and their simultaneous detection. If a large number of heavy atoms accumulate in the inner half of the ejecta then their mutual gravity may lead to enhanced attraction, coalescence and formation of clumps consisting of mostly non-hydrogen elements. From this explanation it follows that dense clumps should form in the inner parts of the ejecta closest to the white dwarf as shown in Figure 8 and it is suggested that the diffuse enhanced and Orion lines form in these clumps. The clumps can be optically thick unlike rest of the ejecta. The radiation field of the hot white dwarf shining on the clumps can trigger either or both of the following: (1) exertion of radiation pressure can accelerate the clumps outwards in the ejecta and (2) increase in the ionization and excitation of the clumps. Under the effect of the radiation pressure exerted by the white dwarf, the clumps move outwards at a velocity larger than the average ejecta velocity (i.e. principal line forming regions) thus explaining the larger blue shifts observed in the absorption lines of the diffuse enhanced and Orion absorption systems. We note that radiation pressure is a function of the temperature and can be estimated as  $1/3 aT^4$  where  $a = 7.565 \times 10^{-16} \text{Jm}^{-3}\text{K}^{-4}$  is the radiation constant. A white dwarf of surface temperature  $10^5 \text{K}$  will exert a radiation pressure  $\sim 2.5 \times 10^4 \text{Jm}^{-3}$ . Clumps of different sizes could suffer different acceleration due to the radiation pressure and if sufficient absorbing and emitting atoms exist, multiple lines at distinct velocities would form. If these lines are sufficiently closely spaced, they would appear wide and would explain the wide diffuse lines that are observed. The diffuse enhanced lines are frequently observed to break up into multiple sharp components which would indicate the decreasing influence of radiation pressure on the disintegrating clumps. We note that the development of and detection of diffuse enhanced and Orion line systems is generally noticeable in slow novae whereas their presence is not always discernible in fast novae. Since clump formation in the ejecta involves several steps which require finite time, the entire process of

clump formation is likely to be more efficient in slow novae which expand slowly and hence higher densities persist longer. In fast novae, the fast expansion can rapidly drop the densities and it is likely that there is not sufficient time for the clumps to form and hence the diffuse enhanced and Orion systems are not always detected. It has been noted that hydrogen is not always detected in the Orion system and which we think lends strong support to the formation of clumps in the ejecta due to mass-based segregation at the rear end of the ejecta which can be depleted of hydrogen. This would indicate that the Orion clumps are mostly composed of the heaviest elements in the ejecta whereas the diffuse enhanced clumps contain intermediate mass elements and hydrogen and this is a justification for their relative location in Figure 8. From the observed velocity displacements, we can infer that the diffuse enhanced clumps and Orion clumps are moving with velocities which are 2–3 times the average expansion velocity of the ejecta quantified by the velocity of the principal system of lines. The clumps would hence be propelled to the leading parts of the ejecta after they are formed (see Figure 8) and before they are destroyed. Both these system of lines are short-lived and disappear when the light curve has fallen by 4 magnitudes from the maximum and the nova has entered the transition phase of evolution. This also gives support to the formation of these lines in the clumps which evaporate or disintegrate as the ejecta expands. After the disappearance of the diffuse enhance and Orion lines and the absorption component of the principal lines, absorption lines disappear from the spectrum indicating the lack of absorbing material in the ejecta.

**Transition phase, dust formation and light oscillations:** Light curves of a few novae have shown a steep fall in their brightness starting about 3.5 magnitudes below maximum (see Figure 1). This has been shown to be due to dust formation in the nova ejecta which absorbs and obscures the optical emission causing the light curve to plunge to a minimum. However it is not known where and how the dust forms in the ejecta. From the above discussion, it appears that the Orion clumps provide an ideal site for dust formation. The clumps contain heavy elements and the inner parts of the clumps are shielded from the hard radiation field of the white dwarf thus facilitating dust formation. The Orion clumps move ahead under the influence of the radiation pressure. If these clumps have formed large quantities of dust and disintegrate or have a large filling factor in the mostly uniform density ejecta, then they can obscure most of the optical continuous emission from the ejecta and the white dwarf, thus causing the steep fall in the brightness of the nova like DQ Herculis. The dust eventually disperses and the continuous emission becomes visible again. Generally it is noted that the light curve begins its drop when the Orion system of lines are detectable and the light curve revives when the ejecta is in the transition phase or has entered the nebular phase when the Orion system of lines have disappeared. This is generally  $\geq 6$  magnitudes below maximum. This signals the end of the transition period in which the stellar type

spectra containing absorption lines evolves into a nebular type spectra containing only emission lines. Some correlation between detection of Orion system of lines like O II, C II, N II and the deep minimum in the light curve of a nova had also been noted (Stratton, 1945) which also lends support to our hypothesis.

While such a steep decline in brightness is a characteristic of slow novae which supports obscuration due to the Orion clumps, some relatively faster novae show light oscillations of 1-2 magnitudes in the transition phase of the light curve (see Figure 1). These light oscillations are accompanied by anti-correlated changes in the velocity displacement, excitation of the Orion lines and colour of the optical light such that a secondary light minimum is accompanied by a larger velocity displacement, higher excitation in the Orion lines and a higher colour temperature **check** and vice versa. Occasionally a correlated change is observed in the principal system of lines and the diffuse enhanced lines but neither are as dramatic as changes in the Orion lines (see Figure 2). We suggest that the oscillations are induced by the varying usage of the white dwarf radiation by the Orion clumps so that the fraction of radiation that reaches becomes variable. We recall that in our model the hot white dwarf contributes  $\leq 2$  magnitudes to the optical light curve. If some of this radiation is used up in exerting radiation pressure on the Orion clumps then it will lead to a minimum in the light curve and a corresponding higher velocity displacement of the Orion absorption lines. If this light is used up in exciting an atom in the Orion clump then the secondary minimum will coincide with a higher excitation Orion line. One can speculate on why the light varies in an oscillatory fashion but we note that there exist novae light curves where the recorded light does not oscillate but shows randomly spaced light variations which are always noted to be less than 2 magnitudes and which show correlation with the changes in the Orion lines. The most obvious explanation could be that once the changes that the light is capable of effecting on the Orion clumps have been done, the light curve recovers and the Orion system reverts to its original state in which case the light can again be absorbed by the Orion clump and the light curve dips. This can continue through the transition period for some novae i.e. for the time that the radiation field can have such an effect on the Orion clumps. In some cases, it has also been noted that a spectral line disappears from the Orion velocity and appears at the principal velocity and vice versa. This is not surprising and merely indicates the changing effect of radiation pressure on a clump so that its expansion velocity varies. About 3 magnitudes below maximum the diffuse enhanced system disappears, around 4 magnitudes below optical peak, the principal absorption features disappear and by 4.5 magnitudes below optical maximum the Orion system of lines have disappeared. After this only emission lines are detected in the nova spectrum and the nova is said to enter the nebular phase of evolution. No spectral lines showing the widths characteristic of the diffuse enhanced or Orion systems are detected again. All lines are found to show the widths characteristic of the principal

system. Thus all the material in the ejecta expands with the velocity of the principal system. The optical continuous emission from the nova continues to decline and get bluer as it enters the nebular phase which is expected since the contribution of the expanding ejecta to the continuous emission is decreasing and that of the white dwarf is increasing.

**Final decline:** Most classical novae take several years to revert back to the brightness and spectrum of the pre-nova stage (e.g. DQ Herculis took 15 years). A large fraction of the time is spent in the final decline phase of the light curve which follows the transition phase of the light curve. The luminosity of the system declines by the last few magnitudes in the final decline to settle down at the pre-nova brightness. The brightness of the ejecta will steadily decrease as it expands and the contribution by the white dwarf will change as accretion restarts and a low temperature envelope forms around it. In some novae, the ejecta is observed as a separate expanding shell around the central binary so that the contributions of the nebula and the white dwarf can be separated. If the light curve of the central object has not reverted to the pre-nova brightness in this case then it gives evidence to the contribution by the white dwarf to the light curve. Similarly the contribution of the nebula to the light curve can also be estimated at that time. However such novae are rare since they have to be very closely to enable the resolution into two components soon after the outburst. Since the white dwarf in the pre-nova phase is characterised by a large accreted envelope it appears that the time taken for the cooler envelope to form on the hot white dwarf will define the time that the nova will take to revert back to its pre-nova state and this could be several years depending on the accretion rates. This time being in decades and not in hundreds of years indicates that the accretion restarts soon after the outburst, the accretion rates are sufficient to build up the pre-nova envelope in decades and that further accretion only goes to increase the density of this envelope with little change in its size.

Recurrent novae which evolve faster on all counts as compared to classical novae also revert to the pre-nova optical state much earlier than classical novae. For example, RS Oph and T CrB reverted back to quiescence brightness in about 95 days after their last outburst and U Sco in about 65 days after its outburst in 2010. Any difference noted between the pre-nova and post-nova brightnesses can then be traced to remnant changes in temperature or extent of this envelope which is disrupted by the outburst.

#### Soft X-rays, radio thermal emission and optical:

The thermonuclear explosion on the white dwarf in a nova outburst could result in one of the following: (1) the entire accreted envelope is energised and ejected (2) part of the envelope is ejected while part of it expands and eventually falls back on the white dwarf (3) the envelope is not ejected and only expands. Observations seem to suggest that (1) is typical of classical and recurrent nova outbursts whereas (3) describes dwarf novae. However it

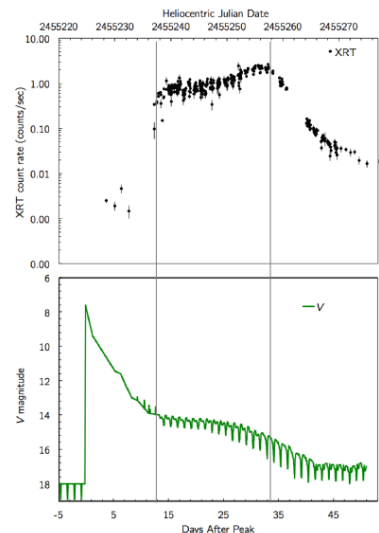


Figure 9: Figure showing X-ray and optical light curves of U Sco after its outburst in 2010 reproduced from Pagnotta et al. (2015). The top curve shows the X-ray (0.3-10 keV) light curve and bottom one shows the behaviour of the V band light curve. Note that the eclipses in the optical light curve revive around day 13 which is when the X-rays are detected. No radio detection has been reported for this nova.

is possible that either (1) or (2) would describe classical novae depending on the energy released and the mass of the accreted envelope which would determine whether all the matter is accelerated beyond the escape velocity or not. We note that in the existing model it was believed that the optical emission arose from the photosphere of the white dwarf i.e. the expanded envelope which had not been ejected. Since we show that the optical emission arises in the ejecta, we have to search for the evidence of an inflated photosphere, if it exists, in other observations.

If we can assume that the detection of soft X-rays which has to be from matter at temperatures  $\geq 10^5$  K implies that the entire accreted envelope has been ejected in the explosion exposing the hot surface of the white dwarf then it would lend support to point (1) made above and hence to the absence of a cooler remnant photosphere from the outburst. We recall that the quiescence surface temperature of the white dwarf has been estimated to be between 8500 and 50000 K (Sion, 1999) which will not emit soft X-rays and thus the detection of soft X-rays after the outburst signalling the ejection of the entire envelope is a plausible one. However we note that the non-detection of soft X-rays does not necessarily imply the presence of a remnant photosphere (point 3 above) since the reasons could be the optically thick ejecta absorbing the soft X-rays and/or accretion restarting so that the hot surface of the white dwarf is beginning to be obscured.

It is commonly observed that hard X-rays, especially from fast novae are detected soon after the nova outburst (e.g. Schwarz et al., 2011) while soft X-ray emission is detected later e.g. it was detected in U Scorpii and V339 Delphini when the optical light curve had dropped by about

6 magnitudes below maximum. In Table 4, the onset and end times for the soft X-ray phase taken from Schwarz et al. (2011) are listed in columns 2 and 3 while the decline in the V band luminosity of the nova from maximum at those times as estimated by eye from the AAVSO light curves are listed in columns 4 and 5. The values in the last two columns should be considered as rough estimates. As listed in Table 4, soft X-rays are generally detected in the transition phase or beginning of the nebular phase i.e. when the peak luminosity has dropped by  $\geq 4.5$  magnitudes. The similarity in the evolutionary stage of the optical light curve when soft X-ray is detected in novae gives strong support to its detection being tied up with the entire ejecta being ionized and becoming transparent to soft X-rays. It rules out the detection epoch of soft X-rays corresponding to a change in the white dwarf photosphere i.e. it contracting sufficiently so that the inner hot portions are detectable which is often cited as the reason in literature. Detection of atomic hydrogen in the ejecta of V339 Delphini till about day 40 post-maximum (Skopal et al., 2014) and the detection of soft X-rays around that time indicates how the opacity of the ejecta to X-rays can be high and be responsible for the delay in its detection. This, then, supports the point (1) listed above in which it is suggested that the nova outburst ejects the entire accreted envelope which leaves behind a hotter white dwarf which should start emitting soft X-rays as soon as the ejecta is adiabatically energised and detached from the white dwarf.

However this does not rule out a thin layer of material, possibly the matter synthesised in the thermonuclear outburst, remaining on the white dwarf - it only shows no evidence for an inflated photosphere of several solar radii. The black body radiation of the hot white dwarf will also contribute to the last  $\leq 2$  magnitudes rise in the optical light curve in some novae. The turn-off times show a larger variation with the slow novae detectable in soft X-rays for longer periods till the nova brightness drops significantly (see Table 4). The turn-off of soft X-rays from novae should indicate onset of obscuration of the hot surface of the white dwarf as the accreted material begins to accumulate on the white dwarf. Thus, it appears that slow novae take longer for the accreted matter to envelope the hot white dwarf which could be indicative of late resumption of accretion or low accretion rates. In nova T Pyxidis, soft X-ray emission was detected between 7.5 hours and 12 days after which it faded (Kuulkers et al., 2011). A long-lived soft X-ray phase began from day 117 (Osborne et al., 2011a) when the nova had faded by about 5 magnitudes from the visible peak. These observations lend strong support to the soft X-rays from the hot white dwarf being emitted as soon as the matter is ejected but being detectable by us only when the atomic hydrogen in the ejecta is ionized in addition to suggesting that matter in the ejecta which if ionized on ejection, recombines to form atomic hydrogen as it expands.

Several novae show a slower or no decline in the V band light curve during the soft X-ray phase (see Figures 9,14) strongly implying a connection between the two. Radio

thermal emission is generally detected at similar epochs as soft X-rays with an onset which precedes detection of soft X-rays by a short interval (see Figure 16). These correlations which are observed in several novae signify a common system of changes in the nova which affect the two wavebands. Such correlations can be instrumental in improving our understanding of novae. We note that soft X-rays which arise on the white dwarf can become detectable when the ejecta is optically thin to the radiation i.e. fully ionized. Radio thermal emission is due to the physical process of free-free emission in the ionized ejecta and the near simultaneous detection of emission at the two distinct wavebands implies that the increasing ionization of the ejecta leads to a rise in the radio thermal emission and also to the ejecta becoming transparent to the soft X-ray emission. In many cases, the radio thermal emission shows the frequency-dependent onset due to optical depth effects. A temperature and hence ionization gradient in the ejecta such that the inner parts are at a higher temperature and ionized and the leading parts are cooler and partially ionized, will delay the onset of the thermal radio emission due to opacity. When the entire ejecta is ionized and isothermal, no further absorption can happen and the radio thermal rapidly becomes detectable. The plateau observed in the optical light curve during the soft X-ray phase means that an additional source of optical emission has been added in the nova system. This could indicate an increase in the temperature of the entire ejecta and hence an increase in the free-free and free-bound emission. One can think of the increased optical emission being due to the contribution from the hot white dwarf to the optical bands or contribution from an ionized band around the companion star ionized by the X-rays from the white dwarf. However these reasons require the ejecta to be optically thick to optical wavelengths till the soft X-ray phase. The optical emission appears bluer in the soft X-ray phase. Since we suggest that the hot white dwarf contributes  $\leq 2$  magnitudes to the optical emission near the maximum, no further rise due to the white dwarf radiation is expected unless parts of the ejecta remain optically thick to the white dwarf emission. We realise that there is some degeneracy in these scenarios and independent data are required to break it.

In the 2010 outburst of the eclipsing recurrent nova U Scorpii, soft X-rays were detected between day  $\sim 13$  and day 33 during which the optical light curve showed a plateau and the dips in the optical light curve due to the eclipse of the white dwarf, which had not been present after the outburst, also resumed around day 13 (Pagnotta et al., 2015) (see Figure 9). The optical light curve had dropped by about 6 magnitudes from the peak. Even in its 1999 outburst, U Sco showed a plateau in the optical emission between days 10 and 33 after peak (Schaefer, 2010) and it was detected in soft X-rays (0.2-2 keV) when it was observed 19-20 days after the optical peak (Kahabka et al., 1999). Similar multi-band behaviour in successive outbursts implies that similar mass is ejected in all the outbursts so that the ejecta properties are similar and the nova evolves on similar timescales. Thus the ejecta



Table 4: X-ray onset/end times from Schwarz et al. (2011). The difference of the optical emission with respect to the peak on the onset/end days of X-rays are listed in the last two columns. These are visual estimates from the V band light curves downloaded from AAVSO website and hence the values are only approximate.

Nova	X-ray		Optical	
	onset	end	below max	
	days	days	onset mag	end mag
KT Eri 2009	71	280	~ 4.5	~ 7.5
RS Oph 2006	35	70	~ 4.5	~ 5.2
U Sco 2011	23	34	~ 6.5	~ 7.5
V1494 Aql 1999	217	515	~ 6.5	~ 10
V1974 Cyg 1992	201	561	~ 5.5	~ 9
V2491 Cyg 2008	40	44	~ 6	~ 6.5
V407 Cyg 2010	15	30	~ 2	~ 2.5
V4743 Sgr 2002	115	634	~ 4.5 – 5	~ 8.5

becomes transparent to soft X-rays at similar epochs in each outburst. Soft X-ray emission was detected at similar epochs following the optical peak in the 1985 and 2006 outbursts of RS Ophiuchi also. This could have been suggested from the very similar optical light curves which are noted for recurrent novae in all outbursts but it is always better to get observational evidence of the same before any theory is hypothesised. It is also worth noting here that differences in the densities of the ambient medium around RS Ophiuchi was noted from radio synchrotron studies of the two outbursts. In spite of this, similar soft X-ray and optical light curve behaviour indicates that these emissions predominantly depend on the ejecta properties and not the ambient matter. Ultraviolet emission (2600 Å) was found to be stronger than the visible band during the soft X-ray phase and returned to normal around day 35 when the soft X-rays were extinguished. (Pagnotta et al., 2015).

This above behaviour observed in U Sco can be explained as follows. The optical emission is predominantly from the ejecta which quickly expands beyond the binary extent and hence no eclipse signatures are observed in the light curve. However if the white dwarf had contributed upto 2 magnitudes to the light curve near maximum then the light curve should have shown eclipse signatures due to the periodic occultation of this contribution. However data show no such signature upto day 13 indicating that there was no contribution of the white dwarf radiation to the light curve till day 13 or that it was present for a short time near the maximum and absent since. Noting that recurrent novae often have optically thick winds blowing from the massive white dwarf due to the high accretion rates, the winds will increase the ambient densities. This matter will be swept-up by the ejecta as it expands and will increase its opacity. A second reasoning is what is generally favoured in literature that the white dwarf after the outburst is surrounded by an inflated photosphere which encloses the companion star and only after it has de-

flated to a size smaller than the binary separation that the eclipses can resume and an inner hot surface which emits soft X-rays is revealed explaining the simultaneous detection of emission at both wavebands. We prefer explaining the plateau and the increasing depth of the eclipses in the optical light curve of U Sco due to the increasing contribution of the white dwarf to the light curve as the ejecta gets transparent and reveals the binary (see Figure 9). On a general note then, the plateau or reduced rate of decline in optical emission that often accompanies the detection of soft X-rays indicates an enhanced contribution to the light curve either from the binary or from increased emission measure of the ejecta. Once the X-ray emission declines, the optical light curve also starts to decline indicating that the extra source of light is also fading.

The V-band eclipse is about 1.3 magnitudes deep in quiescence (Schaefer 2010). We use the detailed eclipse data that has been gathered during the 2010 outburst (Schaefer et al. 2011) to understand the evolution of this system. The eclipse was much shallower when it was first detected after day 13 and a secondary eclipse was also detected which is not observed in the V band during quiescence. Both the primary eclipse and secondary eclipse kept increasing in depth during the soft X-ray phase. After about day 32 when the soft X-ray phase was ending, the secondary eclipses disappeared and the primary eclipse appeared to be similar in depth to that in quiescence (Schaefer et al. 2011). However peculiar behaviour was noted when the second plateau in the optical light curve began around day 41 after outburst. The primary eclipse became shallower by 0.2-0.3 magnitudes and light variations upto 0.6 magnitudes were seen in the non-eclipsing parts of the orbit. This behaviour continued till day 67 when it is believed that the nova returned to quiescence. The primary eclipse seems to have been deepest between days 32 to 41. We note that a scatter of 0.4 to 0.6 magnitudes seems to be present in the non-eclipsing parts even in the quiescent B and I band light curves and a secondary eclipse of magnitude 0.3 is detected in the I band (Figure 45,47 in Schaefer 2010). The outburst behaviour of the eclipsing light curve can be explained in our model as follows. We recall that in this model the outburst ejects the entire accreted low temperature envelope exposing the hot inner surface on the white dwarf and hence the white dwarf should emit soft X-rays soon after ejection. However the soft X-rays will only be detectable when the foreground ejecta is fully ionized and hence transparent to the X-rays. These X-rays can heat and ionize the outer atmosphere of the companion star especially the parts lying close to the orbital plane which could enhance the emission from the companion star. The plateau in the light curve indicates a fresh source of optical emission which adds to the declining ejecta emission. The likely sources could be the white dwarf or the irradiated companion star. That secondary eclipses are seen alongwith the primary eclipse after day 13 in U Sco indicates that the emission from the companion star has increased by about 0.2 magnitudes in the V band due to irradiation by the X-rays and which is eclipsed by the white dwarf during the orbital motion. Such tran-



sient emission from the companion star can contribute to the observed slowing down of the light decay rate. When the X-rays fade, the companion should revert to its quiescent state and the secondary eclipse should fade. That the secondary eclipse is not observed after around day 32 supports the hypothesis. Coming to the primary eclipse, in the first detection after day 13, the eclipse is shallow indicating that the contribution of the white dwarf to the light curve is lower than seen in quiescence. As time passes, the eclipse keeps getting deeper with it being deepest between days 32-41 after the end of the supersoft phase indicating that the V band emission from the white dwarf has returned to its quiescent value which in this case appears to be more than during the outburst. Recall that the end of the soft X-ray phase is hypothesized to be due to accretion restarting and the accreted material forming a cooler envelope around the white dwarf which does not emit in soft X-rays. Thus, it could be that such an envelope was formed after day 32 - ending the soft X-ray phase and returning the eclipsed light curve to the quiescent depths. However the light curve after day 41 shows several peculiarities with light variations upto 0.6 magnitudes in amplitude detected throughout the orbital motion and the primary eclipse being shallower than it was between days 32 and 41. This was also the start of another plateau in the light curve indicating another source of light being added to the light curve. The easiest explanation seems to be a varying source of light contributing to the light curve and giving rise to the light variations which continued all the way to quiescence. Since in quiescence, U Sco shows variations upto 0.5 magnitudes in the B and I bands (Schaefer 2010), this behaviour after day 32 could be due to the same reason.

While the soft X-ray phase in most novae is found to be  $< 3$  years (Schwarz et al. 2011), there do exist novae which are detectable in soft X-rays for a decade or longer. One of them is the fast nova V1500 Cyg which recorded an outburst in 1975. Its progenitor star had  $B = 21.5$  magnitudes. The nova has taken 30-35 years after outburst to decrease to 19 magnitudes (Schaefer et al., 2010b) which is still brighter than quiescence. The soft X-ray phase has also been longer and soft X-rays, albeit faint, are still detectable from the nova (Schaefer et al., 2010b). This supports our model wherein the soft X-rays fade when the cooler accreted envelope forms around the white dwarf and which is also responsible for the nova brightness in the optical bands reverting to the pre-nova values. The long duration of the soft X-ray phase could indicate extremely low accretion rates. Another nova with an exceptionally long soft X-ray phase which lasted for more than 15 years was V723 Cas (Schwarz et al. 2011). A decade-long soft X-ray phase was observed in GQ Muscae which recorded an outburst in January 1983. Soft X-rays were detected in April 1984 (Ogelman et al. 1984) upto 1993 (Shanley et al. 1995). The nova had  $t_3 \sim 40$  days but the light curve entered a plateau after that which lasted for about a year. The soft X-rays turned on when the light curve was within this plateau in 1984. However this nova was somewhat different from the typical case in that the light

curve resumed its faster decline later in 1984 when soft X-rays were still detectable from the system.

We summarize the above:

- The brightening upto the pre-maximum halt and the pre-maximum spectrum are entirely due to the energising of the ejecta matter by the explosion and contains no energy contribution from the white dwarf.
- The final brightening by  $\leq 2$  magnitudes to the optical peak is probably a combination of the rapid isothermal expansion of the optically thick ejecta due to the radiation pressure exerted by the hot white dwarf and contribution from the hot white dwarf radiation. The absorption features of the principal spectrum detected at the light curve maximum has a velocity displacement which is larger than pre-maximum lines which is attributed to the radiation pressure exerted on the optically thick ejecta by the white dwarf radiation field.
- We suggest that mass-based segregation occurs in the ejecta so that the heavier elements accumulate in the inner parts of the ejecta. These facilitate the formation of clumps in which the diffuse enhanced and Orion spectral systems characterised by higher velocity displacements and excitation are suggested to form. All higher velocity displacement features detected post-maximum are attributed to the effect of the radiation pressure on the optically thick clumps.
- It is suggested that dust forms within the Orion clumps. As the Orion clumps move outwards in the ejecta under the influence of radiation pressure, the dust can obscure the optical continuous emission and the light curve can show a rapid fading like in DQ Herculis.
- Some novae show oscillations of amplitude 1-2 magnitudes in the light curve with correlated changes in the Orion system of lines. We suggest this is direct evidence to the contribution of the white dwarf ( $\leq 2$  magnitudes) to the light curve and effect of the radiation field of the white dwarf on the Orion clumps.
- The final decline in the light curve to pre-nova brightness takes several years in many classical novae. We suggest that this timescale is the time needed for the accreted cooler envelope to form around the white dwarf so that its brightness reverts to pre-nova state.
- Soft X-rays arise on the hot surface of the white dwarf and should be present soon after the energetic ejection of the envelope. However detectability depends on the foreground ejecta becoming transparent which happens when it is fully ionized thus delaying the onset of soft X-ray phase to the transition phase of the light curve. The end of the soft X-ray phase signals the restart of accretion and accumulation of a lower temperature envelope on the white dwarf. The soft X-ray phase is generally accompanied by a plateau in

the optical light curve indicating an additional contribution to the light.

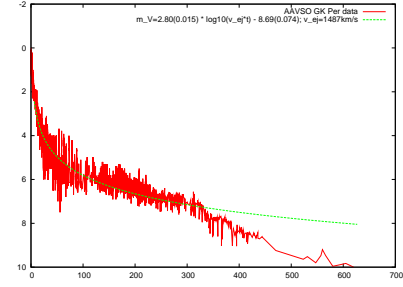
This completes the primary discussion on the updated model which explains the evolution of nova outburst. In the following, we discuss a few observational results on novae in light of the updated model and determine simple parameters of the nova from the model. This also helps us elucidate and fine-tune our model. The list is not exhaustive and more observational results should be examined and it should be possible to explain those with the model. This will help better understand the model and also fix any problems that remain. As with rest of the paper, no effort is spared in keeping the discussion bound by physics, observations, common sense and consistency.

**Emission measure of the ejecta:** In the existing model, the optical continuum is believed to arise in the initially expanding and post-maximum contracting photosphere of the white dwarf while in our model the main contributor to the optical continuous emission is the ejecta and the white dwarf contributes only the last couple magnitudes between the pre-maximum halt and maximum and possibly to the plateau in the light curve. It is also likely that the X-ray irradiated companion star contributes to the light curve during the plateau phase. It appears that optical radiation from central binary in some novae starts contributing to the light curve only at the onset of the plateau and till then the ejecta blocks it. In fact, it appears that the novae which show the coincidence of a plateau in the optical light curve with the appearance of soft X-rays should not show a pre-maximum halt before the maximum light. If it did show a pre-maximum halt then it would mean that light from the binary did penetrate the ejecta. An early transparency of the ejecta followed by an opaque phase might also happen in some novae. Thus, while on a general basis we suggest that the explosive energy is mainly responsible for the sudden brightening of the nova upto the pre-maximum halt and the last  $\leq 2$  magnitudes is due to the white dwarf, we believe that there will be exceptions to this case since a range of physical conditions exist in the nova shell.

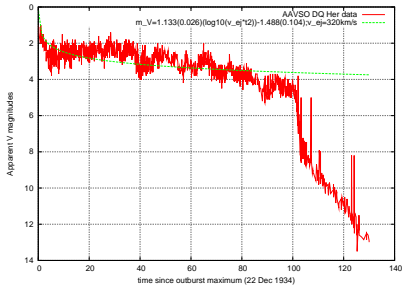
After the maximum, the light curve begins to decline. In our model, the decrease in the optical flux is due to the decreasing densities and hence emission measure in the expanding shell. For simplicity, we assume that drop in emission measure is dominated by the radial expansion of the shell and its thickness is constant. An increasing thickness will lead to a more rapid decline in the emission measure. We hence model the post-maximum light curve with the decreasing emission measure of the expanding ejecta of constant thickness. We assume that the density in the expanding ejecta shell falls off as  $1/r^n$  i.e.  $n_e \propto 1/r^n$  where  $r$  is the radial separation of the shell from the central star. In the optically thin phase, the V band emission at any given time  $t$  after optical maximum will be proportional to the emission measure i.e.  $L_V(t) \propto n_e(t)^2 R$  where  $R$  is the shell thickness which we have assumed to be constant. Since  $r = v_{ej} t$ , we have

$1/r^n = 1/(v_{ej} t)^n$ . Thus,  $L_V(t) \propto 1/(v_{ej} t)^{2n}$  and hence  $M_V = -2.5 \log_{10} L_V + K = 5n \log_{10}(v_{ej} t) + K$ . We use  $v_{ej}$  in  $\text{kms}^{-1}$  and  $t_2$  in days. These function fits to the post-maximum light curve data of three novae are shown in Figure 10. The light curve data have been downloaded from the AAVSO website. The rate at which the density of the ejecta falls as it expands i.e.  $n$  is hence determined. We find that  $n$  is 0.56, 0.23, 0.69 for GK Persei, DQ Herculis and CP Lac respectively. The slowest nova (DQ Herculis) shows the smallest index i.e. the slowest change in density with time, as expected. Thus if we assume that all novae start with the same initial electron densities then at some  $t$  after optical peak, the density in a fast ejecta will be lower than in a slow nova and so will the emission which is another way of saying that  $t_2$  for a fast nova is smaller than for a slow nova when due to the declining emission measure in an expanding ejecta. After about 7 magnitudes below maximum in GK Persei, 3 magnitudes below maximum in DQ Herculis and 9 magnitudes below maximum in CP Lac, the light curve appears to decline more rapidly than expected from the estimated density index  $n$  (see Figure 10). This appears to be the case for the smooth i.e. S type novae shown in Stroepe et. al. (2010). In case of DQ Herculis, the decline is due to dust obscuration of the continuum emission. This exercise supports the dominant contribution to the optical luminosity near maximum being from the ejecta and the decline in the light curve being due to the expansion of the ejected shell.

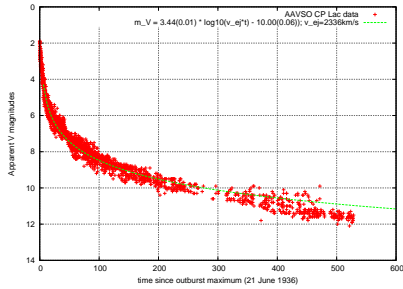
**Radius of ejecta shell at  $t_2$ :** We estimated the radius  $r_2$  of the ejected shell when the peak luminosity had declined by two magnitudes using  $v_{ej}$  and  $t_2$ . These ranged from 3 kpc to 90 kpc (see Figure 11) for the sample of novae listed in Schwarz et al. (2011). Excluding 6 novae with  $r_2 > 30$  kpc, a mean value of  $9.7 \pm 0.7$  AU (see Figure 11a) is determined. The sample of novae listed in McLaughlin (1940) is also overplotted and show the same distribution of shell radii.  $r_2$  shows no correlation with  $v_{ej}$  except that the slow novae show a larger spread in  $r_2$ . In Figure 11(b),  $r_2$  is plotted against  $t_2$  for a nova and a correlation such that slow novae show a larger radial extent of the shell at  $t_2$  seems to be present. The correlation seems tighter for the sample of novae taken from McLaughlin (1940) and a fit to this sample gives  $r_2 = 14.6(\pm 2.06) \log_{10} t_2 - 7.09(\pm 2.76)$  with  $t_2$  in days and  $v_{ej}$  in  $\text{kms}^{-1}$  which is shown by the solid line in Figure 11b. The correlation appears to be present in the sample from Schwarz et al. (2011) but the scatter appears to be larger and the slope slightly different. The radial extent of the shell at  $t_2$  quantifies the required change in the emission measure of the shell to reduce the luminosity by two magnitudes. The correlation of the shell extent with  $t_2$  such that slow novae need a larger shell extent to reduce the emission measure sufficiently for the luminosity to change by two magnitudes could be suggestive of larger initial densities in the ejecta of slow novae compared to fast novae. This could indicate a larger mass ejection in slower novae compared to faster novae and hence explain their distinct speed classes if the outburst energies are comparable. However since the out-



(a)

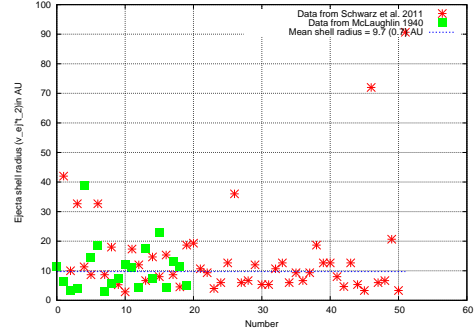


(b)

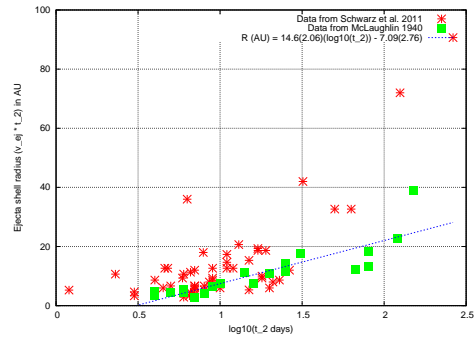


(c)

Figure 10: The V band light curves of three novae downloaded from the AAVSO website: DQ Her(a), GK Per(b), CP Lac(c). The smooth line shows the fit to the light curve estimated from decreasing emission measure of the ejected shell. The principal absorption line velocities are used as proxy to ejecta velocities and are taken from McLaughlin (1960a, 1954).



(a)



(b)

Figure 11: Radial separation  $r_2$  of the shell from the white dwarf at time  $t_2$  estimated for the sample of novae in Schwarz et al. (2011); McLaughlin (1940). In (a)  $r_2$  appears to show a well-defined mean value. (b)  $r_2$  is plotted against  $t_2$  and in which a correlation is detectable which supports a higher mass ejection in slow novae.

burst energy from the CNO thermonuclear reaction is a sensitive function of temperature beyond  $10^8$  K so that it is proportional to  $T^{18}$ , a spread in outburst energies should also be expected. This makes us cautious and we end with the comment that while it does seem possible that slow novae eject a larger mass, we need to investigate this point further before drawing any conclusions.

**Narrow lines post-outburst:** Some novae have shown the presence of narrow emission or absorption lines of helium (He I or He II) and hydrogen located at their rest frequencies within a broader feature in a spectrum taken soon after maximum (e.g. Nova Geminorum 1912, Persei 1901, Aquilae 1918, T Coronae Borealis 1946) and the origin has been suggested to be near the central star (e.g. McLaughlin, 1947; McLaughlin, 1949). Note that these lines were first detected before it was known that novae were binaries with the explosion occurring on a white dwarf. More recently, Munari et al. (2014) detect a narrow He II in KT Eridani. Other novae which have shown such narrow components are U Scorpii, DE Circinus and V2672 Ophiuchi. Their origin on the white dwarf is supported by our model. The outburst leaves behind a hotter white dwarf which will be eventually detected in soft X-rays when the

ejecta becomes transparent to it. In the novae where the ejecta becomes optically thin to the white dwarf radiation in the visible bands around maximum i.e. the novae wherein the white dwarf contributes  $\leq 2$  magnitudes after the pre-maximum halt, high excitation lines forming on the white dwarf, if sufficiently intense should be detectable soon after the maximum. In the novae where the ejecta remains opaque to the optical radiation till much later (for example some of the novae which show a plateau in the light curve near the transition phase), these narrow lines should not be detectable close to the maximum. However if the plateau arises due to an additional non-white dwarf component to the emission then the correlation will not exist. One can speculate that while an absorption line could arise in the photosphere around the white dwarf, an emission line could indicate formation in a wind-like component and which could also signify the restarting of accretion in the system. Novae at minimum show a blue continuum which is sometimes superposed by emission lines of helium and hydrogen (e.g. Humason, 1938). At the end of the outburst, a featureless continuum which is strong in the violet or with emission lines of hydrogen or helium lines at rest frequencies is often observed. The similarity of the narrow lines detected near maximum with the features detected at minimum support the origin of the narrow lines on the white dwarf and can help understand the physical properties of the envelope around the white dwarf.

**Temperatures of novae in outburst:** We can estimate various temperatures for a nova in outburst: (1) colour temperature derived from the continuous spectrum, (2) photoelectric or Zanstra temperature derived from intensities of emission lines relative to the continuous spectrum, (3) excitation temperatures derived from the relative strengths of emission lines of differing excitation potential and (4) electron temperature of the ejecta. McLaughlin (1943) has discussed these temperatures and states that ‘..the different methods yield very different temperatures from observations made on the same date,...’. He also adds that ‘...that different investigators derive different temperatures from the same method’. While this could be indicative of the wide range of excitation conditions and varying abundances in the ejecta, it would be advisable to not consider the determined temperatures as exact values but use the estimated range of values to study trends. It was believed that the colour, photoelectric and excitation temperatures determined the temperature of the central star since the star was believed to be the main source of the continuous emission and the main exciting source for the spectral lines while the electron temperature characterised the ejecta gas. Thus, astronomers expected the colour, photoelectric and excitation temperatures to match and it was surprising that this was not found to be supported by the empirical data. The photoelectric temperatures estimated using spectral lines of He II 4686A, H, N III, N IV, [O III] differ with the lowest temperatures estimated from the hydrogen and oxygen lines and systematically higher temperatures from rest of the

lines. This was believed to reflect the range of excitation conditions which prevailed inside a nova ejecta. The typical photoelectric temperatures were estimated to range from 25000 K to 75000 K (McLaughlin, 1943). The excitation temperatures estimated from the ratio HeII 4686/H $\beta$  was around 70000 K (McLaughlin, 1943). Colour temperatures for novae were found to vary from few thousand K measured near optical maximum and increasing to 20000 K in the decline phase of the light curve (e.g. McLaughlin, 1943). Thus the estimated excitation and photoelectric temperatures were systematically higher than the colour temperatures. Electron temperatures using the intensity ratio of the [O III] lines (i.e. I(5007+4959) / I(4363)) were estimated to range from 6000 to 10000 K showing a tendency towards a decline as the nova faded (McLaughlin, 1960b) and are closer in magnitude to the colour temperatures. This discrepancy, especially the very different values of colour temperatures, were hard to reconcile with the prevalent model. The study of temperatures of novae seems not to have been pursued to any great extent after this.

In the updated model, we can explain the aforementioned discrepancy. We recall that in the updated model, all the energy upto the pre-maximum halt is believed to be due to the explosion owing to the opacity of the ejecta and the earliest contribution of the white dwarf to the energy budget can only be near the maximum. Thus, when measured near the maximum, the photoelectric and excitation temperatures will be proxy to the explosion energy. As the light curve evolves, they will indicate a combination of the explosion energy and the radiation field of the white dwarf and as the fractional contribution of the white dwarf increases, they will be indicative of the temperature of the white dwarf as the explosion energy is not replenished. Thus the photoelectric and excitation temperatures are always high since they denote the temperature of the hot white dwarf or equivalent temperature of the explosion energy. Since in the updated model, the optical continuum at maximum is dominated by the ejecta with some contribution from the white dwarf, the colour temperature is dominated by the low temperature ejecta at the maximum and is comparable to its electron temperature. As the light curve declines, the fractional contribution of the hot white dwarf to the light curve increases as the ejecta fades and hence the colour will get bluer i.e. the colour temperature will rise as the light curve declines as has been estimated. The electron temperature is expected to decrease as the light curve declines since the ejecta is cooling and fading. Thus the excitation and photoelectric temperatures are indicators of the temperature of the same phenomenon - explosion energy, white dwarf and a combination of both and hence are expected to be similar. On the other hand, the colour temperature determined from the optical continuum will be a combination of emission from the ejecta and the white dwarf. It will be closer to the electron temperature of the ejecta near the optical peak and then increase as the light curve declines to finally settle down to the quiescent colour temperature of the system. Thus the measured temperatures can be explained in the updated

model. It would be useful to determine these temperatures for newer novae and further verify this. We recall a comment by McLaughlin (1943) that ‘...the trends of temperature are almost exactly the opposite of what would be expected if the nova phenomenon were due to a simple heating and subsequent cooling of the surface of a star.’

**Outburst winds:** While the occurrence of a single explosive ejection of matter is well established from observations, the existing model also includes a subsequent long-lived wind phase with dramatically lower mass loss rates. In the old model, these winds are believed to be the site of formation of the diffuse enhanced and Orion line systems (e.g. McLaughlin, 1943). In the updated model, we are able to explain most of the observational results with phenomena associated with the main ejecta and have not needed to invoke continuing mass loss from the white dwarf. This prompts us to suggest that the energetic explosion is capable of adiabatically energising and ejecting all the matter above the layer in which the nuclear explosion occurs and hence there remains no matter to eject as winds. It appears certain that the role of white dwarf winds in the post-maximum phase is non-existent or more restricted in the updated model than it was in the old model.

**Synchrotron radio and hard X-ray emission from novae:** While radio thermal emission has been detected in several classical novae, synchrotron radio emission has been detected in only a few novae. The thermal emission is due to the physical process of thermal brehmstrahlung whereas the synchrotron radio emission arises from relativistic electrons accelerated in a magnetic field. The emission sites are hence different with the thermal radio emission arising in the main ejecta and the synchrotron radio appearing to arise in a region which is ahead of the ejecta and might sometimes be coincident with the ejecta. An important argument against the bulk of synchrotron radio emission arising in the ejecta is the differing free-free absorption felt by the emission from the two processes. This would indicate different sources of the free-free absorption and hence support different emitting locations. The detection times are also different with the detection of radio synchrotron preceding detection of the thermal radio emission. There does appear to be a higher rate of detection of radio synchrotron emission from recurrent novae as compared to classical novae. Out of the 11 identified Galactic recurrent novae, radio synchrotron emission has definitely been detected from two - RS Ophiuchi and V745 Scorpii. The companion star in both the novae is a red giant. The classical novae from which synchrotron radio emission has been reported are V1370 Aquilae 1982 (Snijders et al., 1987), QU Vulpeculae 1984 (Taylor et al., 1987), GK Persei 1901 (Reynolds & Chevalier, 1984; Seaquist et al., 1989), V445 Puppis 2000 (Rupen et al., 2001a,b), V1723 Aquilae 2010 (Krauss et al., 2011; Weston et al., 2016). There could be more detections which are hidden in literature. Some of the reasons for the infrequent detection of synchrotron radio in classical novae could be a combi-

nation of lack of observations at sufficiently low radio frequencies where its easier to distinguish between thermal and synchrotron emissions and at appropriate epochs since the radio synchrotron emission from these systems is not as long lived as thermal radio or optical emissions probably indicative of the relatively low energy of the explosion. In both the synchrotron-emitting recurrent novae, the initial ejecta velocities were recorded in excess of  $10000 \text{ kms}^{-1}$  which would have generated a sufficiently large pool of relativistic electron population with  $\gamma \geq 2$ . The relativistic electrons were likely accelerated in the ambient magnetic field. The frequency-dependent onset of the different radio frequencies in both the novae, indicated that the process of free-free absorption was delaying the detection of the synchrotron radiation. The electrons would start emitting synchrotron radiation soon after the outburst since in the updated model, electrons should be instantly accelerated to relativistic velocities alongwith the ejecta especially if expanding with velocities  $> 6000 \text{ kms}^{-1}$ . Synchrotron radio emission has been detected in two outbursts in V745 Sco - in 1989 (Hjellming, 1989) and 2014 (Kantharia et al., 2016) and two outbursts in RS Ophiuchi - in 1985 (Hjellming et al., 1986) and 2006 (e.g. Kantharia et al., 2007) which allowed a glimpse into their evolution. In case of both RS Ophiuchi and V745 Scorpii, the onset of radio synchrotron emission at the same frequency was found to be earlier in the later outburst. It was suggested that the free-free opacity was caused by the white dwarf winds which were blowing when the accretion rate exceeded the critical rate in the recurrent novae (Kantharia et al., 2016). Since the accretion rates vary, the wind rates vary and the free-free absorption also varies with epoch. This was shown to well-explain the behaviour of the radio light curves in successive outbursts demonstrating how synchrotron emission can be used to understand the winds and accretion rates (Kantharia et al., 2016). Radio synchrotron emission from nearby fast classical novae ( $v_{ej} \geq 10000 \text{ kms}^{-1}$ ) should be detectable immediately after the outburst since foreground obscuration is likely to be low owing to the absence of winds from the white dwarf in classical novae wherein the accretion rates are generally much lower than the critical rates.

We note that hard X-ray emission is generally detected soon after the outburst and precedes the detection of soft X-ray emission (Schwarz et al., 2011). Moreover hard X-rays are more frequently detected from fast novae as compared to slow novae (Schwarz et al., 2011). Since the presence of relativistic electrons is more likely in a fast nova wherein the energy imparted to each particle is larger, the above suggests that generation of hard X-rays is connected to the relativistic electron population and the process is likely to be synchrotron or inverse Compton effect. Hard X-rays are also occasionally detected from novae which have lower recorded early ejecta velocities. This could indicate rapid deceleration of the ejecta or another physical process for their generation. Clearly the detection of hard X-rays from a nova is more frequent than of radio synchrotron emission. If emission in both bands is owing to the relativistic electrons, then this difference could ei-

ther be due to different observational sensitivities at the two bands or the absence of a magnetic field and a non-synchrotron origin for the hard X-rays in several cases. This remains to be investigated further by experts.

**Recurrent novae:** The entire evolution is compressed into a shorter time in fast recurrent novae whereas the evolution of slow recurrent novae resemble classical novae. The evolution of the last recorded outburst in the fast recurrent nova V745 Scorpii on 6.7 February 2014 probably just after its optical peak demonstrates the fast evolution. There is a low significance detection of  $\gamma$ -rays  $> 100$  MeV from V745 Sco on 6, 7 February 2014 (Cheung et al., 2014) i.e. near the optical peak in addition to hard X-rays (Mukai et al., 2014). Radio synchrotron emission was detectable at 610 MHz from day 12 to day 217 and indicated that it turned on between days 3 and 12 (Kantharia et al., 2016). Soft X-rays were detected from V745 Sco on 10 February 2014 (day  $\sim 3$  after optical peak), peaked on day 5.5 after the optical peak and faded by February 22 (Page et al., 2015). The soft X-rays were detectable for a total of about 12 days. We note that the existing explanation for the fast ejecta observed in some recurrent novae is attributed to the small masses that are ejected compared to a classical nova. The energy release will continue to be due to the CNO explosion and hence comparable to classical novae. The smaller mass in the recurrent nova will be ejected more violently and the larger energy allocation per particle will lead to the generation of a highly relativistic population of electrons. The rest of the observations can be explained as follows. The lower energy  $\gamma$ -ray photons generated in the thermonuclear reaction would have been the seed photons which were boosted to  $> 100$  MeV energies by inverse Compton scattering by the relativistic electrons. The nuclear reactions were quenched soon after and hence no  $\gamma$ -rays were detected beyond day 2. The relativistic electrons gyrating in the magnetic field either frozen in the ejecta or present in the ambient medium start radiating synchrotron emission. The hard X-rays could indicate inverse Compton scattering or synchrotron radiation from high energy electrons. The detection of soft X-rays around day 3 after optical peak indicates that the ejecta was fully ionized by then and the quenching in 12 days indicates that the accretion had resumed and started forming a low temperature envelope around the white dwarf. If radio observations sensitive to thermal emission existed early on, it would have been possible to detect radio thermal before day 3 although the smaller ejecta mass might have led to lower intensity of radio thermal emission. That the synchrotron radio was detectable for a long time indicates that a large pool of relativistic electrons spanning a large energy range were energised in the explosion.

Fast recurrent novae evolve very quickly and the ejecta velocity also declines rapidly which is unlike classical novae which evolve slowly and the ejecta velocity remains constant for several years. The evolution of fast recurrent novae does not allow the detection of the detailed evolution of the light curve or spectral stages unlike in the

slower classical novae. However slower recurrent novae like T Pyx are seen to show an evolution similar to classical novae supporting similar evolution in classical and recurrent novae. Fast recurrent novae evolve to quiescence within a year of the outburst while slower recurrent novae like T Pyx take longer.

**Dwarf novae:** We have suggested that dwarf novae are due to an episode of smaller energy injection into the accreted envelope on the white dwarf which then isothermally expands causing it to brighten ( $L \propto R^2$ ). There have been suggestions of a thermonuclear origin to this energy output in literature (e.g. Sparks & Starrfield, 1975; Paczynski & Zytkov, 1978) which we think observations support, but the release of gravitational energy has found favour in literature. The continuous emission increases as the photosphere expands reaching a maximum when it is largest and when the energy source is removed, the photosphere contracts and the dwarf nova goes into decline with the entire outburst spread over a short duration of a month or less. A brightening by  $\sim 5$  magnitudes would require the radius of the photosphere to increase by a factor of  $\sim 10$ . We find that observations support this scenario. Dwarf novae show the presence of emission lines during quiescence and absorption lines are detected at the outburst maximum (e.g. Warner, 1995). If the dwarf nova maximum, as mentioned above, is a result of expansion of the envelope to  $\leq 10$  times its quiescent radius then this expanded envelope is the photosphere and the absorption lines at maximum arise in this photosphere. On the other hand the narrow emission lines detected in quiescence could be signatures of accretion winds around the white dwarf in the nova.

**Symbiotic stars:** Symbiotic stars are binary systems consisting of a white dwarf primary and a red giant secondary star and the detected light is a combination of the two components. Symbiotic stars show non-periodic short duration sequence of brightenings and dimmings (e.g. Boyarchuk, 1969) but no mass ejection happens. The brightness variations in symbiotic stars are also accompanied by colour variations such that it gets redder with decreasing brightness (e.g. Boyarchuk, 1969). This supports the occurrence of the brightness variations on the white dwarf so that when the system brightens, the contribution of the hot white dwarf increases and the colour is bluer. When the brightness declines the white dwarf contribution is reducing and the colour gets redder as the red giant dominates. A thermonuclear pulse due to proton-proton reaction on the white dwarf has been found to explain the frequent brightenings in these systems (Paczynski & Zytkov, 1978). The pulse can then lead to an increase in the radius of the white dwarf photosphere like suggested for dwarf novae or it could just trigger an increase in temperature of the envelope around the white dwarf. The spectra of symbiotic stars also follow the light variations such that when the brightness of the symbiotic system decreases, the late type spectrum strengthens and excitation degree of the emission spectrum increases (Boyarchuk, 1969). This be-

haviour is reminiscent of the light oscillations and change in excitation that is noted in classical novae. The observed spectrum consists of lines arising in the white dwarf and the red giant. When the brightness of the white dwarf decreases, the late type spectrum due to the red giant will appear relatively stronger. If the excitation level of the spectrum increases then it would mean that the white dwarf radiation is being used in increasing the excitation. The different radial velocities of lines from symbiotic stars AG Peg, BF Cyg, RW Hya, R Aqr showed that these are binary stars. The radial velocity variation of the Fe II line is significantly lower than that traced by lines of He II, [O III], N III and [Ne III] (Figure 12 in Boyarchuk (1969)). The lines of Fe II arise in the red giant whereas the rest of the lines can form on the white dwarf. Thus we can use the knowledge gained from symbiotic stars in the study of novae.

**[O III] excitation:** In few novae, the [O III] morphology is found to be distinct from that traced by other lines (e.g. DQ Herculis) indicating either a different elemental distribution or different excitation mechanism. Pronik & Pronik (1988) discuss the importance of charge transfer such that  $O^{+++} + H^0 \rightarrow O^{++} + H^+$  in context of the active nucleus in Seyfert galaxies and suggest that this makes an important contribution to the strength of [OIII] lines and also ionizes hydrogen. and in neutral hydrogen regions the charge transfer reaction can enhance the [O III] emission. This requires that H, He are not ionized so that  $n_e \ll 10^6 \text{ cm}^{-3}$ . If  $n_e > 10^7 \text{ cm}^{-3}$ , then collisional deexcitation of the  $O^{++}$  ion will happen and no forbidden lines will result. They also explain variability in [O III] emission due to the above mechanism. The upper level of [O III] transition is populated by electron impact. They also suggest that  $O^{++}$  ions can be formed by removal of electrons from O I by X-rays which is known as the Auger effect. Since we do not know the reason for the distinct distribution of [O III] sometimes noticeable in the nova images, such processes could also be active in the regions around a nova outburst and need to be further investigated.

**Explaining different light curve shapes:** Light curves of novae display a large variety and hence have been prone to classification into different types. We refer to the classification in Strobe et al. (2010) where the authors have classified the light curves into seven types: (1) smooth (S) (2) plateau (P) (3) dust dip (D) (4) oscillations (O) (5) cusp (C) (6) flat top (F) and (7) jitters (J). We attempt to understand these within the framework of the model presented here. We suggest simple explanations and predictions for the types of light curves based on the discussion so far. The *S* type of light curve will arise for a nova in which the white dwarf contributes to the light near the optical maximum and hence should show a pre-maximum halt. No further significant contribution to the optical light is expected and hence no plateau accompanies the soft X-ray detection. The *P* type should arise for a nova in which there is a delayed contribution to the total

light of the system from the white dwarf and/or irradiated companion star. The white dwarf in this case does not contribute near the optical maximum due to opacity of the ejecta and hence such novae should seldom show a pre-maximum halt. The white dwarf contribution is delayed to a later date giving rise to the plateau in the optical light curve and in most cases is found to coincide with the soft X-ray emission which heralds the full ionization of the foreground ejecta. The *P* types can be of any speed class although it is easier to imagine these to be slower novae. The *D* types indicate dust formation in the Orion clumps and the advancing of the clumps to the front of the ejecta so that they can obscure the continuous emission from rest of the ejecta and the white dwarf. When the dust disperses, the light curve revives. These are slow novae since only these have sufficient time for the dust to form inside the Orion clumps and move forward and influence the light curve. The *O* types are the novae wherein the white dwarf contribution to the visible band is significant and the radiation field of the white dwarf has a significant impact on the Orion clumps. These novae should show the pre-maximum halt. The *C* types can be an extension of *P* types wherein the eventual contribution to the light from the white dwarf and possibly companion star are significantly higher than in a *P* type so that the light curve shows a cusp. There should not be a pre-maximum halt for the *C* type. The *F* type is a slow nova since  $t_2$  and  $t_3$  are very long. This could be indicative of a dense slowly expanding ejecta which remains optically thick for a long time and hence the emission remains near maximum for a significant time. The *J* types show jitters of amplitude generally  $\leq 2$  magnitudes detected soon after the maximum and could arise due to varying extra contribution by either the white dwarf or hot spot on the companion heated by the X-ray emission from the white dwarf. Sometimes these jitters lead to maxima perched on a flat light curve.

From the tabulated values in Strobe et al. (2010), we note that while most novae show similar trends in  $t_2$  and  $t_3$  so that a fast nova has short  $t_2$  and  $t_3$ , a large variation is seen in  $t_6$  such that some fast novae show a short  $t_6$  and some show a long  $t_6$ . This kind of behaviour indicates a change in the rate of decline of the light curve beyond  $t_3$  which should help us further understand the nova. For starters, it appears that the fast novae with a long  $t_6$  will be prone to showing a plateau in the light curve which as stated earlier would indicate an additional light contribution to the light curve. A detailed study would be useful before arriving at any firm conclusions on this.

### 3.4 Origin of multifrequency emissions

We can now schematically summarise the model of a nova outburst which emerges from multifrequency observations (see Figure 12). The deduced sites of origin of the multi-band emission are labelled in the figure. The schematic is relevant for a spherical ejecta and depicts the evolutionary states expected for times ranging from just after outburst to  $\sim t_6$  i.e. upto about six magnitudes below op-

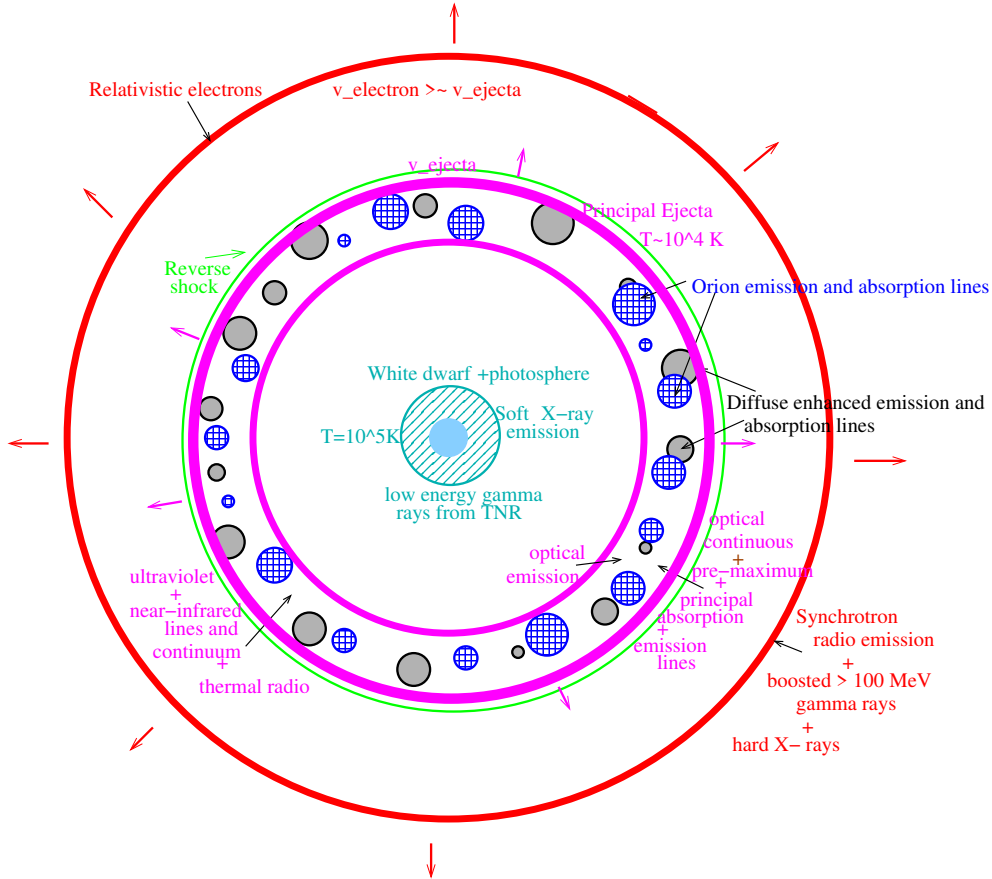


Figure 12: The schematic of a nova outburst labelled with the dominant site of origin of the various multi-wavelength emissions. This schematic will apply to non-rotating (or weakly rotating) white dwarfs which accrete a spherical envelope. A rotating white dwarf will acquire a prolate envelope and the eruption will eject an ellipsoidal envelope which is observed around several novae. The figure is not to scale.

tical maximum. During this period, some of the emissions labelled in the schematic will disappear, new components will appear and some will survive. About six magnitudes below optical maximum, the principal shell of ejecta will be devoid of absorbing clumps and will be emitting nebular lines as it expands around the binary. The white dwarf will begin its journey back to its pre-nova state.

The thermonuclear explosion at the base of the inflated accreted envelope leads to ejection of the overlying layers of matter. The cooler outer parts are ejected leaving behind a thin photosphere at high temperature  $\geq 10^5$  K which emits soft X-rays. The soft X-rays will be visible when the foreground becomes transparent to it which is generally observed to be around the transition or nebular phase of the light curve and are extinguished once accretion restarts and a low temperature envelope forms around the white dwarf. The thermonuclear reactions will release  $\gamma$ -rays of energies  $< 20$  MeV. These  $\gamma$ -rays will be quenched when the thermonuclear reactions stop. These emissions necessarily arise close to the white dwarf as labelled in Figure 12 and propagate outwards. Neither of these emissions are expected from novae in quiescence nor are they detected. Outside the binary lies the expand-

ing ejecta. The radial separation of the ejecta from the white dwarf is continuously increasing and the physical parameters of the ejecta like its density is continuously decreasing as it expands. The ejecta which is shown enclosed by the two magenta circles in Figure 12 contains most of the ejected mass which is typically estimated to be  $\sim 10^{-5} M_{\odot}$  in classical novae and  $\sim 10^{-7} M_{\odot}$  in recurrent novae. Emission at several wavebands arise in the ejecta - optical, ultraviolet, infrared and radio. These can be described further to be optical continuous emission and line spectra, near-infrared continuum and line spectra (including dust emission), thermal radio emission and ultraviolet continuous and line emission. The various optical line systems - pre-maximum, principal, diffuse enhanced and Orion arise in this ejecta. These are labelled in the figure. The clumps which form due to mass-based segregation of elements are also shown. The blue crossed circles indicate the Orion clumps and the grey black circles indicate the diffuse enhanced clumps. The clump formation begins after the maximum and they have formed about a magnitude below the optical maximum especially in slow novae as the detection of diffuse enhanced lines indicate. Spectral lines from these clumps are detectable to about 4



magnitudes below maximum i.e. till the transition phase of the light curve. Dust also forms in the clumps in this period. The clumps move forward within the ejecta under the influence of the radiation pressure exerted by the white dwarf. In some novae, the presence of dust in the leading parts of the ejecta obstructs the optical continuous emission leading to a steep drop in the light curve which eventually recovers in the nebular phase. The clumps disperse and become optically thin as the nova moves to the nebular phase and the diffuse enhanced and Orion lines at higher velocities displacements are not detected again. The electron temperature of the ejecta is around  $10^4$  K. The ejecta continues to expand and the emission lines of the principal system continue to be detectable. In many cases, the ejecta shell is detected several years after the explosion still expanding with similar velocities as inferred from the principal lines. Synchrotron radio emission is detected from some novae, soon after the outburst and is inferred to be arising from a region ahead of the ejecta which in literature is referred to as the forward shock. It is believed that the electrons are accelerated by the forward shock and hence are coexistent with it. However we have shown that electrons in the envelope will be accelerated to relativistic velocities if equal energy is distributed to all particles in the ejecta which means that they are accelerated alongwith rest of the envelope and no separate shock acceleration needs to be invoked. Observations show that the epochs of detection of radio synchrotron and radio thermal are distinct and so is the cause of free-free absorption which indicates that they arise in different locations. Moreover imaging of radio emission following a nova outburst (e.g. RS Ophiuchi) shows that the synchrotron emission arises in a region ahead of the main ejecta from which the thermal radio emission is detected. Hence it appears that relativistic electrons occupy a region ahead of the main ejecta as shown by the red circle in Figure 12. Relativistic electrons should also be present in the main ejecta but their number seems to be insufficient to result in detectable synchrotron radio emission. The population of relativistic electrons in the red circle gives rise to detectable radio synchrotron emission and also hard X-rays. The radio synchrotron requires a magnetic field which would be the field frozen in the ambient medium. The electrons can also inverse Compton boost the low energy  $\gamma$ -ray photons produced in the nuclear reactions to  $\geq 100$  MeV energies thus explaining the detection of such  $\gamma$ -rays from novae as labelled in the figure. If we refer to the red circle as the ‘relativistic electron ejecta’, then it will survive till the electrons lose their energy.

In case of a prolate-shaped envelope being ejected from a rotating white dwarf in the nova explosion, the ejecta in the polar regions will appear to expand further than the equatorial regions. Many times the polar ejecta is observed to expand faster than the equatorial part indicating a possibly more energetic explosion at the polar regions or if the explosion is similar everywhere the non-polar expansion might have been stunted by the presence of an accretion disk. It is difficult to break this degeneracy but we think it should be possible with a further analysis of

observational data.

It is interesting to note that FH Serpentis 1970 was a first timer in several wavebands - thermal radio emission was first detected in this nova (Hjellming & Wade, 1970), dust emission was first detected in this nova when it was found that a decline in the optical light curve was coincident with rise in flux at wavelengths longer than  $2\mu\text{m}$  (Geisel et al., 1970) and an ultraviolet peak was detected after the optical peak leading to models which suggested a constant luminosity phase in novae (Gallagher & Code, 1974).

## 4 Case studies

We summarise and examine existing multi-frequency observational results on a couple classical and a couple recurrent novae in context of the model put forward here. The highlight of the study is that the observed characteristics are well-explained in this model within the purview of known physics. There do remain several details that need to be worked out but the overall framework consistently explains the observables. We also extrapolate some of the model features especially the synchrotron radio emission to supernovae (supernova remnants) and active nuclei but this discussion is left to the next part.

### 4.1 Classical novae

While the shells of several old classical novae detected in optical are spherical in shape e.g. CP Puppis 1942, (Duerbeck & Seitter, 1979); V533 Herculis 1963, V476 Cygni 1920, DK Lacertae 1950 (Slavin et al., 1995) there are also novae which show ellipsoidal or bipolar shells e.g. RR Pictoris 1925 (Duerbeck & Seitter, 1979); T Aurigae 1891 (Gallagher et al., 1980), DQ Herculis (Slavin et al., 1995), V959 Mon (Linford et al., 2015). The enhanced bipolar or prolate morphology of the ejecta is often deduced from the spectral line profiles recorded soon after outburst. Profiles which consist of a central component flanked by high velocity shoulders or a double profile indicate existence of a faster bipolar outflow e.g. RS Oph; (Skopal et al., 2008) and V1535 Sco (Linford et al., 2017), although sometimes it could also result from the equatorial shell if viewed edge-on. A dependence of the axial ratio of a nova shell on the speed class such that slow novae frequently left behind ellipsoidal shells whereas faster novae left behind spherical shells was noted by Slavin et al. (1995). The occurrence of such aspherical remnants has been explored and the possible reasons include a common envelope phase, localised thermonuclear runaways, binary nature of the system and rotation of the white dwarf. As discussed in the paper, an ellipsoidal ejecta gives direct evidence to rotation of the accreting white dwarf which will accumulate the accreted matter in a prolate envelope around it due to the dependence of the accretion rate on latitude. Spherically symmetric matter infall is assumed. In a spherically symmetric or bipolar explosion, the prolate-shaped envelope will form an ellipsoidal or bipolar ejecta. While other physical effects might also contribute to the ellipsoidal envelope,

we believe that the effect due to rotation is the primary reason.

In a few classical novae such as Nova QU Vulpeculae 1984 (Taylor et al., 1987), V1723 Aquilae (Krauss et al., 2011; Weston et al., 2016), a double peaked radio light curve is observed with the first peak indicating a synchrotron origin and the second peak being attributed to thermal free-free emission. However such cases are rare and most radio-detected novae have shown the presence of thermal free-free emission, sometimes detectable for several years after the explosion e.g. HR Delphini 1967. A frequency-dependent behaviour wherein the higher frequencies are detected before the lower radio frequency emission is observed in most novae e.g. T Pyxidis (Nelson et al., 2014), V1974 Cygni (Hjellming, 1996), HR Delphini (Hjellming et al., 1979). Such a behaviour indicates that the radio detection epoch is determined by the optical depth ( $\propto 1/\nu^2$ ) of the foreground/mixed absorbing material. In a few novae, the radio peaks occur simultaneously (e.g. V1723 Aql Weston et al., 2016) indicating that the delay in the onset of radio thermal emission is not due to free-free absorption. Radio emission from classical novae was first detected in the novae HR Delphini and FH Serpentis (Hjellming & Wade, 1970). Radio imaging observations soon after the outburst seem to indicate that synchrotron radio emission arises outside the main ejecta indicating that the relativistic electron population has escaped with larger forward velocities. The synchrotron radio emission which also shows the frequency-dependent onset suffer free-free absorption due to the circumbinary material, mainly the remnant of the white dwarf winds. The thermal radio emission which arises in the ejecta and is generally detected at a later epoch suffers free-free absorption due to the cooler foreground material in the ejecta. The occasional simultaneous detection of thermal radio peaks at later times could be interpreted to be due to partial ionization of the ejecta and hence lower emission measures in the initial stages and the detection being delayed till the entire ejecta was ionized and had sufficient emissivity.

For dust formation to happen in a nova ejecta, high particle density rich in metals and not subjected to intense radiation field of the white dwarf is required (Gehrz, 1988). Our model pinpoints the sites of dust formation to the metal-enriched clumps which are formed due to mass-segregation of elements in the ejecta. The diffuse enhanced and Orion lines are also formed in these clumps. Thus, dust formation in predominantly slow novae which also show the presence of diffuse enhanced and Orion lines should be fairly common as supported by observations. Deep minima in the transition phase have been detected in the slow novae such as DQ Herculis 1934 which showed a deep minimum which started in the transition phase and ended when the nova entered the nebular phase.

After this short summary of a few observations which our model consistently explains, we detail some of the observational results on two well-studied novae DQ Herculis 1934 and V339 Delphini 2013. Although no efforts have been spared to make the summary extensive, it is humanly

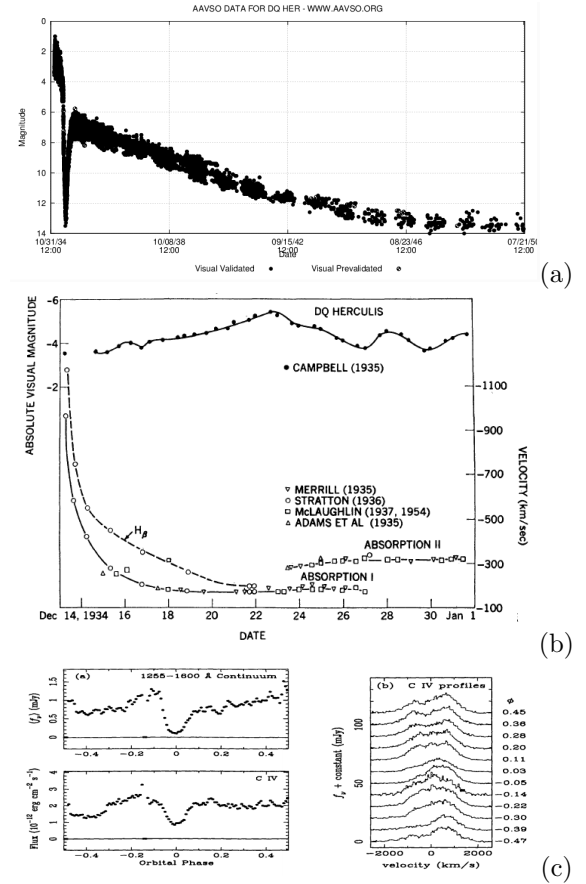


Figure 13: (a) Light curve of DQ Herculis 1934 has been copied from the AAVSO website (<https://www.aavso.org/lcg>). The nova took  $\sim 15$  years to decline to minimum. T Aurigae which showed similar evolution took 30+ years to decline to minimum. (b) This figure reproduced from Sparks (1969) shows the early light and velocity evolution of the pre-maximum (Absorption I) and principal (Absorption II) spectral line systems. (c) This figure reproduced from Eracleous et al. (1998) shows the eclipsing ultraviolet continuum and C IV lines as a function of orbital phase.

impossible to do justice to the vast literature that exists so if any significant observational results have been overlooked, we request the readers to augment this and verify if the model presented here can consistently account for them.

#### 4.1.1 DQ Herculis 1934

DQ Herculis was discovered on the morning of 13 December 1934 in the pre-maximum phase and it peaked in the optical bands on 23 December 1934. This remains one of the best studied novae. In the following, we summarise some of the observational results from literature and our inferences/comments are included in italics:

(1) The visual light curve took almost 15 years to decline to minimum (see Figure 13a). *This would indicate the time required for a quiescent-like envelope to be accreted around the white dwarf. Subsequent accretion would*

increase its density.

(2) DQ Her is an intermediate polar ie has a magnetic field and rotates. *The white dwarf is rotating and hence the accreted matter was accumulated in a prolate-shaped envelope which was ejected in the outburst which continues to be detectable as an elliptical shell.*

(3) In July 1935, Kuiper (1941) found DQ Her was a double star with a separation of 0.2" while the eclipsing binary nature of DQ Herculis with a period of 4<sup>h</sup>59<sup>m</sup> was established by Walker (1954). It is a single line binary and hence the companion spectrum is not detected. From the yellow light, it was estimated that the inclination of the system was 77.3° and the eclipse was 1.4 mag deep in the yellow, 1 mag in blue and 0.8 mag in ultraviolet (Walker, 1956). The radius of the nova was estimated to be  $\sim 0.1R_{\odot}$ , of the companion star to be  $\sim 0.11R_{\odot}$  and the nova was found to become bluer during the primary eclipse while another binary UX UMa would found to become redder in the primary eclipse (Walker, 1956). Maximum blueness is found in the shoulder that precedes the primary eclipse and the colours in the non-eclipsing part indicated that the eclipsed star is bright in the ultraviolet and could be a white dwarf (Walker, 1956). Kraft (1959) suggested that DQ Herculis hosts a white dwarf as the nova star and a companion star which overflows its Roche lobe. A light oscillation of 71 second was also detected (Walker, 1956).

(4) The nova showed several spectral changes within the first ten days after detection starting with a steep fall in the ejecta velocity as shown in Figure 13b reproduced from Sparks (1969). Table 10 in McLaughlin (1960b) lists the evolution of the ejecta velocity in DQ Herculis in the pre-maximum phase after detection with H $\alpha$  showing the highest velocity of  $-1984 \text{ kms}^{-1}$  on 13.3 December 1934 which reduced to  $-320 \text{ kms}^{-1}$  on 21.8 December 1934. *This would indicate that the ejecta rammed into dense circumstellar material and quickly slowed down as it swept up matter. This behaviour is more typical of fast recurrent novae like RS Ophiuchi and V745 Scorpii. Considering that the shell of DQ Herculis continues to expand with a velocity  $\sim 300 \text{ kms}^{-1}$  suggests the existence of relatively tenuous material it has since been expanding into.*

(5) McLaughlin (1937b, 1954) has extensively discussed the observations of DQ Herculis and the following is based on his research papers. The B-type spectrum (starting with  $T_{\text{eff}} \leq 28000 \text{ K}$ ) of 13 December which showed emission bands evolved to a A-type spectrum ( $T_{\text{eff}} \leq 10000 \text{ K}$ ) with P Cygni profiles of hydrogen and other metals including Fe II on 14 December 1934. The velocity displacement of the blue-shifted absorption lines was  $> 500 \text{ kms}^{-1}$  on the night of 13 December which declined to  $\sim 180 \text{ kms}^{-1}$  on December 18 and which was considered the pre-maximum spectrum velocity. *However it should be noted here that the explosion energy was much higher than would be indicated by the pre-maximum spectrum velocity.* Around 21 December before the maximum, the spectrum changed to a F5 type ( $T_{\text{eff}} \sim 6500 \text{ K}$ ). *The evolution of the spectrum to late type stellar types would*

*indicate the expansion of the nova ejecta with no further significant energy input.* During decline from maximum after December 23, a new spectrum of class cF5 containing absorption lines of hydrogen, Fe II, O I and other metals with a displacement of  $-300 \text{ kms}^{-1}$  appeared - this was the principal spectrum and the ejecta has since continued to expand with this velocity. *As suggested in the model, the optically thick ejecta before maximum will be subjected to an extra push by the radiation pressure exerted by the hot white dwarf left behind by the ejection of the cooler envelope in the eruption and which explains the slightly higher velocities of the principal spectrum. If this process makes the ejecta optically thin, then the final  $\leq 2$  magnitudes rise in the light curve could indicate the contribution of the white dwarf. It could also include emission from isothermal expansion of the ejecta thus explaining the change from the spectral type F5 before maximum to the supergiant cF5 post-maximum.* The principal spectral lines evolved to double-peaked profiles with peaks separated by about  $600 \text{ kms}^{-1}$  with some central emission. *These would indicate enhanced emission from the bipolar ejecta.* Diffuse enhanced spectrum appeared in January 1935 with lines of hydrogen, Fe II, Ti II, Cr II, Ca II, Na I at a displacement of  $-550 \text{ kms}^{-1}$  with more components appearing at  $-700$  and  $-800 \text{ kms}^{-1}$ . *The diffuse enhanced clumps formed in the ejecta as heavier elements segregated into clumps. These optically thick clumps acquired an extra acceleration as the radiation pressure due to the hot white dwarf acted on them. Different clumps acquired different velocities which support the radiation pressure scenario. The Fe II, Ti II etc lines could be a combination of the ejecta material and swept-up material which form the clumps in the ejecta as shown in Figure 12.* The diffuse enhanced spectrum faded in mid-February. The Orion spectral lines appeared in March with velocity displacements between  $-300$  and  $-500 \text{ kms}^{-1}$  with more components appearing at  $-1000 \text{ kms}^{-1}$ . All these absorption systems emerged at a secondary minimum in the light curve. *The Orion lines arose in another set of clumps which formed at the rear part of the ejecta (see Figures 8 and 12) and were also accelerated due to the radiation pressure. The excitation and velocity of these clumps are sensitive to the light curve variations so that light recorded by us decreases when the Orion line-forming clumps absorb it and either increase its velocity displacement or excitation. This could be useful in understanding the physical differences between the diffuse enhanced and Orion clump properties.* In April 1935, when the light curve was about 3 magnitudes below maximum, the nova started to fade (see Figure 13a). During this time all the absorption bands and most of the emission features disappeared. The emission bands of hydrogen, Fe II and Ca II were detectable and widened to include the velocities previously occupied by absorption even as the red parts of the emission bands faded. These lines were the last to disappear (also Stratton, 1945). *Since obscuration is due to dust formation in the Orion clumps which are accelerated to the outer parts of the ejecta, it will obscure all the optical continuum and line*

*emission arising in most of the ejecta and white dwarf. The longer time taken by the emission bands of Fe II, Ca II and hydrogen to fade indicate they arise in the outermost part of the ejecta which suggest that the Fe II and Ca II could be from the swept-up material of the companion. The red sides of emission arise on the far side of the ejecta and hence faded before the blue side.* The light curve faded to a minimum of 13 magnitudes on 1 May 1935 after which the nova started to brighten and the nebular spectrum consisting of [O III], hydrogen and '4640' band emission started to appear. Absorption lines did not reappear in the spectrum. The red sides of the emission bands gradually strengthened and when the light curve recovered to about 7 magnitudes below maximum the red part was almost as strong as the violet part of the line. McLaughlin (1935, 1937b) suggested that dust formation in the principal shell in DQ Herculis was responsible for the abrupt drop in the light curve which could explain the spectral changes also. When the dust cleared, the light curve revived and continued its decline which ended around 1950 when the nova was at its pre-outburst brightness (see Figure 13a). *The long time taken to revert to pre-nova condition might indicate low accretion rates.*

(6) In 1940, the central star in DQ Herculis was of photo-visual magnitude 13.4 magnitudes whereas its pre-outburst photographic magnitude was fainter at 14.6 magnitudes (Baade, 1940). *The brighter white dwarf noted in the post-outburst phase gives support to our model wherein the white dwarf is believed to contribute  $\leq 2$  magnitudes increase in the light curve and the hypothesis that the long phase of final decline is due to the time taken by the cooler envelope to be accreted around the white dwarf with similar properties as the pre-nova phase.* The light curve was around 11 magnitudes and the brightness of the nebula was 13.2 magnitudes/arcsec<sup>2</sup> on 1 October 1940 when the photovisual brightness of the star was 13.4 magnitudes (Baade, 1940). *This observation lends strong support to the dominant contribution to the optical light curve by the ejecta as expected by the MMRD and not the expanding photosphere of the white dwarf. The observation demonstrates that the brightness of the white dwarf and nebula were slowly declining to quiescent strengths. If more such data wherein the emission from the white dwarf and ejecta can be separated soon after the outburst are collected then it would be possible to separate the contributions of the white dwarf and the ejected shell to the light curve. This would help study the decline of light from the nebula and white dwarf.*

(7) The expanding shell left behind by the nova outburst which is ellipsoidal is still detectable. In 1940s, the [O III] shell showed a distinct morphology from the N II+H $\alpha$  shell. While the former was detected along the major axis of the shell which was polar, N II+H $\alpha$  were predominantly detected in the equatorial plane (Baade, 1940, 1942; Mustel & Boyarchuk, 1970). Even now the [O III] emission appears to be confined to the end parts of the major axis of the shell while H $\alpha$  and [N II] are detected from the entire shell (Harman & O'Brien, 2003;

Slavin et al., 1995). It appears as if the polar extent of H $\alpha$  and [N II] has increased more than that of [O III]. However this needs to be verified. *A differing morphology in [O III] has been detected in several nova ejecta. We speculate that this could indicate a pre-outburst mass loss which is excited when the electron ejecta traverses through it or could be similar to Auger effect. Since this has been observed in multiple novae, it needs to be examined in detail.* (8) McLaughlin (1960b) discusses the colour, excitation, photoelectric and electron temperatures of DQ Herculis. The colour temperature decreases from 11000 K to 9000 K as the nova rises to maximum brightness and then increases to 18000 K about 4 magnitudes below maximum when the Orion spectrum is strong. The photoelectric and excitation temperatures are found to be high at > 30000 K whereas electron temperature of the ejecta is estimated to be between 6000 and 10000 K. *This behaviour is as expected in our model. We recall that the continuum emission near the maximum predominantly arises in the hot ejecta and hence the colour temperature will be similar to the electron temperature. As the light curve declines, the fractional contribution of the hot white dwarf to the optical continuum increases and the colour temperature increases. The photoelectric and excitation temperatures are a combination of the explosion energy and the hard radiation of the hot white dwarf and which will remain high till the white dwarf forms the cool envelope. At early times these will indicate equivalent temperature signifying the explosion energies and at later times the white dwarf.* (9) Adams & Joy (1936) describe the spectral state prior to (25 March 1935), during (4,15 April 1935) the fading and after the light curve recovered (20 May 1935). We reproduce their summary:

“March 25: Continuous spectrum strong. Prominent absorption lines of hydrogen and calcium showing multiple components and numerous fainter absorption lines of ionized elements. Emission bands of hydrogen broad and diffuse. Faint emission lines of Fe II and [Fe II].

April 4: Continuous spectrum weak. No certain absorption lines. Narrow emission components of hydrogen. Very strong emission lines of Fe II and [Fe II].

April 15: Spectrum similar to that of April 4, but Fe II lines fainter and [Fe II] lines stronger.

May 20: Continuous spectrum very weak or absent. No Fe II or [Fe II] lines. Nebular spectrum fully developed. ” *This summary supports the suggestion that the Fe II lines arise in the swept up circumstellar material.*

(10) While the nebular spectrum of DQ Herculis observed around 1940 (Swings & Struve, 1940) was similar to that in 1935-1936 (Adams & Joy, 1936), significant changes in the dominant spectral lines were noted in 1947 and 1949 (Swings & Jose, 1949, 1952). However there was no change in the expansion velocities which ranged from 222 to 396 kms<sup>-1</sup> and several lines continued to show double components separated by  $\sim 300$  kms<sup>-1</sup> from the centre frequency (Swings & Jose, 1949, 1952) as was observed in the principal spectrum after outburst in 1934. Table 1 in Swings & Jose (1949) lists the changes between spectra of 1940/1942 and 1947/1949 and the main changes can

be summarised to be that [O III] 4959, 5007 weakened, [Ne III], [Fe VII] disappeared and [O II], He II 4686 strengthened. *It is not immediately evident what could have triggered these changes and what they indicated but it is likely that the changes indicate some change in the physical and excitation conditions of the nebula.*

(11) DQ Her is an eclipsing binary and the ultraviolet continuum emission disappears in the eclipse while emission lines (C IV, N V, Si IV, Ne II, He II) show partial eclipse with C IV being the least obscured (see Figure 13c; Eracleous et al. (1998)). Origin of these lines have been suggested to be either winds or the accretion disk. The C IV line (see Figure 13c) shows two components about the rest frequency with the red-shifted component always being detected whereas the blue-shifted component fading twice in an orbital period. In a spectrum taken in 1995, it was found that four spectral lines namely C IV, N V, Si IV, He II have strengthened by 50% compared to 1993 (Silber et al., 1996). The velocity of the He II 4686 line changes with the orbital phase (Kraft, 1958) and a similar behaviour is also exhibited by the higher lines of the Balmer series while it is not seen in  $H\beta$  which prompted the suggestion that the forbidden lines and lower Balmer lines like  $H\beta$  are formed in the nebula around the nova whereas He II and higher Balmer lines arise in a disk/ring around the white dwarf which would explain their partial eclipse and changing radial velocities with orbital phase (Greenstein & Kraft, 1959; Kraft, 1959). *The high ionization lines form close to the white dwarf since they do show a dependence on the orbital phase and possibly form in the inner parts of the accretion disk. Since the white dwarf in DQ Herculis is known to be rotating, an accretion disk should exist. The width of these lines would indicate the rotation velocity of the accretion disk which should be useful in estimating the rotation velocity of the white dwarf and the partial eclipse of the lines might be useful in estimating the radial extent of the disk. Since a cooler envelope should have accumulated on the white dwarf, the radiation escaping from the white dwarf should be of lower temperature making the presence of such highly ionized lines puzzling.*

(12) We used the eclipse parameters in the V band to estimate the luminosities contributed by the binary components. For  $t_2 = 67$  days,  $m_{V,0} = 1.4$  magnitudes,  $m_{V,q} = 15$  magnitudes (McLaughlin, 1960b), we estimate MMRD  $M_{V,0} = -6.9$  mag (Kantharia, 2017) and hence  $M_{V,q} = 6.7$  magnitudes. Using an eclipse depth of 1.3 magnitudes, (Walker, 1956) and  $M_{V,\odot} = 4.83$  magnitudes we estimate  $M_{V,secondary} = 8.0$  magnitudes and  $M_{V,WD} = 7.1$  magnitudes. Both objects emit sub-solar V band luminosity. The companion's luminosity suggests that it is a main sequence star of spectral type between K5 and M0 based on the table in Allen (1973).

(13) The shell of DQ Her is estimated to consist of two components - one with temperature  $\sim 500$  K as inferred from the Balmer continuum radiation which is confined to a small wavelength range and second at  $10^4$  K (Williams et al., 1978). This conclusion is supported by ultraviolet observations (Ferland et al., 1984). Several lines detected

in the nova shell are similar to planetary nebulae except for the excess of permitted recombination lines of C,N,O lines. The existence of high excitation lines at such low electron temperatures has been a perplexing problem. *The excess CNO observed in nova shells as compared to planetary nebulae gives evidence to the underlying energy source being the thermonuclear runaway CNO reaction in which C,N,O are catalysts and are retained whereas the hydrogen and in some cases helium accreted from the companion will be fused to the higher elements and hence be depleted.*

(14) Tails extending outwards from the clumps in the polar regions of the shell of DQ Herculis are detected in  $H\alpha$  and show an increasing radial velocity upto  $800 - 900 \text{ kms}^{-1}$  which are interpreted as being caused by the stellar wind (Vaytet et al., 2007). *There seem to exist at least two observations (this one and the presence of wide emission lines detected in ultraviolet which show partial eclipse) which suggest winds blowing from the white dwarf in DQ Herculis. Since this is a classical nova the accretion rates are likely to be much lower than critical rates and hence the origin of the winds is not clear unless excess surface temperature leads to excess exertion of radiation pressure which blows off the accreted matter. This needs to be examined further*

Thus, although several observational results on DQ Herculis find an explanation in the updated model, there still remain several perplexing results which need to be understood.

#### 4.1.2 V339 Delphini 2013

V339 Del was a fast nova detected on August 14.6, 2013 (Nakano et al., 2013) which reached maximum  $V=4.46$  magnitudes on August 16.44 UT and had a  $t_2 = 10.5$  days (Munari et al., 2013b). It was extensively observed across the electromagnetic spectrum. Here we summarise some observational results from literature and inferences/comments are included in italics:

(1) The nova was in quiescence with  $B \sim 17.1$  magnitudes about 14 hours before discovery (Nakano et al., 2013) indicating a fast rise. It was 6.31 magnitudes and 6.18 magnitudes on August 14.94 and August 15.02 UT 2013 (Tomov et al., 2013). *Strong support to instantaneous release of enormous energy in the nova in a single episode.*

(2) The colour index  $B - V$  changed from about 0.1 to 0.55 between August 15 to August 19.2 which indicated a change in the spectral type from A2 to F8 (Munari et al., 2013b). The colour index  $B - V$  settled down to near 0 around August 25 (Munari et al., 2013b). *The fractional contribution of the hot white dwarf increases as the ejecta fades and hence the colour gets bluer as the light curve declines.*

(3) There was a short plateau in the light curve from August 17.15 to August 19 UT at  $V=4.85$  magnitudes when the colour  $B - I_c$  changed from 0.7 to 1.17 i.e. the nova got redder at the end of the plateau and the emission

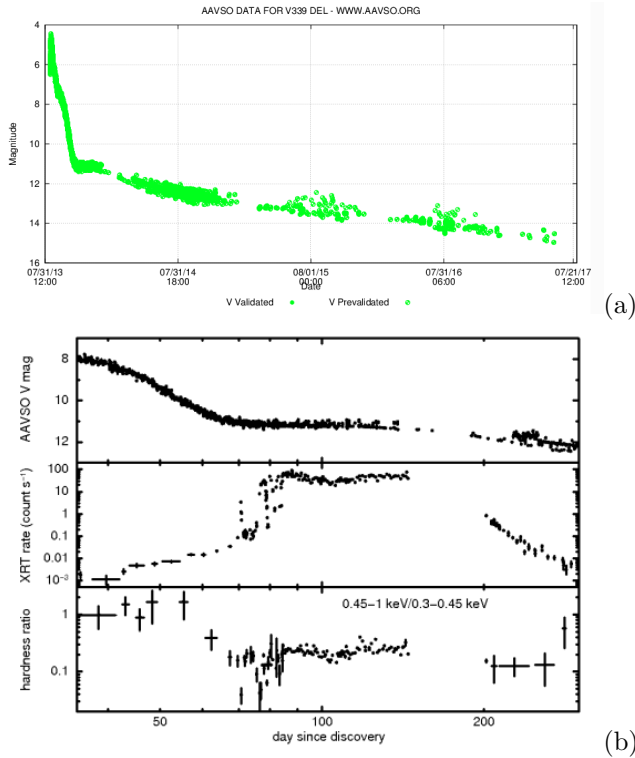


Figure 14: (a) Figure showing V band light curve of V339 Delphini is copied from the AAVSO website. The light curve continues to decline. (b) Figure showing the optical and X-ray light curves of V339 Delphini reproduced from Shore et al. (2016). For comparison, note that radio thermal was detected around day 30 and peaked between days 150-200 after optical detection and was detectable till day 700 or so (Information from an online talk slide by Linford 2015).

lines got fainter (Munari et al., 2013a). There was a longer plateau of brightness in B and V between days 20 (nova had declined by 2.8 magnitudes below maximum) and 37 after maximum. *A plateau in the V band light curve indicates addition of excess V band emission which arrests the decline in the light curve. The plateau indicates new components were added.* The emission component of the  $H\alpha$  line profile changed from trapezoidal on August 14 to flat-topped Gaussian on August 15.83 to Gaussian profile on August 16 (Munari et al., 2013c). *This could indicate the changing morphology of the line forming region indicative of increasing ionization in the ejecta.* It was a Fe II type nova (Munari et al., 2013b) *Although V339 Delphini was a fast nova, the ambient medium due to the main sequence companion appears to have been sufficiently dense to allow the fast ejecta to sweep up sufficient matter for the lines to be detectable.*

(4) The absorption component of the  $H\alpha$  line was detected at  $-1600 \text{ km s}^{-1}$  in the pre-maximum phase and the displacement of the absorption component declined to around  $-730 \text{ km s}^{-1}$  in the post-maximum phase on August 19 (Skopal et al., 2014). The absorption features disappeared by around August 20 while the emission lines got wider and bands with full width at zero intensity

(FWZI) of about  $5000 \text{ km s}^{-1}$  were detectable upto day 40 (Skopal et al., 2014). *The wide emission bands seen after maximum till day 40 probably also included diffuse enhanced and/or Orion lines.*

(5) It was surmised that atomic hydrogen was present in the ejecta of V339 Del from the detection of the broad emission band at 6825 Å which is produced due to Raman-scattering of O VI 1032 Å line photons by neutral hydrogen atoms (Skopal et al., 2014). The line was detected post-maximum around 17 August and had both an absorption and emission component till 21 August after which only an emission component was detected till end September i.e. about day 40. This indicated that the ejecta got completely ionized around day 40 (Skopal et al., 2014) when the light curve was about 3.5 magnitudes below maximum. We note that radio thermal was detected around day 23 near 96 GHz (Chomiuk et al., 2013) and soft X-rays started rising around day 40 (see Figure 14). *All three observations are consistently explained since the detection of soft X-rays is delayed till the atomic hydrogen in the ejecta is ionized and the increasing ionization leading to increasing emissivity of thermal radio.* It was surmised that the optically thick phase in the ejected shell ended around day 77 (Munari et al., 2013b). As seen in Figure 14 soft X-rays reached maximum around that time and the optical light curve showed a plateau. *The plateau in the light curve indicates the addition of an extra component of light possibly from the white dwarf as it becomes visible.*

(6) Dust formed in the shell after 21 September, 2013 (Shenavrin et al., 2013). *Wide Orion lines were detected before this, indicating the presence of clumps and the formation of dust in the Orion clumps.*

(7) The nebular phase was established in October 2013 when the strengths of  $H\beta$  and [OIII] were comparable and the light curve had declined by 6 magnitudes from the peak (Munari et al., 2013b).

(8) Mass of the ejecta was estimated to have been  $2 - 3 \times 10^{-5} M_{\odot}$ . The ejected shell appeared to be bipolar in nature (Shore et al., 2016). *This would indicate the rotating white dwarf in V339 Del which would lead to the formation of a prolate-shaped accreted envelope and hence the aspherical morphology of the ejected shell.*

(9) Detected in  $\gamma$ -rays between days 2 and day 11 after the optical peak (Hays et al., 2013; Ackermann et al., 2014). V339 Del was not detected in non-thermal synchrotron on Aug 28 2013 (day  $\sim 12$ ) (Roy et al., 2013). *The detection of energetic  $\gamma$ -rays for a few days near optical maximum supports the hypothesis that low energy  $\gamma$ -rays from the thermonuclear reaction form the seed photons which are inverse Compton accelerated to  $> 100 \text{ MeV}$  energies by relativistic electrons. This would confirm the presence of relativistic electrons and the non-detection of radio synchrotron could be due to lack of magnetic field or it could be a faint signal.*

(10) The light curve of V339 Delphini shows a pre-maximum halt around 15 August 2013 before the final rise to maximum. *This would indicate that the ejecta was transparent to optical emission of the white dwarf*

which pushed the light curve to the maximum. However when combined with the formation of atomic hydrogen in the ejecta after maximum and the appearance of plateaus in the light curve, it indicates the changing physical conditions in the ejecta so that a fully ionized ejecta recombined and its opacity changed.

(11) Modelling of the evolving spectral energy distribution (SED) of V339 Delphini that was carried out by Skopal et al. (2014). They fitted the SED from  $\sim 3500$  Å to  $\sim 9500$  assuming that in early times, all the emission was from the expanding pseudophotosphere of the white dwarf resembling a star of type A to F and that at a later date some contribution by the emission from the nebula was included. They present the evolution of the radius of the white dwarf defined by the extent of the pseudophotosphere, its effective temperature  $T_{eff}$  and its luminosity  $L_{WD}$ . Interestingly, there is a steep increase in  $T_{eff}$  and  $L_{WD}$  just after the pre-maximum halt when the light curve embarks on its final rise and which in their modelling also leads to an increase in the radius of the pseudophotosphere (Figure 3 in Skopal et al., 2014). After the optical maximum, the  $T_{eff}$  and  $L_{WD}$  decline and then seem to be constant whereas the radius of the pseudophotosphere continues to rise at least till 20 August. *In the model presented here, all the energy input prior to the pre-maximum halt is due to the explosion energy which sets the ejecta in motion and the optical emission is dominated by the ejecta. The influence of the white dwarf radiation begins at the pre-maximum halt when it exerts a radiation pressure on the optically thick ejecta explaining the higher principal velocities compared to pre-maximum spectrum that are generally observed. If the ejecta becomes optically thin in the process, then the white dwarf radiation can escape and will contribute to the blue/optical SED thus increasing the observed luminosity and effective temperature of the nebula. Interestingly, an abrupt rise in both  $T_{eff}$  and  $L_{WD}$  immediately following the pre-maximum halt is deduced from the evolving SED. This gives strong support to the contribution of the hot white dwarf to the SED which increase the bluewards emission as is observed. We note that the SED indicates a rise in temperature and luminosity after the pre-maximum halt which is what is expected in our model.*

## 4.2 Recurrent novae

From the different onset times of radio synchrotron emission at a given frequency recorded in two successive outbursts in RS Ophiuchi and V745 Scorpii, both of which happen to be novae hosting a red giant companion, Kantharia et al. (2016) suggested a scenario in which the winds, blown by the massive white dwarf accreting at super-critical rates, would form a halo around the nova. The size and densities of the halo will keep varying with the varying accretion rates and the winds are responsible for the free-free thermal absorption of the radio synchrotron emission leading to the frequency-dependent onsets and varying onset times at the same radio frequency

for different outbursts (Kantharia et al., 2016). Thus, if the white dwarf in a recurrent nova experiences super-critical accretion rates between two outbursts, then a dense halo of ionized material will form around the nova and will delay the onset of synchrotron emission. When the accretion rate falls then the halo will expand and disperse thus leading to a rapid onset of synchrotron radio emission. The onset epoch of the radio synchrotron emission in successive outbursts helps study the varying accretion rates of the system. Due to the multiple processes involved, there will be a time lag between the change in accretion rates and change in the physical state of the wind halo and hence free-free absorption. This would be applicable to all novae with super-critical accretion rates which comprise most of the recurrent novae.

The interval between the recorded outbursts in RS Ophiuchi have been 9, 26, 12, 13, 9, 18, 21 years. The inter-outburst period seems to have increased in the last two outbursts indicating a decreasing accretion rate and hence reduced winds. The synchrotron radio emission in 2006 at a given radio frequency was detected earlier as compared to its previous outburst in 1985 which would indicate that the wind halo is getting tenuous as expected from the inter-outburst period. The free-free absorption is hence decreasing accelerating the onset of radio synchrotron emission. The long-term pattern in the inter-outburst periods suggests that the accretion rates should soon increase and lead to the wind halo becoming larger, the inter-outburst period reducing (i.e. the next outburst in RS Oph should occur well before 2032) and the onset of radio synchrotron emission in the next outburst being delayed compared to 2006. In the recurrent nova which consistently have a super-critical accretion rate, the optically thick wind halo extent will keep increasing and will lead to a larger delay in the onset of radio synchrotron emission with each outburst. From observations, one can infer that this is possibly the case for U Scorpii and T Pyxidis with the latter actually showing the existence of a large halo around it which is optically visible. In this case, the radio synchrotron will only be detected at later dates if the electron population has not aged. While it is surmised from observations that accretion rates in novae change, it is not known what triggers the variations. While accretion would be disrupted during the outburst, it is possible that changes in local physical conditions could also trigger variations in the accretion rate. However this needs to be investigated further before any firm conclusions can be drawn.

Recurrent novae generally return to optical quiescence within a year of outburst - much faster than classical novae which take at least a few years. U Scorpii is particularly fast and returns to the pre-nova phase in about two months and hence there is high likelihood of missing outbursts when it is in the day sky. The thermal radio light curves also follow the same trend. Recurrent novae in quiescence show variability on several timescales with amplitudes ranging from 1 to 2.5 magnitudes (Schaefer, 2010). The brightness of some recurrent novae dips a year or so before the outburst while in others the brightness dips af-



ter the outburst (Schaefer, 2010). Moreover the range of quiescence luminosities of recurrent novae is larger than of classical novae (Schaefer, 2010) and the contributory factors could be the larger range in types of the companion star - main sequence to red giant in addition to possible differences between the accreting white dwarfs as shown in Table 3.

#### 4.2.1 RS Ophiuchi

The last two outbursts in RS Ophiuchi occurred in 1985 and 2006 and have been well studied at multiple wavelengths. RS Ophiuchi has also been studied in the inter-outburst period. We examine the observational results:

(1) The optical light curves are similar in all outbursts in terms of maximum luminosity and decline characteristics (see Figure 15a).

(2) Radio emission at early times shows a bipolar morphology extending along the east-west which indicates an expansion rate of about 1.3 mas/day as noted in both the 1985 and 2006 outbursts (Hjellming et al., 1986; Taylor et al., 1989; O'Brien et al., 2006; Sokoloski et al., 2008). The outer parts of the east-west emission is attributed to the synchrotron process and this is substantiated from the spectral index of the eastern lobe between 1.7 and 5 GHz which was estimated to be  $\sim 0.5$  ( $S \propto \nu^{-\alpha}$ ) (Sokoloski et al., 2008). The extended east-west emission fades faster at higher radio frequencies while the central part of the radio emission is thermal and longer lived so that at later dates, only the central emission is detectable (Sokoloski et al., 2008) (see Figure 15b) and this should arise in the main ejecta of the explosion. *The bipolar-shaped synchrotron emission indicates a rotating white dwarf in RS Ophiuchi which would have accreted a prolate-shaped envelope and formed an accretion disk in the equatorial plane. The origin of radio synchrotron at a further distance from the binary compared to thermal emission indicates a faster ejection speed for the relativistic electrons especially from the poles. If the accretion disk is destroyed in the outburst then the radio synchrotron emission even if present in the equatorial plane might remain undetectable due to enhanced free-free absorption.*

(3) There was a rapid decline in the ejecta velocity as deduced from the fast evolving widths of the Pa $\beta$  and O I lines (Das et al., 2006). The initial FWHM of few thousand  $\text{kms}^{-1}$  had dropped to a few hundred  $\text{kms}^{-1}$  around day 50 (see Figure 15c). A triangular-shaped H $\alpha$  with FWZI of about 7600  $\text{kms}^{-1}$  was detected on day 1.38 which narrowed down to a FWHM of 420  $\text{kms}^{-1}$  on day 57 and was  $\sim 100 \text{ kms}^{-1}$  on day 209 after outburst (Skopal et al., 2008). *This rapid decline in high initial ejecta velocities is commonly observed in recurrent novae and rarely in classical novae. This supports the presence of high densities in the circumstellar environment due to the winds blown by the white dwarf which leads to deceleration of the ejecta.*

(4) Emission in [O III] 5007A and [Ne V] 3426A was resolved into a east-west oriented double ring around the

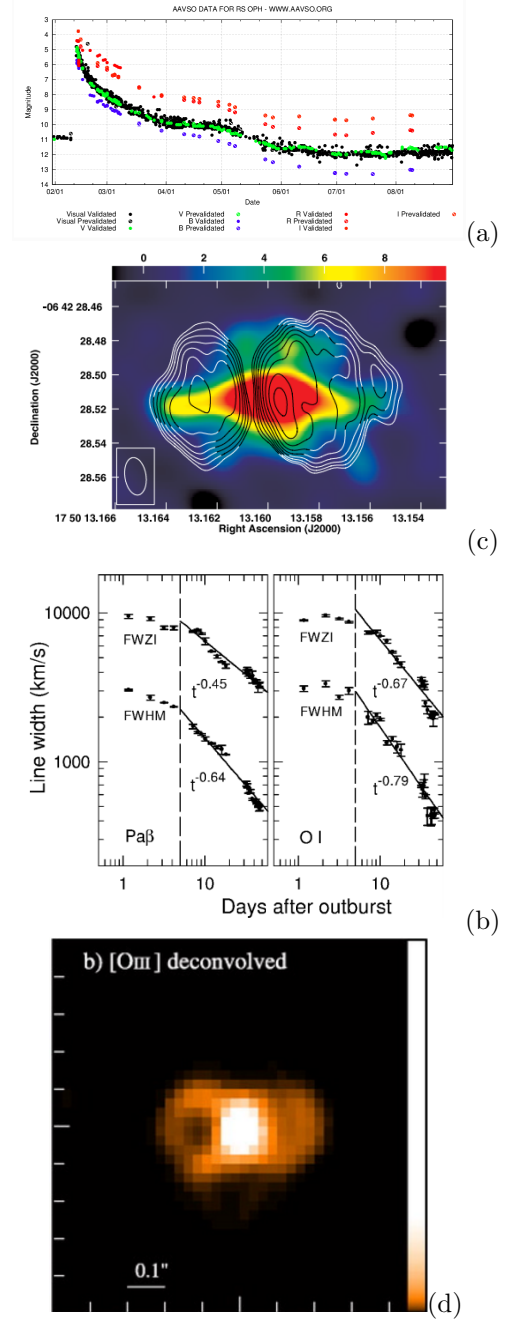


Figure 15: (a) Light curve of RS Ophiuchi in its 2006 outburst copied from the AAVSO website. Note the rapid rise and the rapid initial decline. (b) Radio image of RS Ophiuchi at 43 GHz (colour) and at 1.7 GHz (contours) about 7-8 weeks after outburst reproduced from Sokoloski et al. (2008). Thermal emission in central parts is surrounded by non-thermal emission. (c) Figure showing the rapid evolution in the line widths of Pa $\beta$  and O I reproduced from Das et al. (2006). This behaviour is very different from classical novae which show constant widths of the principal spectrum detectable from near optical maximum to nebular phase and beyond. (d) Image of the [OIII] 5007 emission on day 155 in shown in this figure reproduced from Bode et al. (2007). Note the double ring structure and the extent is similar to the synchrotron radio emission.



nova following its 2006 outburst (see Figure 15d) and their extent indicated an expansion rate of about 1.2 mas/day (Bode et al., 2007). The extent of the [O III] rings appear to be coincident with the radio synchrotron emission (see Figure 15b,d). The double ring structure in [O III] imaged on days 155 and 449 after outburst is well fitted by a model containing an outer faster moving bipolar outflow and an inner slower moving denser ejecta (Ribeiro et al., 2009). The image of day 449 is consistent with a linear expansion of the bipolar outflow from day 155 and no expansion of the inner ejecta (Ribeiro et al., 2009). *The central region is the main ejecta from the explosion as traced by the radio thermal emission also. The synchrotron emission locates the relativistic electrons which precede the main ejecta and could have been swept out by the blast wave after the explosion. The co-existence of [O III] emission with synchrotron emission can be due to either pre-existing matter excited by the electrons or some of the material which was also carried out by the blast wave.*

(5) Soft X-rays were strong around day 55 after the outburst in 1985 and declined soon after that (Mason et al., 1987). Soft X-rays were detected on day 26 after the outburst in 2006 when the light curve had declined by more than 4 magnitudes, strengthened on day 29 and started to decline around day 60 (Bode et al., 2006; Osborne et al., 2011b). *The similar behaviour of X-rays in the 1985 and 2006 outbursts is expected from similar ejecta properties of both outbursts which is expected from the similar behaviour of optical light curves. One can infer that the ejected mass is comparable in all outbursts and the different accretion rates only lead to a varying inter-outburst period and wind halo extents. In both epochs, accretion restarted before day 60.*

(6) Hard X-rays (14-25 keV) were detected for only six days after discovery in 2006 (Bode et al., 2006). Radio synchrotron emission was detected in the first observation at 5 GHz on day 4 after outburst in 2006 when it was dominated by synchrotron emission and by day 13, the radio emission was a combination of thermal and non-thermal emissions (Eyres et al., 2009). This is also inferable from the result that the east-west size of the radio source was about 200 mas on day 63 at 1.7 GHz whereas it was 90 mas on day 59 at 22 GHz (Eyres et al., 2009). *Hard X-rays if mainly due to the relativistic electrons will show some correlation with radio synchrotron detection. The radio size differences indicate the presence of two distinct emitting regions as mentioned above and which also fits the optical observations.*

(7) No evidence of dust formation is found in the ejecta. Features due to silicate dust detected between days 208 to 430 after outburst were interpreted as being from the circumnova environment (Evans et al. 2007). *Since RS Ophiuchi is a fast recurrent nova, its evolution is rapid and there might not be sufficient times for clumps and subsequently dust to form.*

(8) From the radio (1.5 to 23 GHz) study of RS Ophiuchi during its outburst in 1985 (Hjellming et al., 1986) and

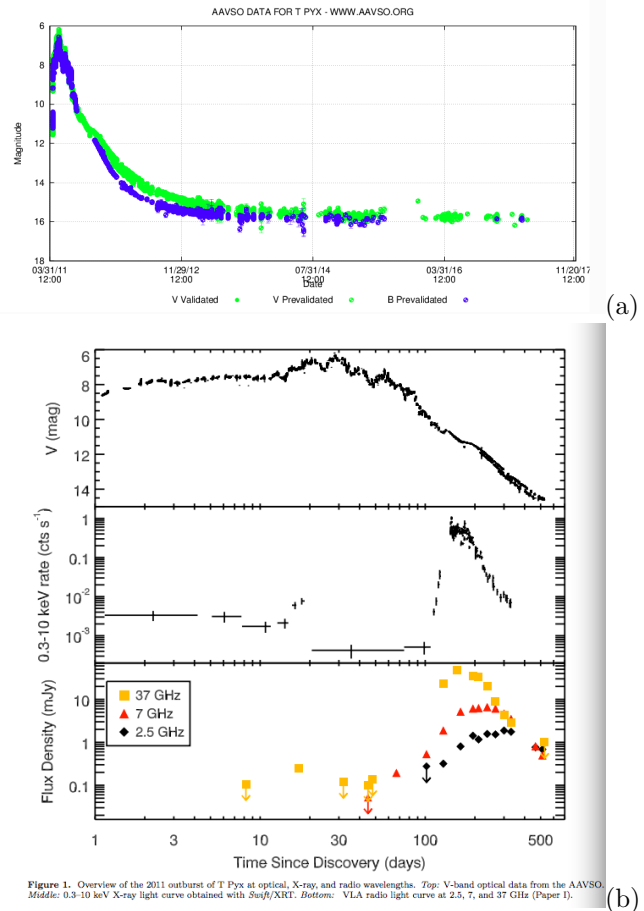


Figure 16: (a) Light curve of T Pyx copied from the AAVSO website. (b) Figure showing the optical, X-ray and radio light curve of T Pyx during its 2011 outburst reproduced from Chomiuk et al. (2014). Note the tight correlation between onset of soft X-rays and thermal radio emission.

study of classical novae (e.g. Hjellming et al., 1979), four main differences between the two were pointed out by Hjellming et al. (1986): (a) brightness temperatures for RS Ophiuchi  $\gg 10^4$  K with it being highest at 1.5 GHz, (b) light curve had timescales  $< 1$  yr whereas it took several years or decades for classical novae to go to quiescence, (3) decay power laws with index in the range  $-1$  to  $-2$  rather than the  $-2.3$  to  $-2.5$  generally noted for classical novae and (4) spectral index of radio emission during the decay was different from  $-0.1$  which is generally estimated for classical novae. Hjellming et al. (1986) inferred that the radio emission from RS Ophiuchi likely consisted of two components - a synchrotron emission and a gyrosynchrotron emission component. *These were interesting first results. Subsequent studies have brought out the different locations of the two components and also determined them to be synchrotron and thermal emission.*

### 4.2.2 T Pyxidis

The last outburst in T Pyx which was the first nova in which recurrent outbursts were recorded, was detected in the pre-maximum phase on 14 April 2011 and reached maximum brightness around 12 May 2011. The previous outbursts in T Pyx were recorded in 1890, 1902, 1920, 1944, 1966 with inter-outburst periods of 12, 18, 24, 22, 45 years. Some of the main observational features of T Pyx which have been surmised are:

(1) T Pyx is a slow nova and had a long pre-maximum halt from day 3.3 to day 13 after detection on 14 April 2011 before it peaked at 6.33 magnitudes on 12.22 May 2011 (day 27.9 after discovery) (Surina et al., 2014). It spent almost three months near maximum emission (see Figure 16). The four main phases of a typical light curve evolution (Figure 1) have been identified in the light curve of T Pyx and the detailed spectral evolution from the initial rise to transition stage has been presented in Surina et al. (2014). The nova is a Fe II type. Since T Pyx was detected in its initial rise which is rare it gave a glimpse into the elemental composition and the spectrum prior to the pre-maximum halt. The spectra taken between days 0.8 and 2.7 showed the presence of high excitation emission lines of C III, N III, Ne II, O II, N II, He I and Ne I which disappeared between 3 to 14 days (i.e. in the pre-maximum halt phase) and the Fe II lines started getting stronger (Surina et al., 2014). *This interesting result which is rarely studied due to few novae being detected in the initial rise phase would indicate the composition of the ejecta before the heavier elements started sinking to the rear part of the ejecta and the ejecta had swept up sufficient circumstellar material to show their spectral signatures.* The ejecta velocity derived from the P Cygni profiles of Balmer lines and Fe II lines does show a tendency for the latter estimates to be lower than the former between days 3.3 to about day 20. Near maximum the ejecta velocities appear well-matched and post-maximum, the Balmer line velocities increase (Figure 10 in Surina et al., 2014).

(2) T Pyx shows a light curve and spectrum evolution typical of classical novae (McLaughlin, 1960b; Surina et al., 2014).

(3) Following its outburst in 1920, three strongly displaced absorption systems with velocities between  $-1000$  and  $-1900$   $\text{kms}^{-1}$  were detected from T Pyx (Adams and Joy 1920) and which corresponded to the principal, diffuse enhanced and Orion systems (McLaughlin, 1960b).

(4) In its 2011 outburst, the ejection velocity estimated from the Balmer lines of hydrogen was  $\sim 4000$   $\text{kms}^{-1}$  about 0.8 days after detection, which declined to  $\sim 2000$   $\text{kms}^{-1}$  after 2.7 days and then remained constant  $\sim 1500$   $\text{kms}^{-1}$  till near maximum (i.e. 28 days after discovery) after which it increased (Surina et al., 2014). *The dramatic reduction in the initial ejecta velocities is commonly observed in recurrent novae likely indicative of a dense circumstellar medium due to the winds blowing from the white dwarf. One would note  $1500$   $\text{kms}^{-1}$  as the pre-maximum velocity and the increase at maximum as*

*the principal spectrum velocities. The original expansion velocities were much higher as expected for a massive white dwarf*

(5) The outburst showed evidence for a bipolar ejecta (Chesneau et al., 2011). *The white dwarf in T Pyx is rotating, has an accretion disk and a prolate shaped accreted envelope which gives rise to the bipolar ejecta.*

(6) Soft X-ray emission was detected around 7.5h after discovery in the initial rise (Kuulkers et al., 2011) which faded around day 12 (see Figure 16b). Interestingly this early detection of faint soft X-rays coincides with the detection of high ionization lines described in point 1 above (Surina et al., 2014). *This indicates that the white dwarf had ejected the accreted envelope soon after the explosion and exposed the hot underlying surface which was emitting in soft X-rays. The pre-maximum ejecta was fully ionized and transparent to soft X-rays upto about day 12 which also increased the excitation of the ejecta.* T Pyx started brightening again in soft X-rays from day 117 (Osborne et al., 2011a). This renewed X-ray activity consisted of supersoft X-rays of energy 30-50 eV (Chomiuk et al., 2014) (see Figure 16b). This also coincided with a period of reduced rate of decline in the light curve at the end of which the soft X-rays started declining. Thermal radio emission was detected around day 69 and was detectable for more than 500 days (Nelson et al., 2014). In fact the steep rise in soft X-rays coincided with a steep increase in the radio thermal emission (Chomiuk et al., 2014) as shown in Figure 16b. *The near coincidence of the increase in thermal radio emission from the ejecta and X-ray emission from the white dwarf surface is expected in the model since X-rays ionize the ejecta and propagate outwards while the increasing ionization leads to increasing free-free emissivity and detectability in thermal radio.*

(7) Hard X-rays were detected on days 14-20 after discovery (Chomiuk et al., 2014) and there was an isolated radio detection at 33 GHz on day 17 (Nelson et al., 2014). T Pyx was not detected in  $\gamma$ -rays (Chomiuk et al., 2014) or in radio synchrotron (Roy et al., 2012). *The non-detection of  $\gamma$ -rays and radio synchrotron emission could either be due to lack of relativistic electrons or deep absorption in the large dense nebula surrounding the nova. If hard X-rays is due to a leptonic process such as synchrotron or inverse Compton also then their detection indicates that relativistic electrons did exist.*

(8) The Balmer lines of hydrogen  $H\alpha$ ,  $H\beta$ ,  $H\gamma$  displayed P Cygni profiles in the spectra taken soon after discovery to about 48.6 days (Surina et al., 2014). Around day 42, the Balmer lines started showing a double component profile and the emission lines of Fe II and Ca II disappeared around day 48 and the Orion line features started appearing around day 70 (Surina et al., 2014). The 4640 emission which is generally seen towards the end of the Orion stage was apparent between 70 and 80 days (Surina et al., 2014). The  $H\beta$  lines continued showing P Cygni profiles at least upto day 69 (Nelson et al., 2014). Alongside the existing absorption near  $-1900$   $\text{kms}^{-1}$  a new absorption feature  $\sim -3000$   $\text{kms}^{-1}$  is seen to be

present in a spectrum from day 69 (Nelson et al., 2014) when the optical light curve was about 2 magnitudes below maximum and would indicate the appearance of the Orion spectral component. The spectrum observed on day 155 was nebular with detection of several coronal and forbidden lines and the light curve had faded by five magnitudes (Surina et al., 2014). *The higher velocity components would be diffuse enhanced or Orion features. Lines with double components is typically observed in diffuse enhanced lines and the highly displaced component at  $-3000 \text{ km s}^{-1}$  detected on day 63 was probably an Orion line since the 4640 band was detected between days 70 and 80 when the light curve had faded by about 2 magnitudes from maximum.*

(9) An expanding shell of radius  $\sim 5''$  surrounded by a faint halo of radius  $10''$  has been detected around T Pyx (Duerbeck & Seitter, 1979; Shara et al., 1997; Schaefer et al., 2010b). Its spectrum resembles that of a planetary nebula with solar abundances (Williams, 1982) and does not show CNO enhancement. We note that CNO enhancement is commonly observed in nova shells. The shell is hot and consists of numerous knots with expansion velocities between  $500$  and  $715 \text{ km s}^{-1}$  for a distance of  $3.5 \text{ kpc}$  to the nova (Schaefer et al., 2010b). It has been suggested that the shell and halo are remnants of previous outbursts. *As noted earlier, the supercritical accretion rates on the white dwarf in recurrent novae can set up vigorous winds and the shell+halo might be a result of the matter blowing out as winds. The matter in the wind would then principally consist of matter accreted from the companion star which has not undergone any processing on the white dwarf and hence should result in solar-like abundance as observed. The extended emission around T Pyx of radius  $10''$  corresponds to a size of  $0.17 \text{ pc}$  at a distance of  $3.5 \text{ kpc}$ . If the winds started blowing in 1890 at a mean speed of  $\sim 1000 \text{ km s}^{-1}$  then they would have travelled out to about  $0.1 \text{ pc}$  in the 120 years between 1890 and 2010. Alternatively the winds could have been quasi-continuous with varying speeds. The radial inhomogeneties observed in the shell would support the varying wind rates and hence varying accretion rate of T Pyx, mostly hovering near the supercritical rates.*

(10) In the 1966 outburst, a slowly evolving light curve and line velocities of  $900$  and  $2000 \text{ km s}^{-1}$  were reported and the spectral development through diffuse enhanced and Orion spectra was also noted (Catchpole, 1969).

(11) The quiescent brightness of T Pyx has been decreasing so that it is fainter by  $1.9$  magnitudes in B band than it was 120 years ago and this has been attributed to decreasing accretion rates (Schaefer et al., 2010b). *A possible reason for fading could be the winds blowing from the white dwarf. If there was dust formation in the winds then it could lead to fading of B band emission but brightening in the infrared.*

(12) T Pyx is not a soft X-ray source in quiescence and its optical emission spectrum is of low excitation compared to several other novae like V Sge (Selvelli et al., 2008). *Novae in quiescence are not expected to be soft X-ray emitters due to the accreted envelope which will be cooler*

*( $< 10^5 \text{ K}$ ) and hence not emit X-rays.*

(13) Ejected mass in the 2011 outburst is estimated to be  $10^{-4}$  to  $10^{-5} M_{\odot}$  (Chomiuk et al., 2014) which is similar to classical novae but about two orders of magnitude higher than generally surmised in recurrent novae. For an inter-outburst period of 45 years, this translates to an accretion rate of  $2.2 \times 10^{-6}$  to  $2.2 \times 10^{-7} M_{\odot} \text{ yr}^{-1}$ . *Such high accretion rates are close to or exceed critical rates for the massive white dwarf and support blowing of intense winds which accumulate around the white dwarf as the halo.*

### 4.3 Evolution of novae to SN 1a

This section speculates on the different possibilities regarding evolution of the binary stars in novae. Let us consider the binary system in a nova which consists of a white dwarf primary and a Roche lobe-filling main sequence companion. If the separation between the stars has not changed significantly since their birth, then it would imply that in its red giant phase, the white dwarf engulfed the companion star even as it evolved to a white dwarf and this left the companion star unaltered. The alternate scenario is that the two stars were at a larger separation when the white dwarf was in its red giant phase and have subsequently lost orbital angular momentum which has reduced the separation. While the mass loss in the red giant phase can carry away some of this angular momentum, the rest could have been converted into a spin component of the white dwarf increasing its rotation speed as the binary has become compact. The next issue to address would be the evolution of the binary when the secondary star will enter the red giant phase and engulf the white dwarf assuming that the separation will remain the same. This could enhance the accretion rates on the white dwarf as the giant star loses mass and could either initiate coalescence of the cores to a neutron star or some of the accreted matter can enter the hot degenerate core and explosively detonate. In the latter case, the energy input to the core would lift the degeneracy and disrupt the white dwarf which we would view as a supernova type 1a. Alternatively the white dwarf might accrete the entire outer envelope of the secondary thus forcing the secondary to enter the white dwarf phase without passing through a giant phase. In this case a double degenerate system can result and if these spiral in then again a supernova type 1a might result.

Then there are novae which host a red giant companion and the orbital separation is large. If there has been no change in the separation between the binary members then the white dwarf in its red giant phase would have filled up its Roche lobe while the companion star which would have been a main sequence star would have had a smaller Roche lobe. The white dwarf would have gradually lost its outer envelope even as the secondary evolved to a red giant phase so that the binary as detected by us show the presence of a white dwarf and red giant companion. If the white dwarf is massive then it is possible that some of the accreted matter will seep into the degenerate core

and explode as a SN 1a. On the other hand it is possible that the red giant companion will lose its outer envelope accelerated due to accretion by the white dwarf. Eventually the secondary will settle down as a white dwarf giving rise to a wide double degenerate system. It is difficult to comment on further evolution of such a system.

Thus while it appears possible that some novae might evolve to supernova explosions, we need to examine relevant observational data spanning novae to other binaries to be able to derive any firm conclusions.

## 5 Conclusions

This study was aimed at understanding the nova outburst that optically brightens the binary system consisting of a white dwarf and a gaseous companion star by 8-20 magnitudes. With the availability of multi-band observing facilities, the multi-wavelength observational results on novae can be used to build a consistent model. Using all these data, the existing model commonly used to explain nova outbursts has been updated and is presented in the paper. This study has also resulted in several significant inferences which are applicable to other astrophysical systems. One of the significant results is the pointing out that the explosion should adiabatically energise the overlying layers increasing their internal energy and that equal distribution of this energy to all particles which includes electrons will result in the electrons acquiring relativistic velocities due to their small mass. No shock acceleration needs to be invoked for this.

The main conclusions are:

1. Several old classical novae ( $< M_{V,q} > \sim 2.6$  magnitudes) are brighter than the combination of an isolated white dwarf ( $M_V \sim 11$  magnitudes) and a late type main sequence star ( $M_V > 4.6$  magnitudes). It is suggested that this is expected since an accreting white dwarf should be surrounded by a cooler accreted envelope. If this envelope is  $\geq 10$  times the radius of the core of a white dwarf and radiating black body emission then it can enhance the black body emission from the white dwarf by a factor  $\geq 100$  and hence explain the discrepancy. If this is a realistic scenario, then no soft X-rays should be detectable from old novae which is indeed the case. Soft X-rays are detected during the outburst which is expected since the outer cooler envelope is ejected in the explosion exposing the hot ( $\sim 10^5$  K) surface of the white dwarf. The soft X-ray phase ends in different novae at different times which we suggest can be consistently explained as the time taken by the white dwarf to accrete sufficient matter to form a cooler envelope so that it no longer shines in soft X-rays. Thus, a large accreted cooler envelope around the white dwarf defines its physical state in quiescence. Further evidence to the presence of a brighter white dwarf in a nova is presented using data on eclipsing novae.
2. The updated model to explain novae in a nutshell is: The base of the accreted envelope will be compressed and heated. When it reaches temperatures  $\geq 10^8$  K then an energetic CNO explosion will be detonated, the huge en-

ergy release will be adiabatically transmitted to the overlying layers of normal matter which will acquire radial velocities in excess of the escape velocity of the white dwarf and be violently ejected. The ejected matter will consist of electrons, ions and atoms and assuming that each particle is equally energised, the light electrons would have acquired relativistic random velocities especially if the ejecta expansion velocity  $\geq 10000$  kms $^{-1}$ . Detection of radio synchrotron outside the main ejecta indicates that relativistic electrons could have been ejected with the blast wave or could have acquired higher expansion velocities thus preceding the main ejecta. The energy input to the envelope would effectively result in two velocity components per a particle species namely an outward expansion velocity and a random component. The explosion should result in a blast wave and a shock wave should set up by the supersonic ejecta which is often referred to in literature as the reverse shock. The location of the relativistic electrons would define the position of what is known in literature as the forward shock.

The rapid rise in the optical emission is owing to the instantaneous energising of the main hydrogen-rich ejecta which leads to rapidly decreasing optical depths due to expansion, heating and ionization thus triggering emission by the free-free and free-bound processes. An important change from the previous model is that in this model the optical continuum emission near the maximum is predominantly from the ejecta. This is strongly supported by the empirical result that most novae follow the maximum magnitude relation with decline time (MMRD) which strongly advocates the common origin of the optical continuous and spectral line emission. The spectral lines are known to arise in the ejecta.

In the updated model, all the energy input till the pre-maximum halt is from the explosion which is often characterised by the velocity displacement of the pre-maximum spectrum and the brightness of the nova. However it is important to keep in mind that several novae show a decline in the expansion velocity in the initial rise phase indicating that the explosion energy was higher by a factor of few than that estimated from the pre-maximum velocity displacement. Later additions from the radiation field of the white dwarf in form of radiation pressure and excitation of lines or continuing winds constitute a trivial fraction of the total energy. Observations indicate that the radiation field of the white dwarf contributes the last  $\leq 2$  magnitudes rise to the optical maximum before the light curve begins its decline. The ejecta fades as it expands, the uniform density component goes optically thin and its emission measure drops. Another important difference in our model is that the diffuse enhanced and Orion systems of spectral lines are shown to form in clumps which coalesce due to mass-based segregation in the ejecta. The optically thick clumps are formed in the inner parts of the ejecta and are subject to the radiation field of the white dwarf. The higher velocity displacement and wider emission lines of these systems are well explained by the action of radiation pressure on the optically thick clumps accelerating them to a range of velocities while the higher excitation

is explained as being caused by the radiation field of the white dwarf shining on the clumps. The insides of these clumps are shielded from the harsh radiation field of the white dwarf and contain metals making them ideal formation sites for dust. These clumps are pushed forward in the ejecta with 1.5 to 2 times the principal velocities due to the radiation pressure exerted by the hot white dwarf. In slow novae where there is sufficient time to form dust inside these clumps, the dust can obscure the optical emission from the entire ejecta and white dwarf and lead to a deep minimum indicating that the clumps have moved to the front of the ejecta. The dust disperses as the ejecta enters the nebular phase and the light curve revives continuing its expected slow decline to minimum. As the light curve declines, the fractional contribution of the hot white dwarf radiation field goes up whereas that of the cooler ejecta goes down which explains the increasing colour temperature during the decline. The high excitation and photoelectric temperatures are indicative of the explosion energy in the early times and of the hot white dwarf at later times and hence are always high.

Most classical novae take several years to go back to their pre-nova brightness which as pointed out in the previous point indicates the time it requires to accrete an envelope similar to their pre-eruption size. It is also suggested that the envelope size has to be a combined function of the mass of the white dwarf and the orbital separation but which in some cases can be modified by an outburst leaving behind a dwarf nova. It is suggested that dwarf novae outbursts are powered by a low energy thermonuclear explosion on the surface of the accreting white dwarf which isothermally inflates the accreted envelope to  $\leq 10$  times the radius of the core of the white dwarf so that the nova brightens and then declines when the envelope deflates. The quiescent and maximum size of this envelope will be a function of the orbital separation in dwarf novae, which is supported by the observed correlations.

3. An ellipsoidal or bipolar shell left behind by the nova outburst is often observed. We explain this as proof of a rotating, accreting white dwarf in the nova. Rotation of the white dwarf leads to a latitude-dependent effective potential due to the combined effect of the gravitational and centrifugal forces that will be felt by the infalling particles. This translates to a latitude-dependent accretion rate such that it is maximum at the poles and minimum at the equator. This will lead to the formation of a prolate-shaped accreted envelope around the white dwarf (see Figure 5) due to higher mass accretion at the poles as compared to the equator. This aspherical envelope will be ejected in a nova explosion. The lower mass accretion rates in the non-polar regions will lead to the infalling mass accumulating in an accretion disk around the white dwarf. This explains the formation of the accretion disk around rotating accreting objects and the tight correlation observed between the presence of an accretion disk and bipolar ejection. Both the formation of an accretion disk and bipolar ejection from compact objects result from latitude-dependent accretion rates. The existing explanation for the formation of an accretion disk attributed to the angular momentum

of the infalling particles is inadequate.

In case of a non-rotating accreting spherical white dwarf, the potential felt by the infalling particle will be the same over the entire surface and hence a spherical envelope will form around the white dwarf. The nova outburst will lead to a spherical ejecta.

This treatment will be applicable to several other astrophysical systems which form accretion disks.

4. Astronomical objects, although they reside at humongous distances, give us a near-perfect demonstration of the validity of the laws of physics that have been derived over centuries. These, along with the electromagnetic signals that these objects emit and their gravitational footprint allow us to probe the universe in which we reside.

## Acknowledgements

I gratefully acknowledge using ADS abstracts, arXiv preprints, AAVSO data, gnuplot, LaTeX, xfig, Wikipedia and Google search engines enabled by the internet and the world wide web, in this research. If you happen to use any of the figures copied from literature, please credit the original reference since I have only used these to better demonstrate a point.

## References

- Ackermann, M., Ajello, M., Albert, A., Baldini, L., Ballet, J., Barbiellini, G., Bastieri, D., Bellazzini, R., Bissaldi, E., Blandford, R. D., Bloom, E. D., Bottacini, E., Brandt, T. J., Bregeon, J., Bruel, P., Buehler, R., Busson, S., Caliandro, G. A., Cameron, R. A., Caragiulo, M., Caraveo, P. A., Cavazzuti, E., Charles, E., Chekhtman, A., Cheung, C. C., Chiang, J., Chiaro, G., Ciprini, S., Claus, R., Cohen-Tanugi, J., Conrad, J., Corbel, S., D'Ammando, F., de Angelis, A., den Hartog, P. R., de Palma, F., Dermer, C. D., Desiante, R., Digel, S. W., Di Venere, L., do Couto e Silva, E., Donato, D., Drell, P. S., Drlica-Wagner, A., Favuzzi, C., Ferrara, E. C., Focke, W. B., Franckowiak, A., Fuhrmann, L., Fukazawa, Y., Fusco, P., Gargano, F., Gasparri, D., Germani, S., Giglietto, N., Giordano, F., Giroletti, M., Glanzman, T., Godfrey, G., Grenier, I. A., Grove, J. E., Guiriec, S., Hadasch, D., Harding, A. K., Hayashida, M., Hays, E., Hewitt, J. W., Hill, A. B., Hou, X., Jean, P., Jogler, T., Jóhannesson, G., Johnson, A. S., Johnson, W. N., Kerr, M., Knödseder, J., Kuss, M., Larsson, S., Latronico, L., Lemoine-Goumard, M., Longo, F., Loparco, F., Lott, B., Lovellette, M. N., Lubrano, P., Manfreda, A., Martin, P., Massaro, F., Mayer, M., Mazziotta, M. N., McEnery, J. E., Michelson, P. F., Mitthumsiri, W., Mizuno, T., Monzani, M. E., Morselli, A., Moskalenko, I. V., Murgia, S., Nemmen, R., Nuss, E., Ohsugi, T., Omodei, N., Orienti, M., Orlando, E., Ormes, J. F., Paneque, D., Panetta, J. H., Perkins, J. S., Pesci-Rollins, M., Piron, F., Pivato, G., Porter, T. A., Rainò, S., Rando, R., Razzano, M., Razzaque, S., Reimer, A., Reimer, O., Reposeur, T., Saz Parkinson, P. M., Schaal,

- M., Schulz, A., Sgrò, C., Siskind, E. J., Spandre, G., Spinelli, P., Stawarz, L., Suson, D. J., Takahashi, H., Tanaka, T., Thayer, J. G., Thayer, J. B., Thompson, D. J., Tibaldo, L., Tinivella, M., Torres, D. F., Tosti, G., Troja, E., Uchiyama, Y., Vianello, G., Winer, B. L., Wolff, M. T., Wood, D. L., Wood, K. S., Wood, M., Charbonnel, S., Corbet, R. H. D., De Gennaro Aquino, I., Edlin, J. P., Mason, E., Schwarz, G. J., Shore, S. N., Starrfield, S., Teyssier, F., & Fermi-LAT Collaboration. 2014, *Science*, 345, 554
- Adams, W. S. & Joy, A. H. 1936, *Contributions from the Mount Wilson Observatory / Carnegie Institution of Washington*, 545, 1
- Allen, C. W. 1973, *Astrophysical quantities*.
- Baade, W. 1940, *PASP*, 52, 386
- . 1942, *PASP*, 54, 244
- Banerjee, D. P. K. & Ashok, N. M. 2012, *Bulletin of the Astronomical Society of India*, 40, 243
- Bethe, H. A. 1939, *Physical Review*, 55, 434
- Bode, M. F., Harman, D. J., O'Brien, T. J., Bond, H. E., Starrfield, S., Darnley, M. J., Evans, A., & Eyres, S. P. S. 2007, *ApJ*, 665, L63
- Bode, M. F., O'Brien, T. J., Osborne, J. P., Page, K. L., Senziani, F., Skinner, G. K., Starrfield, S., Ness, J.-U., Drake, J. J., Schwarz, G., Beardmore, A. P., Darnley, M. J., Eyres, S. P. S., Evans, A., Gehrels, N., Goad, M. R., Jean, P., Krautter, J., & Novara, G. 2006, *ApJ*, 652, 629
- Boyarchuk, A. A. 1969, *Communications of the Konkoly Observatory Hungary*, 65, 395
- Catchpole, R. M. 1969, *MNRAS*, 142, 119
- Chandrasekhar, S. 1931, *ApJ*, 74, 81
- . 1939, *An introduction to the study of stellar structure*
- Chesneau, O., Meilland, A., Banerjee, D. P. K., Le Bouquin, J.-B., McAlister, H., Millour, F., Ridgway, S. T., Spang, A., ten Brummelaar, T., Wittkowski, M., Ashok, N. M., Benisty, M., Berger, J.-P., Boyajian, T., Farrington, C., Goldfinger, P. J., Merand, A., Nardetto, N., Petrov, R., Rivinius, T., Schaefer, G., Touhami, Y., & Zins, G. 2011, *A&A*, 534, L11
- Cheung, C. C., Jean, P., & Shore, S. N. 2014, *The Astronomer's Telegram*, 5879
- Chomiuk, L., Linford, J., Finzell, T., Sokoloski, J., Weston, J., Zheng, Y., Nelson, T., Mukai, K., Rupen, M., & Mioduszewski, A. 2013, *The Astronomer's Telegram*, 5382
- Chomiuk, L., Nelson, T., Mukai, K., Sokoloski, J. L., Rupen, M. P., Page, K. L., Osborne, J. P., Kuulkers, E., Mioduszewski, A. J., Roy, N., Weston, J., & Krauss, M. I. 2014, *ApJ*, 788, 130
- Cordova, F. A., Mason, K. O., & Nelson, J. E. 1981, *ApJ*, 245, 609
- Darnley, M. J., Ribeiro, V. A. R. M., Bode, M. F., Hounsell, R. A., & Williams, R. P. 2012, *ApJ*, 746, 61
- Das, R., Banerjee, D. P. K., & Ashok, N. M. 2006, *ApJ*, 653, L141
- Duerbeck, H. W. & Seitter, W. C. 1979, *The Messenger*, 17, 1
- Eggen, O. J. & Greenstein, J. L. 1965, *ApJ*, 141, 83
- Eggleton, P. P. 1983, *ApJ*, 268, 368
- Eracleous, M., Livio, M., Williams, R. E., Horne, K., Patterson, J., Martell, P., & Korista, K. T. *Astronomical Society of the Pacific Conference Series*, Vol. 137, , *Wild Stars in the Old West*, ed. S. Howell. Kuulkers & C. Woodward, 438
- Evans, A. & Gehrz, R. D. 2012, *Bulletin of the Astronomical Society of India*, 40, 213
- Eyres, S. P. S., O'Brien, T. J., Beswick, R., Muxlow, T. W. B., Anupama, G. C., Kantharia, N. G., Bode, M. F., Gawronski, M. P., Feiler, R., Evans, A., Rushton, M. T., Davis, R. J., Prabhu, T., Porcas, R., & Hassall, B. J. M. 2009, *MNRAS*, 395, 1533
- Ferland, G. J., Pepper, G. H., Langer, S. H., MacDonald, J., Truran, J. W., & Shaviv, G. 1982, *ApJ*, 262, L53
- Ferland, G. J., Williams, R. E., Lambert, D. L., Slovak, M., Gondhalekar, P. M., Truran, J. W., & Shields, G. A. 1984, *ApJ*, 281, 194
- Fowler, R. H. 1926, *MNRAS*, 87, 114
- Gallagher, J. S., Hege, E. K., Kopriva, D. A., Butcher, H. R., & Williams, R. E. 1980, *ApJ*, 237, 55
- Gallagher, J. S. & Starrfield, S. 1978, *ARA&A*, 16, 171
- Gallagher, III, J. S. & Code, A. D. 1974, *ApJ*, 189, 303
- Gaposchkin, C. H. P. 1957, *The Galactic Novae* (Dover Publications, Inc, New York, 1957.)
- Gehrz, R. D. 1988, *ARA&A*, 26, 377
- Geisel, S. L., Kleinmann, D. E., & Low, F. J. 1970, *ApJ*, 161, L101
- Greenstein, J. L. 1957, *ApJ*, 126, 23
- Greenstein, J. L. & Kraft, R. P. 1959, *ApJ*, 130, 99
- Greenstein, J. L., Oke, J. B., & Shipman, H. L. 1971, *ApJ*, 169, 563
- Harman, D. J. & O'Brien, T. J. 2003, *MNRAS*, 344, 1219
- Hays, E., Cheung, T., & Ciprini, S. 2013, *The Astronomer's Telegram*, 5302

- Helton, L. A., Gehrz, R. D., Woodward, C. E., Wagner, R. M., Vacca, W. D., Evans, A., Krautter, J., Schwarz, G. J., Shenoy, D. P., & Starrfield, S. 2012, *ApJ*, 755, 37
- Hjellming, R. M. 1989, *IAU Circ.*, 4853
- Hjellming, R. M. in , *Astrophysics and Space Science Library*, Vol. 208, *IAU Colloq. 158: Cataclysmic Variables and Related Objects*, ed. A. Evans J. H. Wood, 317
- Hjellming, R. M., van Gorkom, J. H., Taylor, A. R., Sequist, E. R., Padin, S., Davis, R. J., & Bode, M. F. 1986, *ApJ*, 305, L71
- Hjellming, R. M. & Wade, C. M. 1970, *ApJ*, 162, L1
- Hjellming, R. M., Wade, C. M., Vandenberg, N. R., & Newell, R. T. 1979, *AJ*, 84, 1619
- Humason, M. L. 1938, *ApJ*, 88, 228
- Joy, A. H. 1954, *AJ*, 59, 326
- Kahabka, P., Hartmann, H. W., Parmar, A. N., & Negueruela, I. 1999, *A&A*, 347, L43
- Kantharia, N. G. 2017, *ArXiv e-prints* 1703.04087 <https://arxiv.org/pdf/1703.04087>
- Kantharia, N. G., Anupama, G. C., Prabhu, T. P., Ramya, S., Bode, M. F., Eyres, S. P. S., & O'Brien, T. J. 2007, *ApJ*, 667, L171
- Kantharia, N. G., Dutta, P., Roy, N., Anupama, G. C., Ishwara-Chandra, C. H., Chitale, A., Prabhu, T. P., Banerjee, D. P. K., & Ashok, N. M. 2016, *MNRAS*, 456, L49
- Kato, T., Ishioka, R., Uemura, M., Starkey, D. R., & Krzemiński, T. 2004, *PASJ*, 56, S125
- Kerr, R. P. 1963, *Physical Review Letters*, 11, 237
- Kraft, R. P. 1958, *PASP*, 70, 598
- 1959, *ApJ*, 130, 110
- 1962, *ApJ*, 135, 408
- 1964a, *Leaflet of the Astronomical Society of the Pacific*, 9, 137
- 1964b, *ApJ*, 139, 457
- Krauss, M. I., Chomiuk, L., Rupen, M., Roy, N., Mioduszewski, A. J., Sokoloski, J. L., Nelson, T., Mukai, K., Bode, M. F., Eyres, S. P. S., & O'Brien, T. J. 2011, *ApJ*, 739, L6
- Krzeminski, W. 1965, *ApJ*, 142, 1051
- Kuiper, G. P. 1941, *ApJ*, 93, 133
- Kuulkers, E., Page, K. L., Ness, J.-U., Osborne, J. P., Balman, S., Starrfield, S., Beardmore, A. P., Bode, M. F., Darnley, M. J., Drake, J. J., Evans, P. A., Eyres, S. P. S., O'Brien, T. J., Orío, M., Schaefer, B. E., Schwarz, G. J., Takei, D., & Walter, F. M. 2011, *The Astronomer's Telegram*, 3285
- Linford, J. D., Chomiuk, L., Nelson, T., Finzell, T., Walter, F. M., Sokoloski, J. L., Mukai, K., Mioduszewski, A. J., van der Horst, A. J., Weston, J. H. S., & Rupen, M. P. 2017, *ArXiv e-prints*:1703.03333
- Linford, J. D., Ribeiro, V. A. R. M., Chomiuk, L., Nelson, T., Sokoloski, J. L., Rupen, M. P., Mukai, K., O'Brien, T. J., Mioduszewski, A. J., & Weston, J. 2015, *ApJ*, 805, 136
- Marshak, R. E. 1940, *ApJ*, 92, 321
- Mason, K. O., Córdova, F. A., Bode, M. F., & Barr, P. 1987, in *RS Ophiuchi (1985) and the Recurrent Nova Phenomenon*, ed. M. F. Bode, 167
- McLaughlin, D. B. 1935, *Popular Astronomy*, 43, 323
- 1937a, *ApJ*, 85, 362
- 1937b, *Publications of Michigan Observatory*, 6, 107
- 1939a, *Popular Astronomy*, 47, 410
- 1939b, *Popular Astronomy*, 47, 538
- 1940, *ApJ*, 91, 369
- 1941, *Popular Astronomy*, 49, 292
- 1942, *ApJ*, 95, 428
- 1943, *Publications of Michigan Observatory*, 8, 149
- McLaughlin, D. B. 1947, *PASP*, 59, 81
- McLaughlin, D. B. 1949, *Publications of Michigan Observatory*, 9, 13
- 1953, *ApJ*, 117, 279
- 1954, *ApJ*, 119, 124
- 1960a, *ApJ*, 131, 739
- McLaughlin, D. B. 1960b, in *Stellar Atmospheres*, ed. J. L. Greenstein, 585
- Mestel, L. 1952, *MNRAS*, 112, 598
- 1965, *Stellar Structure - Stars and Stellar Systems*, 8, 297
- Mukai, K., Page, K. L., Osborne, J. P., & Nelson, T. 2014, *The Astronomer's Telegram*, 5862
- Munari, U., Dallaporta, S., Cherini, G., Valisa, P., Cetrulo, G., Milani, A., & Ghirrotto, L. 2013a, *The Astronomer's Telegram*, 5304
- Munari, U., Hamsch, F.-J., & Frigo, A. 2017, *MNRAS*, 469, 4341
- Munari, U., Henden, A., Dallaporta, S., & Cherini, G. 2013b, *Information Bulletin on Variable Stars*, 6080
- Munari, U., Mason, E., & Valisa, P. 2014, *A&A*, 564, A76



- Munari, U., Valisa, P., Milani, A., & Cetrulo, G. 2013c, *The Astronomer's Telegram*, 5297
- Mustel, E. R. & Boyarchuk, A. A. 1970, *Ap&SS*, 6, 183
- Nakano, S., Itagaki, K., Denisenko, D., Lipunov, V., Gorbvskoy, E., Parkhomenko, A., Tlatov, A., Dormidontov, D., Senik, V., Shurpakov, S., Vollmann, W., Masi, G., Schmeer, P., Nocentini, F., Reichert, U., Izzo, L., D'Avino, L., Yusa, T., Bacci, P., & Ye, Q. 2013, *Central Bureau Electronic Telegrams*, 3628
- Nelson, T., Chomiuk, L., Roy, N., Sokoloski, J. L., Mukai, K., Krauss, M. I., Mioduszewski, A. J., Rupen, M. P., & Weston, J. 2014, *ApJ*, 785, 78
- O'Brien, T. J., Bode, M. F., Porcas, R. W., Muxlow, T. W. B., Eyres, S. P. S., Beswick, R. J., Garrington, S. T., Davis, R. J., & Evans, A. 2006, *Nature*, 442, 279
- Osborne, J. P., Beardmore, A. P., Page, K. L., Kuin, P., Walter, F. M., Schaefer, B. E., Kuulkers, E., Shore, S., Bode, M. F., Schwarz, G. J., Drake, J. J., Ness, J.-U., Balman, S., Starrfield, S., Darnley, M. J., Eyres, S. P. S., O'Brien, T. J., Orío, M., Oksanen, A., & Streamer, M. 2011a, *The Astronomer's Telegram*, 3549
- Osborne, J. P., Page, K. L., Beardmore, A. P., Bode, M. F., Goad, M. R., O'Brien, T. J., Starrfield, S., Rauch, T., Ness, J.-U., Krautter, J., Schwarz, G., Burrows, D. N., Gehrels, N., Drake, J. J., Evans, A., & Eyres, S. P. S. 2011b, *ApJ*, 727, 124
- Paczyński, B. 1965, *Acta Astron.*, 15, 197
- Paczynski, B. & Zytzkow, A. N. 1978, *ApJ*, 222, 604
- Page, K. L., Osborne, J. P., Kuin, N. P. M., Henze, M., Walter, F. M., Beardmore, A. P., Bode, M. F., Darnley, M. J., Delgado, L., Drake, J. J., Hernanz, M., Mukai, K., Nelson, T., Ness, J.-U., Schwarz, G. J., Shore, S. N., Starrfield, S., & Woodward, C. E. 2015, *MNRAS*, 454, 3108
- Pagnotta, A., Schaefer, B. E., Clem, J. L., Landolt, A. U., Handler, G., Page, K. L., Osborne, J. P., Schlegel, E. M., Hoffman, D. I., Kiyota, S., & Maehara, H. 2015, *ApJ*, 811, 32
- Pickering, W. H. 1901, *ApJ*, 13, 277
- Pronik, V. I. & Pronik, I. I. 1988, *Soviet Ast.*, 32, 244
- Reynolds, S. P. & Chevalier, R. A. 1984, *ApJ*, 281, L33
- Ribeiro, V. A. R. M., Bode, M. F., Darnley, M. J., Harman, D. J., Newsam, A. M., O'Brien, T. J., Bohigas, J., Echevarría, J. M., Bond, H. E., Chavushyan, V. H., Costero, R., Coziol, R., Evans, A., Eyres, S. P. S., León-Tavares, J., Richer, M. G., Tovmassian, G., Starrfield, S., & Zharikov, S. V. 2009, *ApJ*, 703, 1955
- Robinson, E. L. 1975, *AJ*, 80, 515
- Robinson, E. L., Nather, R. E., & Kepler, S. O. 1982, *ApJ*, 254, 646
- Roy, N., Kantharia, N. G., Chomiuk, L., Nelson, T., Anupama, G. C., Bode, M. F., Eyres, S. P. S., O'Brien, T. J., & Prabhu, T. P. 2012, *The Astronomer's Telegram*, 4452
- Roy, N., Kantharia, N. G., Dutta, P., Anupama, G. C., Ashok, N. M., & Banerjee, D. P. K. 2013, *The Astronomer's Telegram*, 5376
- Rupen, M. P., Dhawan, V., & Mioduszewski, A. 2001a, *IAU Circ.*, 7717
- Rupen, M. P., Mioduszewski, A. J., & Dhawan, V. 2001b, *IAU Circ.*, 7728
- Sanford, R. F. 1947, *PASP*, 59, 87
- Schaefer, B. E. 2010, *ApJS*, 187, 275
- Schaefer, B. E., Pagnotta, A., Allen, B., Campbell, T., Krajci, T., Richards, T., Roberts, G., Stein, W., Stockdale, C., Dvorak, S., Gomez, T., Harris, B. G., Sjoberg, G., Tan, T. G., Oksanen, A., & Handler, G. 2010a, *The Astronomer's Telegram*, 2452
- Schaefer, B. E., Pagnotta, A., & Shara, M. M. 2010b, *ApJ*, 708, 381
- Schwarz, G. J., Ness, J.-U., Osborne, J. P., Page, K. L., Evans, P. A., Beardmore, A. P., Walter, F. M., Helton, L. A., Woodward, C. E., Bode, M., Starrfield, S., & Drake, J. J. 2011, *ApJS*, 197, 31
- Seaquist, E. R., Bode, M. F., Frail, D. A., Roberts, J. A., Evans, A., & Albinson, J. S. 1989, *ApJ*, 344, 805
- Selvelli, P., Cassatella, A., Gilmozzi, R., & González-Riestra, R. 2008, *A&A*, 492, 787
- Shara, M. M., Zurek, D. R., Williams, R. E., Prialnik, D., Gilmozzi, R., & Moffat, A. F. J. 1997, *AJ*, 114, 258
- Shenavrin, V. I., Taranova, O. G., & Tatarnikov, A. M. 2013, *The Astronomer's Telegram*, 5431
- Sherrington, M. R. & Jameson, R. F. 1983, *MNRAS*, 205, 265
- Shore, S. N., Mason, E., Schwarz, G. J., Teyssier, F. M., Buil, C., De Gennaro Aquino, I., Page, K. L., Osborne, J. P., Scaringi, S., Starrfield, S., van Winckel, H., Williams, R. E., & Woodward, C. E. 2016, *A&A*, 590, A123
- Silber, A. D., Anderson, S. F., Margon, B., & Downes, R. A. 1996, *AJ*, 112, 1174
- Sion, E. M. 1999, *PASP*, 111, 532
- Skopal, A., Drechsel, H., Tarasova, T., Kato, T., Fujii, M., Teyssier, F., Garde, O., Guarro, J., Edlin, J., Buil, C., Antao, D., Terry, J.-N., Lemoult, T., Charbonnel, S., Bohlsen, T., Favaro, A., & Graham, K. 2014, *A&A*, 569, A112

- Skopal, A., Pribulla, T., Buil, C., Vittone, A., & Errico, L. RS Ophiuchi (2006) and the Recurrent Nova Phenomenon, ed. , A. EvansM. F. BodeT. J. O'Brien & M. J. Darnley, 227
- Slavin, A. J., O'Brien, T. J., & Dunlop, J. S. 1995, MNRAS, 276, 353
- Snijders, M. A. J., Batt, T. J., Roche, P. F., Seaton, M. J., Morton, D. C., Spoelstra, T. A. T., & Blades, J. C. 1987, MNRAS, 228, 329
- Sokoloski, J. L., Rupen, M. P., & Mioduszewski, A. J. 2008, ApJ, 685, L137
- Sparks, W. M. 1969, ApJ, 156, 569
- Sparks, W. M. & Starrfield, S. 1975, Memoires of the Societe Royale des Sciences de Liege, 8, 407
- Stratton, F. J. M. 1920, MNRAS, 80, 540
- . 1945, MNRAS, 105, 275
- Strope, R. J., Schaefer, B. E., & Henden, A. A. 2010, AJ, 140, 34
- Surina, F., Hounsell, R. A., Bode, M. F., Darnley, M. J., Harman, D. J., & Walter, F. M. 2014, AJ, 147, 107
- Swings, P. & Jose, P. D. 1949, ApJ, 110, 475
- . 1952, ApJ, 116, 229
- Swings, P. & Struve, O. 1940, ApJ, 92, 295
- Taylor, A. R., Davis, R. J., Porcas, R. W., & Bode, M. F. 1989, MNRAS, 237, 81
- Taylor, A. R., Pottasch, S. R., Seaquist, E. R., & Hollis, J. M. 1987, A&A, 183, 38
- Tomov, T., Ilkiewicz, K., Swierczynski, E., Belcheva, M., & Dimitrov, D. 2013, The Astronomer's Telegram, 5288
- Vaytet, N. M. H., O'Brien, T. J., & Rushton, A. P. 2007, MNRAS, 380, 175
- Walker, M. F. 1954, PASP, 66, 230
- . 1956, ApJ, 123, 68
- . 1961, ApJ, 134, 171
- Warner, B. 1987, MNRAS, 227, 23
- . 1995, Cataclysmic Variable Stars (Cambridge University Press, 1995)
- Weston, J. H. S., Sokoloski, J. L., Metzger, B. D., Zheng, Y., Chomiuk, L., Krauss, M. I., Linford, J. D., Nelson, T., Mioduszewski, A. J., Rupen, M. P., Finzell, T., & Mukai, K. 2016, MNRAS, 457, 887
- Williams, R. E. 1982, ApJ, 261, 170
- . 1992, AJ, 104, 725
- Williams, R. E., Hamuy, M., Phillips, M. M., Heathcote, S. R., Wells, L., & Navarrete, M. 1991, ApJ, 376, 721
- Williams, R. E., Woolf, N. J., Hege, E. K., Moore, R. L., & Kopriva, D. A. 1978, ApJ, 224, 171